Ocean Colour System Vicarious Calibration Tool

Tool Documentation (DOC-TOOL)

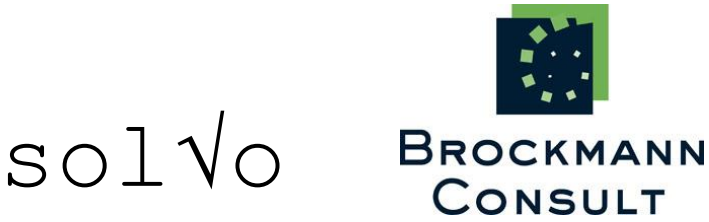

DOCUMENT CHANGE RECORDS

Version	Date	Authors	Description
1.0	30.11.2020	Constant Mazeran (SOLVO) Ana Ruescas (Brockmann Consult)	First version of the document

TABLE OF CONTENTS

1 INTRODUCTION

1.1 BACKGROUND ON OC-SVC

The concept of System Vicarious Calibration (SVC) for Ocean Colour (OC) mission was introduced by Gordon (1987) as a practical mean to meet stringent accuracy requirements of the water-leaving radiance, which only forms a small portion of the radiance measured by the sensor at top of atmosphere (TOA). The OC-SVC method inherently considers as a whole the system comprising the sensor and the processing chain, from TOA radiometry up to the marine signal. In essence, it consists of computing the expected TOA radiometry that results from both the physics embedded in the processor (radiative transfer modelling) and high-quality sea-truth measurements concurrent with space acquisitions, from the visible (VIS) to the near-infrared (NIR) part of the solar spectrum. SVC gains are then defined as the ratio between the expected and actual TOA radiometry at each match-up and each relevant wavelength, and are finally averaged over the mission life-time. In practice, the individual gains are computed such that they make the system exactly match the in situ measurement. The gains are thus intrinsic to a given system, and in particular any change in the processing chain requires their update.

Due to the complexity of the OC processing chain, various implementations of SVC have been attempted since the end of the 1980s, using either the combination of atmospheric and marine in situ data (e.g. Gordon 1998, Eplee et al. 2001), or marine reflectance only (Gordon 1987; Franz et al. 2007) or even reflectance model for retrospective satellite dataset (Werdell et al., 2007). Still, all published methods have considered a unique type of atmospheric correction (AC) in the processing chain, namely the approach of Gordon and Wang (1994) which assumes:

- A decoupling between NIR and VIS: two bands in the NIR are used to detect the atmosphere (aerosol content), and the atmospheric correction is successively applied in the VIS;
- A decoupling between all visible bands: the correction of the atmosphere is applied independently band per band.

For historical reasons we will refer the class of AC algorithms that fulfils these criteria to as *standard* atmospheric correction (e.g. Gordon and Wang, 1994; Antoine and Morel, 1999), in contrast to alternative approaches coupling all bands in the visible and in the NIR (e.g. POLYMER, Steinmetz et al. 2011). These assumptions on the processing chain have implicitly driven the existing SVC methods. Notably, they have made possible the independent (successive) vicarious calibrations of the NIR and visible bands, which we will also refer to as *standard SVC*. Schematically, the marine signal resulting from standard AC can be explicitly computed at a given band λ_i by (all radiometric quantities are in unit of reflectance):

$$\rho_w(\lambda_i) = \frac{\frac{\rho_t(\lambda_i)}{t_g(\lambda_i)} - T\rho_G(\lambda_i) - \rho_{path}(\lambda_i)}{t(\lambda_i)} \quad (1)$$

Where ρ_t is the TOA reflectance (after Level-1 instrumental calibration), t_g is the transmittance for gaseous absorption, $T\rho_G$ is the sun glint reflectance at TOA, ρ_{path} is the total atmospheric path reflectance (Rayleigh scattering, aerosol scattering and multiple-scattering between both) and t the total upward and downward transmittance of the atmosphere; other terms like white-caps can be similarly corrected. Assuming that the corrective terms rely either on ancillary data and models (gaseous absorption, sun glint) or bands in the NIR already calibrated (atmospheric scattering functions), this expression shows that a relative error $\frac{\Delta\rho_t}{\rho_t}$ at a given band λ_i in the VIS leads directly to a relative error at sea level at the same band of:

$$\frac{\Delta\rho_w}{\rho_w}(\lambda_i) = \frac{\Delta\rho_t}{\rho_t}(\lambda_i) \Big/ \frac{t_g t\rho_w(\lambda_i)}{\rho_t(\lambda_i)} \quad (2)$$

The denominator of (2) represents the contribution of marine reflectance to TOA signal. This equation justifies the well-known rule: "*If $t\rho_w$ is 10% of ρ_t, and we want ρ_w with an uncertainty of ±5%, one would expect that it would be necessary to know ρ_{TOA} with an uncertainty of no more than ±0.5%*" (Gordon 1998). The impossibility, to date, to achieve this accuracy at TOA by instrumental calibration alone is the essential motivation to implement operational OC-SVC routine and underlying infrastructure for long-term in situ measurements (e.g. Clark et al., 2003 for MOBY infrastructure). Conversely, the basic relationship (2) has been exploited in detail by Zibordi et al. (2015) to derive specifications on the quality of the in situ data used in the SVC process, in the context of Climate Data Records.

A simple and successful method for OC-SVC considered as reference in the present context is that of Franz et al. (2007), operationally applied by NASA to SeaWiFS, MODIS, VIIRS, and applied with minor adaptation also by ESA to MERIS (Lerebourg et al. 2011) and OLCI (Deru et al., 2019). Taking advantage of the explicit formulation of the signal in Eq. (1), the true (or targeted) radiometry (superscript t) in ideal condition outside Sun glint is given, for any band in the VIS or NIR, by

$$\rho_t^t(\lambda_i) = t_g(\lambda_i)\left(\rho_{path}^t(\lambda_i) + t^t(\lambda_i)\rho_w^t(\lambda_i)\right) \quad (3)$$

Comparison with actual sensor acquisition provides vicarious calibration gains:

$$g(\lambda_i) = \frac{\rho_t^t(\lambda_i)}{\rho_t(\lambda_i)} \quad (4)$$

The targeted quantities in Eq. (3) come from (i) various assumptions for NIR SVC and (ii) indirect measurements for VIS SVC:

i. First, SVC in the NIR is achieved over oligotrophic waters, where the marine signal can reasonably be considered negligible, i.e. ρ_w^t=0 (black pixel assumption). Then, the method assumes that the aerosol model is known (maritime atmosphere) and that one of the two bands used in the aerosol detection is well calibrated (typically the farthest, 865 nm). It is then

possible to predict ρ_{path}^{t}, hence the TOA signal, and compute gains at all other NIR wavelengths.

ii. Then, SVC in the VIS is achieved over an instrumented site with long-term radiometric measurement, ρ_{w}^{t}, at all VIS bands. It is done after application of the NIR calibration: the aerosol detection at the two NIR bands is then supposed to be free from any bias, so that path reflectance and diffuse transmittance derived by the AC become reference quantities, $\rho_{path}^{t}(\lambda)$ and $t^{t}(\lambda)$, at any wavelength λ. Ideally the site is characterized by a clear atmosphere that minimizes potential residual error of the NIR SVC and AC.

It is important to emphasise that the overall algebra of Eqs. (2)-(3)-(4) is intrinsically linked to the standard AC scheme, in particular to the decoupling between all bands as well as to the supposed perfect calibration of NIR bands for the VIS SVC. Recent investigations have demonstrated the impossibility to use such explicit computation of gains for non-standard AC (Mazeran 2018; Mazeran et al., 2019). The generalised definition of SVC is that individual spectral gains minimize the discrepancy between the targeted in situ measurement and the satellite marine reflectance.

1.2 PURPOSE OF THE SOFTWARE

The purpose of the OC-SVC software tool (hereafter referred to as SW-TOOL) is to compute in a controlled manner the OC-SVC gains required by EUMETSAT in its daily operation of OC missions. The SW-TOOL is able to handle in a generic way any OC sensor and processing chain, as far as the interfaces (data format and calling procedure) follows some conventions described in this manual.

The SW-TOOL is operated through a Graphical User Interface (GUI) giving access to two main functionalities: first the computation of individual SVC gains over a match-up database (MDB) between satellite data and high quality in situ marine reflectance; second the post-processing and analysis of these individual gains, up to the provision of mission average gains which shall be applied in operation. The full process is compliant with protocols and requirements inherited from the OC community and EUMETSAT own practices, implemented in the SW-TOOL through data selection, data screening and post-processing. A third functionalities is an optional pre-processing of the database, to restrict its coverage before running the SVC and speed up the processing to only useful match-ups.

The core module of the SW-TOOL is able to handle in a generic way any Level-2 OC processor, comprising in particular standard AC (aerosol detection in the NIR, such as the Baseline AC of OLCI IPF) and more advanced AC (full NIR-VIS inversion, such as the Alternative AC of OLCI IPF). To do so, the numerical computation of the individual gains relies on an iterative algorithm, running the Level-2 processor as a black-box and minimizing the discrepancy between the targeted (in situ) and satellite marine reflectance. Importantly, this minimization formalism allows to implement in one single algorithm the computation of gains both in the VIS and in the NIR, by the adequate selection of bands and reference data by the user (e.g. NIR SVC gains can be computed by selecting a database with zero marine reflectance in the NIR, fixing calibration of one band, limiting the aerosol detection to one model and computing gains at other NIR bands).

This document comprises the theoretical foundation of the algorithm (section 2), a user manual (section 3) and a demonstration on OLCI-A and OLCI-B data supporting EUMETSAT reprocessing for OLCI collection 003 to be released in 2021 (section 4).

1.3 REQUIREMENTS AND DESIGN

1.3.1 METHODOLOGY AND PROTOCOLS

Protocols for match-up selection - This requirement refers to the protocols used in the OC community to select data for SVC gains computation. Because the computation can be time-consuming, the protocols have to be applied in a first stage to limit the SVC process to the useful match-ups. This generates a sub-set of the MDB, locally stored in the SW-TOOL data files.

The criteria coded in the SW-TOOL comprise:

- Time difference between the satellite and in situ acquisitions;
- Thresholds on the Sun zenith angle and satellite viewing zenith angle;
- Threshold on the chlorophyll concentration;
- Threshold on the AOT;
- List of Level-1b and Level-2 flags to discard the pixels;
- Size of the Region of Interest (ROI) around the in situ station, in number of pixels;
- Percentage of required valid pixels in the ROI;
- Definition of statistical screening (outliers rejection based on mean and standard-deviation of the reflectance in the ROI);
- Homogeneity test through CV criteria on remote-sensing reflectance (spectrally dependent);
- Possibly manual screening based on specific discrete variables provided in the MDB (in situ status, in situ deployment, satellite granules…).

The criteria are proposed in the GUI (see section 3.5) so that users are able to manually modify the thresholds; default values come from the literature. The list of criteria itself can be modified in a configuration file, for instance to add thresholds or manual screening on new quantities that are dynamically added to the GUI.

Protocols for gain computation – The SW-TOOL is compliant with the method of Franz et al. (2007) summarised in section 1, when applied to standard AC. The two-step NIR-VIS approach is achieved by launching two successive jobs with their specific options. All requirements on the NIR and VIS datasets are fulfilled by the selection of appropriate MDBs by the user. However, the SW-TOOL is more generic as it shall handle any Level-2 processor as a black-box, including non-standard AC. This precludes to compute gains with the explicit Eqs. (3)-(4). We refer to section 2 for all numerical details on the gain computation.

Required adaptation to the per-pixel methodology – With SVC gains being stored in a given Auxiliary Data File (ADF) read by the Level-2 processor at granule level, the Level-2 black-box approach

necessitates to define only one gain per match-up (and not individual gains per-pixel). This unique gain (spectral) is linked to one unique marine reflectance per match-up (for each spectral band). This unique reflectance results from standard protocols used in ocean colour data validation (Bailey and Werdell, 2006; Cazzaniga et al., 2019b; Zibordi and Voss, 2019). The criteria correspond to those listed above, possibly with other thresholds defined by the user. The process includes optionally the normalisation for BRDF effects (Morel et al., 2002), when it is not included in the Level-2 processor. This process at match-up level, although slightly different than the usual approach at pixel level, implies by construction a perfect consistency between the vicarious calibration of the sensor and the validation of the marine reflectance. Typically, for standard AC, the averaged satellite Rrs defined by validation protocols over a calibration target exactly matches the in situ Rrs used in the individual gain computation. This is not ensured in the averaging of per-pixel gains.

Protocols for gain averaging - When gains at match-ups level are ready, a final post-processing step computes the mission average gains and produces statistics and plots to analyse their distribution and sensitivity to various parameters (time, angles, etc.). First, a screening of the gains is applied, based on the list of criteria given previously (possibly with slightly different thresholds than those used in the pre-screening and spatial averaging). Then, the averaging of the remaining gains is done using the Mean of the Semi-Interquartile Range (MSIQR; Franz et al., 2007), which amounts of removing the 25% lowest and 25% highest values of the gains' distribution. The purpose is to remove outliers that would have passed the screening step. On top of simple mean and standard-deviation, another interesting indicator to check the suitability of gains with respect to stability requirement in ocean colour (0.5% on marine reflectance over a decade) is the Relative Standard Error of the Mean (RSEM) proposed by Zibordi et al. (2015). It is computed at a given band λ_i by:

$$RSEM(\lambda_i) = \left. \frac{\sigma(\lambda_i)}{\bar{g}(\lambda_i)} \right/ \sqrt{N_y} \tag{5}$$

where $\bar{g}$ is the mean gain, σ the standard-deviation of the individual gains and N_y the number of individual gains (i.e. good match-ups), scaled over a decade (i.e. $N_y = 10\ N/Y$ where N and Y are the actual number of match-ups and measurement years, respectively).

SVC assessment – Validation of SVC gains is not possible in the strict sense of the term, beyond the verification that individual gains fulfils their roles on the calibration dataset. Instead, the impact of the mission average gains shall be assessed on independent validation datasets. This validation is explicitly out of scope of the SW-TOOL.

1.3.2 SOFTWARE DESIGN

Modularity – The SW-TOOL is built on four main components further detailed in next sections (Figure 1): the GUI to launch easily these modules by the user (section 3.1.3), a pre-processing capability of the MDB (section 3.1.4), the core module to compute individual gains (section 3.1.5), the post-processing for gains averaging and analysis (section 3.1.6).

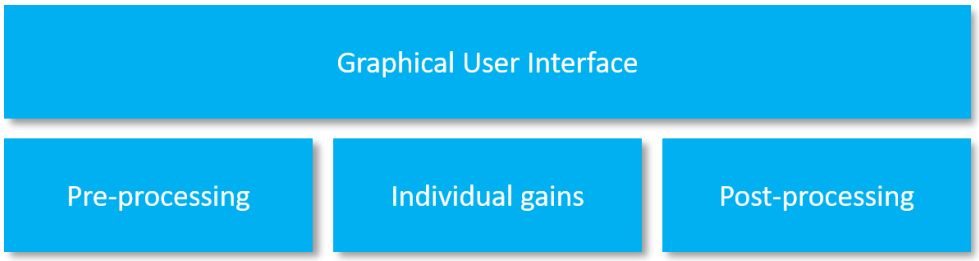

Figure 1 Main components of the SW-TOOL

The software is fully developed in Python and distributed directly in source code on EUMETSAT Gitlab server.

Versatility – The code is generic in term of sensors, options and Level-2-processor. The hard-coding of sensor names only appears in low level routines when specific process is strictly required (e.g. to handle the format of the ADF and PDUs). The code reads a configuration file, easily editable in text format (section 3.1.1), that defines once for all the list of OC sensors with their characteristics (bands, flags …) and default options of the user which can be further modified in the GUI. The Level-2 processor is invoked as a black-box by a so-called *wrapper*, using a pre-defined list of required arguments handled by the SW-TOOL and possibly other specific options/arguments for the given processor (section 3.4.1.4).

Traceability – Each run of the SW-TOOL (pre-processing, gains computation, post-processing) generates an output configuration file summarising exhaustively the data and options selected by the user, to keep perfect traceability in the SVC gains computation (section 3.5.2).

Verification – When each individual gain has been computed, it is applied at TOA on the individual match-up and the Level-2 processor is launched one more time. This creates a new temporary MDB after individual SVC. The impact of all individual gains is then assessed by plotting the satellite marine reflectance of this MDB against the targeted values. For standard AC, the individual SVC shall make the satellite data perfectly match the in situ measurements (3.5.2.2). For non-standard AC, the individual gains shall still improve the retrieval for being considered valid.

2 ALGORITHM THEORETICAL BASELINE

2.1 GENERIC SVC FORMULATION

The computation of individual gains in the SW-TOOL relies on the generic formalism initially developed in the ESA OC-CCI project (Mazeran 2018; Mazeran et al., 2019), but differs in its numerical implementation and extends its genericity. This formalism was introduced to deal with any non-standard AC, such as POLYMER (Steinmetz et al., 2011), also comprising the standard AC (e.g. Antoine and Morel, 1999), and is applicable to any Ocean Colour sensor. In this context, the fully normalized remote-sensing reflectance, R_{rs} is formally defined as a function of the TOA radiance, L_t, by:

$$R_{rs}(\lambda_i) = f_i\big(L_t(\lambda_1), \cdots, L_t(\lambda_n)\big), \;\; i = 1 \dots m \tag{6}$$

Where the m functions f_i express the link between the TOA and BOA radiometry and n is the number of bands at TOA actually used by the AC (possibly lower than the total number of the sensor bands). These functions also depend on other non-radiometric parameters such as ancillary data, geometrical conditions, physical constants, etc., not made explicit in the present context. In the standard OLCI processor, the remote sensing reflectance at a given band in the VIS is simply a linear expression of the TOA radiance, ρ_t, at this same band, i.e. there is no spectral coupling in the f_i functions because the aerosol detection is done in other bands in the NIR:

$$\text{Standard AC:} \quad R_{rs}(\lambda_i) = \frac{C_{BRDF}}{\pi}(\lambda_i) * \frac{\frac{\rho_t(\lambda_i)}{t_g(\lambda_i)} - T\rho_G(\lambda_i) - \rho_{path}(\lambda_i)}{t(\lambda_i)}, \;\; i = 1 \dots m \tag{7}$$

Where C_{BRDF}/π is a normalisation factor accounting for BRDF correction and conversion to unit of remote-sensing reflectance. For other processing chains, the link may be more complex and possibly even not explicit (e.g. OLCI alternative AC with neural networks).

Traditionally, SVC consists in multiplying the TOA radiance $L_t(\lambda_1), \cdots, L_t(\lambda_n)$ by a set of n gains $\boldsymbol{g} = (g_1, g_2, \cdots, g_n)$. Note that applying SVC on a subset of bands is possible in the SW-TOOL, and is here implicitly considered by the same notation assuming that some of the g_i are fixed to unity. In the generic framework, the application of gains can be done wherever in the Level-2 processor (what for instance occurs in OLCI IPF, after gaseous and glint correction). Hence, the remote-sensing reflectance is formally expressed as a function of the gains through:

$$R_{rs}(\lambda_i) = F_i(g_1, g_2, \cdots, g_n), \;\; i = 1 \dots m \tag{8}$$

This is just another writing of functions f_i, directly expressed with respect to gains instead of TOA radiometry. When SVC gains are applied at TOA, as was done in the OC-CCI, functions F_i are simply defined by $F_i(g_1, g_2, \cdots, g_n) = f_i\big(g_1 * \rho_t(\lambda_1), \cdots, g_n * \rho_t(\lambda_n)\big)$. In any case, the SW-TOOL never

requires the explicit formulation of functions F_i, but only needs the capability to compute them for various sets of gains.

For a given match-up, the SVC is defined as an optimal problem: find a spectral gain $\boldsymbol{g} = (g_1, g_2, \cdots, g_n)$ which minimises the discrepancy between the retrieved R_{rs} and targeted R_{rs}^t given by sea-truth measurement, defined by following χ^2 cost function:

$$\chi^2(\boldsymbol{g}) = \sum_{i=1}^{m} \left(R_{rs}^t(\lambda_i) - F_i(\boldsymbol{g})\right)^2 \quad (9)$$

While all previous equations are, in general, applicable at pixel level, they are used in the present context at match-up level, i.e. on the average macro-pixel. Indeed, the SW-TOOL requirement to process a full match-up with a unique gain (stored in one ADF), implies that the optimal problem shall be solved as a whole on the macro-pixel. This means that R_{rs} comes from spatial averaging over the macro-pixel, through standard validation protocols (tuned by the user in the SW-TOOL). In other words, the unique spectral gain $\boldsymbol{g}$ per match-up minimizes the discrepancy between the sea-truth R_{rs}^t and the averaged R_{rs}, as done in standard validation protocols. Such procedure hence discards the need for spatial averaging of gains per match-up, and avoid any inconsistency between averaging in the SVC process and in the validation process. When the optimal problem can be solved exactly (see below for standard AC), it is ensured that the match-up averaged R_{rs} is exactly equal to R_{rs}^t for the m bands of interest.

In this context, *individual gain* hence means *gain per match-up*. The individual gains g_i are then post-processed to unique mission average spectral gain $\bar{g}_i$.

2.2 DIMENSIONALITY OF THE SVC OPTIMISATION PROBLEM

Computation of SVC gains is not necessarily done at all bands, and especially not simultaneously. For instance, in the standard approach, gains are computed first in the NIR, with some assumptions on fixed gains. Then gains in the VIS are computed, with fixed gains in the NIR. The spectral dimensionality of the SVC optimisation problem allows such capability in the SW-TOOL. With $l \leq n$ and $l \leq m$, one has:

- n is the number of bands at TOA used by the processor to identify the marine and atmospheric unknowns. Basically, it could be considered as the full set of sensor bands, although some may not be used for retrieving R_{rs} (e.g. absorption bands) and thus cannot be vicariously calibrated. It typically refers to $L_t(\lambda_1), \cdots, L_t(\lambda_n)$. This number is intrinsic to sensor and a processing chain and cannot be changed in the SW-TOOL.
- l is the number of SVC gains to be computed; it refers to quantity $\boldsymbol{g} = (g_1, g_2, \cdots, g_l)$. This number may change from one run to another run of the SW-TOOL, for instance SVC in the NIR, then in the VIS. Implicitly, the remaining $n - l$ gains are fixed during the optimization problem, to values given by the user and possibly different from unity (e.g. NIR gains fixed while computing VIS gains). Note also that the l gains $g_1, \cdots, g_l$are applied to a set of l bands here noted $\lambda_1, \cdots, \lambda_l$ for the sake of simplicity, without implying that these bands are ordered by

their actual wavelength (i.e. λ_1 does not have to represent the shortest wavelength of the sensor, etc.).

- m is the number of bands at BOA used as observation in the χ^2 minimisation; it refers to quantities R_{rs}^t and R_{rs}. In practice, the spectral coverage of in situ R_{rs}^t may be more limited than that of the satellite R_{rs} and restricts necessarily m. In any case, this number has to be equal or higher than the number of unknown gains, l. The case $m = l$ can be used for standard AC which amounts to a simple diagonal matrix inversion (see below). With $m > l$, the SVC becomes a classical overdetermined optimisation problem. Two options are proposed in the GUI to select the bands used in the χ^2:
  - Take exactly bands used for SVC, i.e. $m = l$;
  - Take all available in situ bands, which can typically cover the case $m > l$. The in situ bands are automatically detected in the input match-up database.

2.3 NUMERICAL IMPLEMENTATION

The minimum of the cost function is solution of the non-linear system:

$$\nabla \boldsymbol{F}^T(\boldsymbol{g})(\boldsymbol{R_{rs}^t} - \boldsymbol{F}(\boldsymbol{g})) = 0 \tag{10}$$

Where bold variables refer to vector notation (spatial dimension), $\nabla \boldsymbol{F}(\boldsymbol{g})$ is the Jacobian matrix of $\boldsymbol{F}$, evaluated at current $\boldsymbol{g}$, and the *T* superscript stands for its transpose. The Jacobian matrix of size $m * l$ is defined by:

$$\nabla \boldsymbol{F} = \begin{pmatrix} \frac{\partial R_{rs}(\lambda_1)}{\partial g_1} & \cdots & \frac{\partial R_{rs}(\lambda_1)}{\partial g_l} \\ \vdots & \ddots & \vdots \\ \frac{\partial R_{rs}(\lambda_m)}{\partial g_1} & \cdots & \frac{\partial R_{rs}(\lambda_m)}{\partial g_l} \end{pmatrix} \tag{11}$$

The numerical resolution of the non-linear system is based on a first order Taylor expansion around a fixed set of gains (*nominal gains*), $\boldsymbol{g}^0$:

$$\boldsymbol{F}(\boldsymbol{g}) \approx \boldsymbol{F}(\boldsymbol{g}^0) + \nabla \boldsymbol{F}(\boldsymbol{g}^0)(\boldsymbol{g} - \boldsymbol{g}^0) \tag{12}$$

By definition of the optimal problem, $\boldsymbol{F}(\boldsymbol{g})$ is supposed to be equal to the target $\boldsymbol{R_{rs}^t}$ and $\boldsymbol{F}(\boldsymbol{g}^0)$ is given by the processor at the fixed gains $\boldsymbol{g}^0$, noted $\boldsymbol{R_{rs}^0}$. This allows Eq. (10) to be solved approximately with the $l \times l$ linear system:

$$\nabla \boldsymbol{F}^{\mathrm{T}} \nabla \boldsymbol{F}(\boldsymbol{g} - \boldsymbol{g}^0) = \nabla \boldsymbol{F}^{\mathrm{T}}(\boldsymbol{R_{rs}^t} - \boldsymbol{R_{rs}^0}) \tag{13}$$

Where $\nabla \boldsymbol{F}$ is implicitly defined at $\boldsymbol{g}^0$. This solution can be interpreted as the first iteration of the Gauss-Newton algorithm minimising χ^2, and the fixed spectral gain $\boldsymbol{g}^0$ as a first guess. This $\boldsymbol{g}^0$ corresponds to the spectral gain stored in the *nominal* ADF used by the SW-TOOL to compute $\boldsymbol{R_{rs}^0}$. The Jacobian matrix is computed around this first gain $\boldsymbol{g}^0$ by numerical derivative:

$$\frac{\partial R_{rs}(\lambda_i)}{\partial g_j} \approx \frac{F_i(g_1^0, \cdots, g_j^0 + h_j, \cdots, g_l^0) - F_i(g_1^0, \cdots, g_j^0 - h_j, \cdots, g_l^0)}{2h_j} \quad \text{with } h_j \ll 1 \qquad (14)$$

In practice for each calibration scene, these terms are computed by applying the Level-2 processor for $2 * l$ sets of gains (i.e. $2 * l$ ADFs). The choice of step h_j depends on how quickly F_i varies with respect to g_j. This has no importance for standard AC (see below). For non-standard AC such as POLYMER, numerical tests have convinced us to consider a relative step instead of an absolute step, i.e. $h_j = s * g_j^0$ with $s = 0.5\%$. Importantly, too small increments would yield totally erroneous estimates of the Jacobian because then numerical differences reach the limit of numerical accuracy and become meaningless.

2.4 CONVERGENCE FOR STANDARD AC

In the general case, the method assumes small deviation between $\boldsymbol{g}$ and $\boldsymbol{g}^0$. If non-linearities in the Level-2 processor are too important, it may be important to start from a realistic first guess to converge towards the solution $\boldsymbol{g}$ – or, alternatively, the procedure should be iterated. The situation simplifies advantageously for standard AC. Eq. (7) shows indeed that R_{rs} is a linear function of the TOA radiometry, with a fixed offset given by the path reflectance. In OLCI standard AC, the gains are not directly applied to the TOA reflectance, but to the reflectance corrected for gas and glint, ρ_{gc}:

$$R_{rs}(\lambda_i) = F_i(g_1, g_2, \cdots, g_n) = \frac{C_{BRDF}(\lambda_i)}{\pi} * \frac{\rho_{gc}(\lambda_i) * g_i - \rho_{path}(\lambda_i)}{t(\lambda_i)} \qquad (15)$$

The only non-linearity could be due to the BRDF correction, using R_{rs} at various bands in the chlorophyll estimate (see Morel et al., 2002). It is negligible, as will be shown hereafter and could be, if too high, totally removed by computing C_{BRDF} by the fixed R_{rs}^t which is expected to be reached at convergence.

Hence, function $\boldsymbol{F}$ is linear with respect to $\boldsymbol{g}$ and the SVC optimisation for gains in the VIS can be solved with $m = l$. The square Jacobian matrix does not depend on $\boldsymbol{g}$ and the numerical estimates given by Eq. (14) are exact, whatever $\boldsymbol{g}^0$:

$$J = \begin{pmatrix} \frac{C_{BRDF}(\lambda_1)}{\pi} * \frac{\rho_{gc}(\lambda_1)}{t(\lambda_1)} & \cdots & 0 \\ \vdots & \ddots & \vdots \\ 0 & \cdots & \frac{C_{BRDF}(\lambda_m)}{\pi} * \frac{\rho_{gc}(\lambda_m)}{t(\lambda_m)} \end{pmatrix} \qquad (16)$$

The linear system given in Eq. (13) is diagonal and can be solved explicitly at all bands:

$$
\begin{aligned}
g_i &= g_i^0 + \frac{1}{\frac{C_{BRDF}(\lambda_i)}{\pi} * \frac{\rho_{gc}(\lambda_i)}{t(\lambda_i)}} * \left(R_{rs}^t(\lambda_i) - R_{rs}^0(\lambda_i)\right) \\
&= g_i^0 + \frac{1}{\frac{C_{BRDF}(\lambda_i)}{\pi} * \frac{\rho_{gc}(\lambda_i)}{t(\lambda_i)}} * \left(R_{rs}^t(\lambda_i) - \frac{C_{BRDF}(\lambda_i)}{\pi} * \frac{\rho_{gc}(\lambda_i) * g_i^0 - \rho_{path}(\lambda_i)}{t(\lambda_i)}\right) \\
&= \frac{t(\lambda_i)\frac{\pi}{C_{BRDF}(\lambda_i)} * R_{rs}^t(\lambda_i) + \rho_{path}(\lambda_i)}{\rho_{gc}(\lambda_i)} \\
&= \frac{t(\lambda_i)\rho_w^t(\lambda_i) + \rho_{path}(\lambda_i)}{\rho_{gc}(\lambda_i)}
\end{aligned}
\tag{17}
$$

Where ρ_w^t corresponds to the denormalised in situ marine reflectance, i.e. in the geometry of the sensor. This demonstrates that the solution $\boldsymbol{g}$ does not depend on $\boldsymbol{g}^0$. Furthermore, we recognize exactly the standard definition of SVC gains explicitly given as a function of the path reflectance and transmittance (Franz et al., 2007). The resolution of the SVC optimal problem in the SW-TOOL hence exactly amounts to the standard SVC procedure when applied to standard AC. Eq. (9) and its resolution can thus be considered as a generalisation of SVC for any AC.

In practice, the individual gains computed by the optimal problem can be considered as validated when they bring R_{rs} to R_{rs}^t at the calibrated bands. This check is done by the SW-TOOL at the end of the SVC run. We emphasize that for non-standard AC, this may not be the case, or even may be theoretically impossible (see Mazeran et al., 2017, for POLYMER).

3 USER MANUAL

3.1 CONTENT OF THE SOFTWARE

3.1.1 OVERALL STRUCTURE

The software comprises essentially five Python modules with one configuration file (Figure 2), complemented by a folder giving a stand-alone Level-2 processor:

1. `main.py` contains the code of the GUI and of the SVC module.
2. `pre_processing.py` contains the routines to pre-process the Level-1 MDB.
3. `post_processing.py` contains the function to post-process the individual gains.
4. `MDB_utils.py` contains various routines related to the handling of the MDB.
5. `utils.py` contains various routines specific to the sensors and ADF.
6. `ocsvctool.cfg` defines all parameters used in the software: file paths, options of the processing and characteristics of the sensors considered for SVC.
7. `wrappers/AC_example/` is a directory containing a simplified OLCI-A Level-2 processor (`AC_example_wrapper.py`) and a pre-computed Level-2 MDB on the MOBY site. The purpose of this stand-alone processor is to test quickly the software without external dependency.

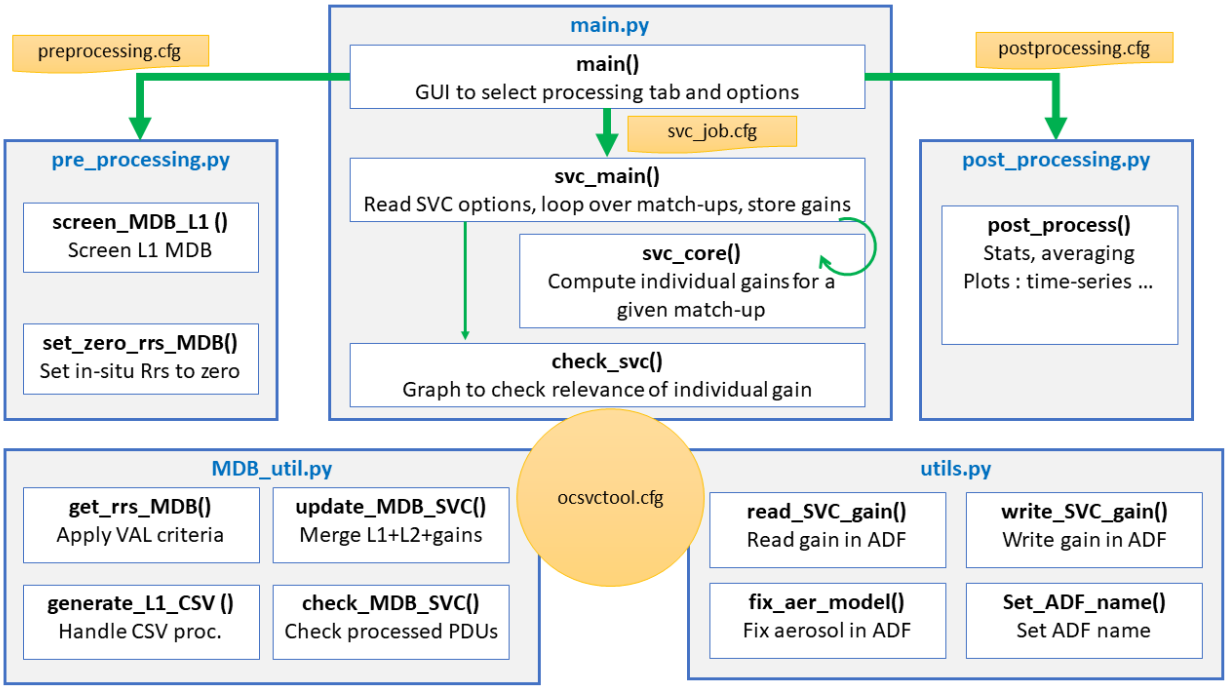

Figure 2 Overall structure of the software and main functions.

3.1.2 CONFIGURATION FILES

The configuration file `ocsvctool.cfg` is organized with sections, each containing keys and values, listed below. This file can be easily edited by the user. When a list is given for a value, it should be comma separated without spaces.

- [GLOBAL]
  - sensors = list of sensors defined in this configuration files
  - debug = True or False
  - delete_individual_ADF = True or False
  - parallel = True or False
  - proc_mode = PDU or CSV
  - nmatchup = number of match-ups to process

  - MDB_dir = user MDB directory path
  - OUT_dir = user output directory path
  - ADF_dir = user ADF directory path
  - PDU_dir = user PDUs' directory path
  - wrapper_dir = user wrapper directory path
- [FACILITY]
  - center = short name of processing center
  - name = long name of processing center
  - organisation = organisation of processing center
  - site = site of processing center
  - country = country of processing center
- [SVC]
  - thresholds = var1, var2, …, varN
  - var1 = threshold of var1
  - …
  - varN = threshold of varN
  - MP = size of macro-pixel
  - percentage = percentage
  - outlier = coefficient to remove outlier (std-dev over mean)
  - CV_range : lambda_min, lambda_max
  - CV = coefficient of variation between lambda_min and lambda_max
- [PREPROCESSING]
  - thresholds = var1, var2, …, varN
  - var1 = threshold of var1
  - …
  - varN = threshold of varN
  - MP = size of macro-pixel
  - percentage = percentage
  - outlier = coefficient to remove outlier (std-dev over mean)
  - CV_range : lambda_min, lambda_max
  - CV = coefficient of variation between lambda_min and lambda_max
- [POSTPROCESSING]
  - thresholds = var1, var2, …, varN
  - var1 = threshold of var1

    - …
    - varN = threshold of varN
    - MP = size of macro-pixel
    - percentage = percentage
    - outlier = coefficient to remove outlier (std-dev over mean)
    - CV_range : lambda_min, lambda_max
    - CV = coefficient of variation between lambda_min and lambda_max
    - max_rrs_diff = maximum allowed absolute difference between in situ and satellite Rrs after individual SVC
    - manual_screening = field1, field2, ….,fieldN
- [sensor1]
    - bands_sat = list of all bands of sensor1
    - level1_flags = list of all Level-1 flags of sensor1
    - level2_flags = list of all Level-2 flags of sensor1
    - ADF_filter = pattern to filter ADF filename of sensor1
    - pre_flags = default flags considered to screen the MDB in pre-processing
    - val_flags = default flags consider to average Rrs at macro-pixel level
    - cal_flags = default flags consider to average the individual gains
    - aer_models =list of aerosol models in the ADF (when relevant) of sensor1
- [senso2]
    - *as sensor1*
    - …

Other configuration files, with same format, are generated by the SW-TOOL. They store the options selected by the user in the GUI to keep perfect traceability on the SVC:

- `preprocessing.cfg`: options of the MDB pre-processing
- `svc_job.cfg`: options of the SVC processing
- `postprocessing.cfg`: options of the gains post-processing

3.1.3 GUI

The GUI is developed with the Python tkinter module, which is the Python wrapper around the standard Tcl/Tk GUI toolkit. The main window contains three tabs, for the three main capabilities, and is opened by default on the SVC tab (Figure 3). These three capabilities are not automatically launched one after another: it is the responsibility of the user to select in the GUI the desired modules.

The various functions in `main.py` related to the GUI only are not further described in this document.

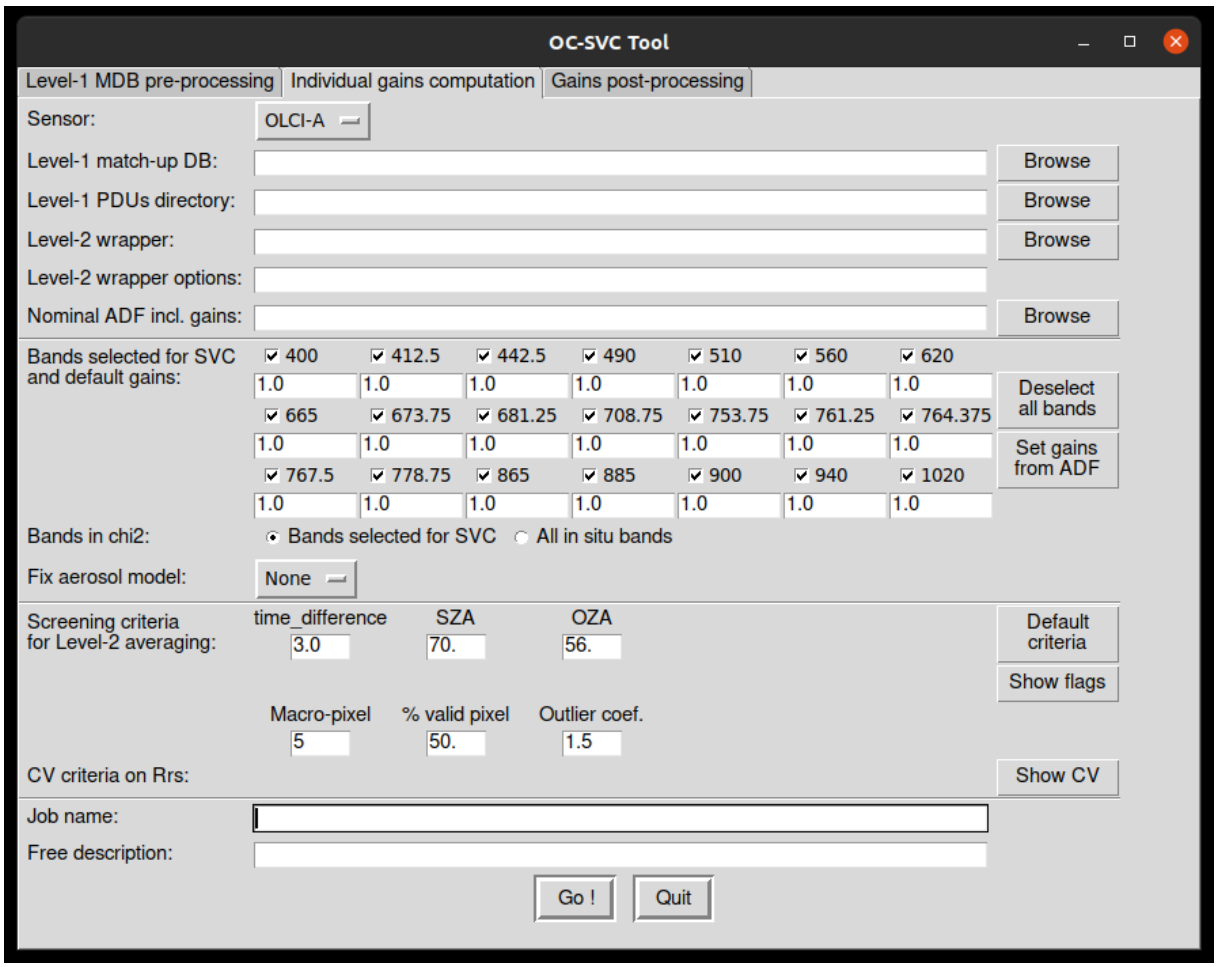

Figure 3 Window of the GUI, opened on the 'Individual gains computation' tab

3.1.4 LEVEL-1 MDB PRE-PROCESSING

The pre-processing tab implements various functionalities that can be used optionally to pre-process the Level-1 MDB before the SVC computation. Screening allows to reduce the MDB to the useful match-ups, hence speed up the SVC processing.

All functions are implemented in the `MDB_util.py` module.

3.1.4.1 SCREENING L1 MDB WITH RESPECT TO L2 DATA

Function `screen_MDB_L1()` - This function requires an existing Level-2 MDB, generated in a consistent manner with the Level-1 MDB (i.e. same in situ data, same orbits, etc.).

3.1.4.2 PRE-PROCESSING FOR NIR SVC

Function `set_zero_rrs_MDB()` - This function adds new fields with insitu_Rrs equal to zero, at bands defined by the user in the GUI. It is used typically for SVC in the NIR, where the native MDB does

not contain any in situ data. Latitude and longitude are also created. If time_difference was missing in the MDB, it is created and set to zero for all match-ups. Hence, the output MDB is fully compatible for being used by the SVC module, as if coming from in situ data.

3.1.5 INDIVIDUAL GAINS COMPUTATION

The functions related to gains computations are implemented in the `main.py` module. The process handles the Level-1 MDB and the corresponding Level-1b PDUs archive stored on the user disk space, both being univocally linked through the PDU filenames registered in the MDB. The black-box Level-2 processor is assumed to process the Level-1 PDUs in their native format (specific to the sensor), while the SW-TOOL deals only in a generic way the MDB (Figure 4).

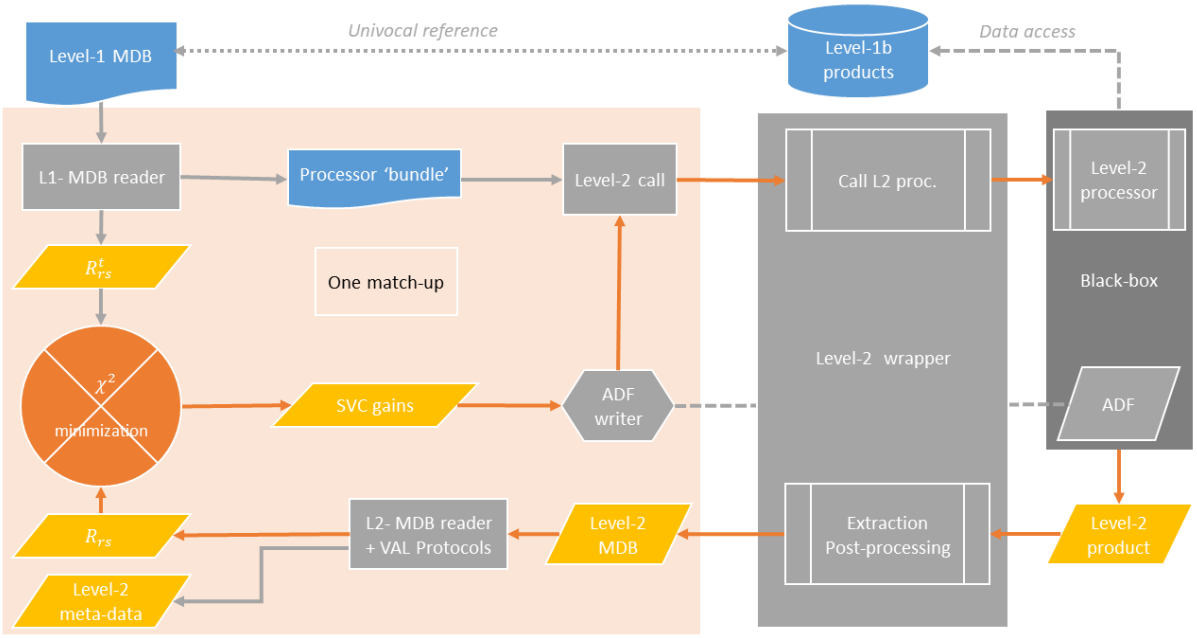

Figure 4 Dataflow for individual gain computation

Function `svc_main()` – This function read the configuration of the SVC job, loop over the Level-1 match-ups for calling `svc_core()` and storing gains in a Level-2 MDB, and finally calls `svc_check()`.

Function `svc_core()` – For a given match-up, this function computes the individual gains as described in section 2.3. The computation of the Jacobian matrix requires various calls to the Level-2 processor, for various set of spectral gains written in dedicated ADFs. This process can be parallelized (see section 3.5.1.5). The linear system is then inversed and provides the gains. Numerical implementation The function calls a last time the Level-2 processor with the individual gains.

Function `svc_check()` - This function compare the in situ and satellite data after individual calibration (scatter plots).

3.1.6 GAINS POST-PROCESSING

Function `post_process()` – This function reads the Level-2 MDB containing individual gains, applies screening criteria, compute mission average gains and produces various plots

3.2 OPERATIONAL ENVIRONMENT

3.2.1 HARDWARE CONFIGURATION

The SW-TOOL runs on Linux environment. It has been tested on various environments, including EUMETSAT Offline Environment, for these distributions: Ubuntu 16.04 LTS, Ubuntu 18.04 LTS and Ubuntu 20.04 LTS.

In term of disk space, the software itself (code) is less than 1MB. On installation about 41 MB is required due the stand-alone Level-2 processor provided as example (the pre-computed Level-2 MDB of this processor) and the git local files for version control.

Importantly, more disk space is required for:

- The Level-1 MDB. Typically, the OLCI Level-1 MDB at MOBY covering 3 years is about 30 MB. The MDB at SPG is about 100 MB.
- The archive of Level-1 PDUs matching the calibration site(s). Depending on the Level-2 processor capability, minifiles can be used to reduce the space.
- The Level-2 processor(s) and associated ADFs. The OLCI ADF containing SVC gains is about 1.4GB, alone. This size may be multiplied by an order of magnitude when SVC is launched in parallel mode, see section 3.2.3 Operational constraints.

3.2.2 SOFTWARE CONFIGURATION

The software requires Python 3 (tested with Python 3.5.2, 3.6.9, 3.7.4 and 3.8.2). Check which Python version is installed by typing:

```
python3 --version
```

Following packages must be installed:

- argparse
- collections
- configparser
- csv
- datetime
- functools
- glob
- locale

- matplotlib (in particular version 3.1.3 and 3.3.0 tested)
- netCDF4 (in particular version 1.2.2 and 1.5.4 tested)
- numpy
- os
- re
- shutil
- subprocess
- sys
- time
- tkinter
- utils

To access to the SW-TOOL, it is recommended to use EUMETSAT Gitlab server. Hence installation of the Git version control system is required (https://git-scm.com/download/linux). On Ubuntu it can be installed by:

```
sudo apt-get install git
```

During the SVC process, the modification of the OLCI ADF also impacts the associated XML manifest. This requires installing the XMLStarlet toolkit (http://xmlstar.sourceforge.net/download.php). For instance on Ubuntu it can be installed by:

```
sudo apt-get install xmlstarlet
```

3.2.3 OPERATIONAL CONSTRAINTS

3.2.3.1 CPU TIME

Pre-processing and post-processing takes a couple of minutes at most. On the other hand, the gain computation can be highly time-consuming, depending on the processing time taken by the Level-2 processor for one PDU. Typically, computing gains at l bands for one-matchup requires launching $2 * (l + 1)$ times the processor. Hence, the capability to process only small tiles around the match-ups is highly recommended to save CPU time.

Copying/modifying/deleting the ADFs generated during the process may also take time depending on their size.

3.2.3.2 DISK SPACE

To save CPU time during the Jacobian matrix computation, an option allows to launch the required $2 * l$ jobs in parallel. In this case, there are potentially $2 * l$ ADFs generated in parallel. User shall make sure to have enough free disk space available. For instance, calibration of 10 bands for OLCI will require about 14 GB to store the ADFs in parallel.

3.2.3.3 DISK ACCESS

The software requires real-time access to the various dataset (MDB, PDUs, ADFs) and real-time call to the Level-2 processor. Interaction between the SW-TOOL and potentially lengthy external commands (Level-2 processor, ADF removing on the disk) are handled with the *subprocess* Python package and its *wait()* function to be sure the commands terminates before further actions start. This implementation has solved problems of synchronisation encountered in complex environment where the software and the Level-2 processor were not installed on the same system.

3.2.4 EXTERNAL DEPENDENCIES

The only algorithmic external dependency of the SW-TOOL relates to the Level-2 processor. This processor must be installed and ready to ingest the Level-1 PDUs referred in the Level-1 MDB and stored on the disks. It is launched as a black box on the Linux system as a subprocess, through a wrapper (executable script) whose predefined input/outputs are described in section 3.4.1.4. Hence all ancillary and auxiliary data required by the processor shall be accessible on the disks and, likely, configured in this dedicated wrapper.

3.3 PRODUCT SPECIFICATION AND INPUT OUTPUT DATA DEFINITION

3.3.1 INPUT DATA

3.3.1.1 LEVEL-1 MATCH-UP DATABASE

The match-up database read by the software shall follow the netCDF format of the MDB files generated by EUMETSAT in its regular Ocean Colour Cal/Val activity (see https://ocdb.eumetsat.int, section Matchups). All required fields by the software should be present by default, as listed in Table 1. The dimensions of the arrays shall also follow EUMETSAT standard convention: *satellite_id*, *insitu_id, rows, columns, satellite_bands.*

Importantly, it should be noted that:

- In the *PDU processing mode* (see section 3.5.1.6), the Level-2 processor does not use any of the MDB satellite variables, since it only handles the real Level-1 PDUs. These MDB variables are however used in the SW-TOOL for screening purpose. On contrary, in *SVC mode*, the processor does not read the PDUs and process the satellite data as stored in the MDB. Hence all physical units may be different as far as they are consistent with what requires the Level-2 processor.
- In *SVC mode*, other fields are probably required by the Level-2 processor (but not the SW-TOOL per se), like the TOA radiance (*satellite_Oaxx_radiance* in OLCI) and possibly other variables (solar flux, etc.). Hence the Level-1 MDB shall include all required satellite inputs to the Level-2 processor.

- For the given calibration site, the fields related to the in situ reflectance (*insitu_Oaxx_Rrs*) shall be limited to the spectral bands effectively measured. There is no use to fill the MDB with a band never measured (doing this can even discard all match-ups, see section 3.5.2.2 about χ^2 computation). On the other hand, a measurement at a given band may be punctually missing, for a given match-up, what will discard only that match-up if that band is used in the SVC process; missing data in the MDB are detected as *not a number* or *masked* data when Python reads the netCDF file.

Table 1 Minimum set of fields required in the Level-1 MDB by the OC-SVC tool. (*) refers to units that can be different as far as there are consistent with what requires the Level-2 processor.

netCDF object	Parameter	Unit	Data Type	Description
Variables	satellite_PDU	none	string	OLCI source PDU name
	insitu_time	second	double	In situ acquisition time, in seconds since 1970-01-01
	time_difference	seconds	double	Absolute time difference between satellite acquisition and in situ acquisition
	insitu_latitude	degree	double	in situ latitude of the calibration site
	insitu_longitude	degree	double	in situ longitude of the calibration site
	insitu_Oaxx_Rrs	sr^{-1}	double	Above water in situ Remote Sensing Reflectance at band xx matching satellite band, corrected for BRDF.
	satellite_time	seconds		Satellite acquisition time, in seconds since 1970-01-01
	satellite_detector_index	none	int	Satellite detector index (can be set to zero if not relevant to the sensor)
	satellite_quality_flags	none	unint	Classification and quality flags
	satellite_humidity	%	double	Relative humidity
	satellite_total_ozone	kg/m^2(*)	double	Total columnar ozone
	satellite_total_columnar_water_vapour	kg/m^2(*)	double	Total column water vapour
	satellite_sea_level_pressure	hPa (*)	double	Mean sea level pressure

netCDF object	Parameter	Unit	Data Type	Description
	satellite_altitude	m (*)	double	DEM corrected altitude
	satellite_horizontal_wind	m/s (*)	double	Horizontal wind vector at 10m altitude
	satellite_OAA	degree	double	Observation (Viewing) Azimuth Angle
	satellite_OZA	degree	double	Observation (Viewing) Zenith Angle
	satellite_SAA	degree	double	Sun Azimuth Angle
	satellite_SZA	degree	double	Sun Zenith Angle
Attributes	site	N/A	string	Calibration site name
	description	N/A	string	Description of the site and MDB
	creation_time	N/A	string	Date of creation of the MDB

The SW-TOOL generates an output database merging the Level-1 input database, the Level-2 data and associated gains generated during the process (see output in section 3.3). This generation assumes that dimensions *satellite_id* and *insitu_id* are placed in the first and last position, respectively (routine `update_MDB_SVC()`). For instance, the dimension of variable *satellite_Oa01_radiance* is *(satellite_id, rows, columns)* and dimension of variable *insitu_Oa01_Rrs* is *(satellite_id, insitu_id)*. Furthermore, the merged MDB contains only once the *dimensions* and *variables* initially present in both the Level-1 and Level-2 match-ups, e.g. dimension *satellite_bands* or variable *satellite_lambda0*. In this case the Level-1 variable is prevailing because it systematically contains more bands. No conflicts were identified in current Level-1 and Level-2 MDBs.

Note: if some attributes are missing in the original MDB, or have a wrong value, this be corrected with the attribute editor of the standard NetCDF Operator (NCO) toolkit (http://nco.sourceforge.net). For instance, adding the site name “MOBY” to the MDB_L1.nc file is done by this command:

```
ncatted -O -a site,global,c,c,MOBY -h MDB_L1.nc
```

To set the minimum valid value -180 to variable satellite_OAA:

```
ncatted -O -a valid_min,satellite_OAA,m,f,-180. -h MDB_L1.nc
```

3.3.1.2 LEVEL-1 PDUS

The Level-1 PDUs can have any format as far as:

i. The Level-2 processor can process this format;
ii. The exact filenames of the PDUs are stored in the Level-1 MDB.

3.3.1.3 ADF

ADF purpose – In the SW-TOOL, SVC gains are supposed to be stored in an ADF read by the Level-2 processor. This is typically the case for the OLCI IPF but other means may exist for other processors, such as invoking gains in command line or defining them directly in a piece of code. Furthermore, another option of the Level-2 processor is the list of aerosol models possibly fixed during the SVC process. **To be generic, the SW-TOOL deals with only one ADF containing the gains and aerosol models, in a format fixed per sensor (not per processor).** It thus the role of the wrapper to make the interface between the ADF used in the SW-TOOL and the inputs required by the processor (see section 3.4.1.4).

ADF format – The filetype of the ADF, fixed once for all per sensor, can be either a single file or a directory containing files, of any format (this has to be defined in function `get_ADF_filetype()` of module `utils.py`). Currently only OLCI-A and OLCI-B are implemented in the low-level routines of the SW-TOOL. For these sensors, the choice was made to keep the nominal ADF format used by the operational Level-2 processor (OLCI IPF), referred to as `OL_2_ACP_AX`. This ADF is in Sentinel-SAFE format, i.e. it is a **directory** containing a netCDF file and an XML manifest. This ADF can be downloaded from EUMETSAT Data Center (https://archive.eumetsat.int).

For the strict purpose of the SW-TOOL, the OLCI netCDF file shall contain these fields, as formatted in the nominal OLCI ADF:

- group: glint_whitecaps
  - variable: gain_vicarious
- group: alternate_AC
  - variable: gain_vicarious_AAC
- group: standard_AC
  - variable: nb_passes
  - variable: aerosols

Note that SVC is conducted only with the `gain_vicarious` variable (OLCI standard AC), and that the other variable `gain_vicarious_AAC` (OLCI alternative AC) simply contains a copy of these gains. Regarding the aerosol fields, they are actually only required when the Level-2 processor handles the list of models and when the user choose to fix one model during the SVC.

Also, the checksum of the netCDF file is computed for any new ADF (new gains) and written in the manifest (`xfdumanifest.xml`) – in particular, this is required by the IPF. For the strict use of the SW-TOOL, the manifest requires at least these metadata:

- /xfdu:XFDU/dataObjectSection/dataObject[@ID="ADFData"]/byteStream/
  - checksum

    - @size
- /xfdu:XFDU/metadataSection/metadataObject[@ID="generalProductInformation"]/metadataWrap/xmlData/sentinel3aux:generalProductInformation/
    - sentinel3aux:fileName
    - sentinel3aux:productSize
    - sentinel3aux:creationTime
- /xfdu:XFDU/metadataSection/metadataObject[@ID="processing"]/metadataWrap/xmlData/sentinel-safe:processing/sentinel-safe:facility/
    - @name
    - @organisation
    - @site
    - @country

ADF content – A *nominal* (or default) ADF containing nominal SVC gains is required to produce nominal Level-2 data. The SW-TOOL uses these gains as a first iteration. For standard AC, we have seen in section 2.4 that the new gains computed in the VIS do not depend on the value of the nominal gains at the same bands. However, they do depend on the nominal gains in the NIR. This is why the procedure for standard AC is to compute gains in the NIR, and then use the resulting ADF as nominal for the SVC in the VIS. For non-standard AC, all gains are spectrally coupled and the choice of the nominal gains can influence the retrieval. **Hence, for any type of AC, user shall be careful on the content of the nominal ADF, i.e. nominal gains are all bands.**

3.3.2 OUTPUT DATA

3.3.2.1 PRE-PROCESSING OUTPUTS

The pre-processing module creates an output directory at the level of the input MDB, named by the user in the GUI (by default pre_processing_*date*T*time*), which contains the new MDB and the options of the user:

- pre_processing_*date*T*time*/
    - preprocessing.cfg
    - *input_MDB*_screened.nc *or input_MDB*_screened_zeroRrs.nc

3.3.2.2 INDIVIDUAL GAIN OUTPUTS

The core module creates an output directory, at the level defined by default by the user in the `ocsvctoolf.cfg` file (*OUT_dir*, see Configuration in section 3.4.1.2), named by the user in the GUI (by default oc_svc_*sensor_date*T*time*). This directory contains the options of the user and two sub-directories, one for the nominal run (gains set to values in the input ADF) and another one after the individual calibration. For each of them, a dedicated MDB contains the Level-1 data, the Level-2 data (for corresponding gains) and the individual gains, per matchups. Scatter plots compare the in situ and satellite Rrs, at all available bands.

The list of outputs is:

- *OUT_dir*/oc_svc_*sensor_date*T*time* /
  - svc_job.cfg
  - nominal_run/
    - MDB_nominal.nc
    - check_nominal_400.png
    - check_nominal_412.png
    - ….
  - svc_run/
    - MDB_svc.nc
    - check_svc_400.png
    - check_svc_412.png
    - ….

3.3.2.3 POST-PROCESSING OUTPUTS

The post-processing module applies to a given SVC job. It thus creates a directory in the same SVC directory, named by the user in the GUI (by default post_processing_*date*T*time*). This directory contains the final mission average gains, in text file and in the ADF format, the MDB processed after application of the averaged gains and various plots of the individual gains versus time and other variables, at all bands (see the OLCI demonstration in section 4 for examples):

- *OUT_dir*/oc_svc_*sensor_date*T*time* /
  - post_processing_*date*T*time*/
    - postprocessing.cfg
    - gains_avg.txt (without MSIQR)
    - gains_avg_MSIQR.txt
    - S3A_OL_2_ACP_AC…..nc/ (or any other relevant ADF for the sensor)
    - MDB_post.nc
    - *site*_individual_gains.png (all individual gains)
    - *site*_mean_gains.png (only mean gains)
    - *site*_RSEM_MSIQR.png
    - *site*_satellite_detector_index_*band*.png
    - *site*_satellite_OZA_*band*.png
    - *site*_satellite_SZA_*band*.png
    - *site*_time-series_*band*.png

Plots of gains versus other parameters can be added in the module `post_processing.py`, by complementing the `x_vars` array with any fields existing in the Level-1 MDB:

```
x_vars = ['satellite_SZA', 'satellite_OZA',
'satellite_detector_index']
```

3.4 INSTALLATION

3.4.1 SET UP AND INITIALISATION

3.4.1.1 DOWNLOAD

The SW-TOOL shall be downloaded from EUMETSAT Gitlab server http://gitlab.eumetsat.int, project OC/External/OC-SVC-TOOL. In a terminal, go to a working directory and clone the Git repository:

```
git clone --depth=1 --branch=dev_solvo
https://gitlab.eumetsat.int/OC/External/oc-svc-tool.git
```

This will create a directory `oc-svc-tool`. Option --depth will only include the up-to-date version of the code, without the history of past commits, and option – branch will checkout the relevant `dev_solvo` branch.

All Python modules and the `ocsvctool.cfg` files are downloaded in the `oc-svc-tool` directory.

3.4.1.2 CONFIGURATION

Edit your default paths and preferences in the `ocsvctoolf.cfg` file:

```
[GLOBAL]
MDB_dir = USER_DEFAULT_DIRECTORY
OUT_dir = USER_DEFAULT_DIRECTORY
ADF_dir = USER_DEFAULT_DIRECTORY
PDU_dir = USER_DEFAULT_DIRECTORY
wrapper_dir = USER_DEFAULT_DIRECTORY
```

Edit also the facility section, that will be used in the metadata of the final ADF containing mission average gains (used at least for OLCI nominal ADF format):

```
[FACILITY]
center = USER_DEFAULT_NAME
name = USER_DEFAULT_NAME
organisation = USER_DEFAULT_NAME
site = USER_DEFAULT_NAME
country = USER_DEFAULT_NAME
```

In the `[SVC]`, `[PREPROCESSING]` and `[POSTPROCESSING]` sections, you can also edit the screening options, which will appear by default in the GUI:

```
thresholds = time_difference,SZA,OZA
time_difference = 3.0
OZA = 60.
SZA = 70.
```

```
MP = 5
percentage = 50.
outlier = 1.5
CV_range = 560, 560
CV = 0.2
```

3.4.1.3 UPDATE OF THE CODE

The latest version of the code can be downloaded with Git. Be sure that you are working on the `dev_solvo` branch:

```
git branch
```

Then in the `oc-svc-tool` directory, pull the recent changes:

```
git pull origin dev_solvo
```

Be careful that the local version of `ocsvctool.cfg` may be overwritten by that on the server. It is thus recommended to back-up the local version with users's preference, e.g. to `ocsvctool.cfg.backup`, and copy it after any code update to `ocsvctool.cfg`. Check if the new version of `ocsvctool.cfg` contains new keys, and in such a case add them to your own configuration file.

3.4.1.4 LEVEL-2 WRAPPER

The SVC module calls the Level-2 processor through a so-called wrapper. The role of the wrapper is to launch through a unique generic command line any Level-2 processor, for any Level-1 product, ADF and region of interest, and get back the Level-2 output.

The wrapper is specific to the Level-2 processor and has to be developed by the user.

The wrapper must be an executable script in Linux, for instance a Python or bash script. To give right to the user to execute the wrapper, type in the terminal:

```
chmod u+x wrapper_executable
```

Check that the shebang of the wrapper really allows to execute the wrapper from command line. For instance for a Python 3 script the shebang could be something like `#!/usr/bin/env python3`, to be adapted to the environment of the user.

Note that the SW-TOOL exports systematically the environment variables which may be necessary by the wrapper when calling the Level-2 processor (e.g. `$HOME`, `$SHELL`, etc.).

Wrapper inputs – The calling sequence must follow this convention:

```
wrapper_executable --ADF ADF_file --PDU PDU_file --lat lat_IS --lon
lon_IS --outdir output_dir [options]
```

where:

- `ADF_file` is the auxiliary data file containing the SVC gains, as used in the SW-TOOL (see section 3.3.1.3); other auxiliary data files required by the Level-2 processor shall be handled directly in the wrapper itself;
- `PDU_file` is the Level-1 PDU to be processed;
- `lat_IS` and `lon_IS` are the latitude and longitude of the calibration site;
- `output_dir` is the output directory where the Level-2 product will be created;
- `options` are a list of optional parameters to be given to the Level-2 processor for user' specific purpose, outside the SW-TOOL specifications.

The in situ coordinates shall ideally be considered inside the wrapper to limit the PDU processing to the strict ROI required by the SVC process.

Wrapper output – The Level-2 output of the wrapper must be a file name `MDB_L2.nc`, formatted into a MDB consistent with EUMETSAT Level-2 MDB in term of format (variables, attributes). The strictly required fields are given in Table 2. Other Level-2 outputs can be added (e.g. chlorophyll, aerosol products…) under the same naming convention `satellite_variable`; since the SW-TOOL will copy all fields of the Level-2 MDB into the merged MDBs (`MDB_nominal.nc`, `MDB_svc.nc`, `MDB_post.nc`), these Level-2 variables can be used for further screening (see screening options in section 3.5.1.8).

Table 2 Content of the MDB_L2.nc to be produced by the Level-2 wrapper

Parameter	Unit	Data Type	Description
satellite_Oaxx_Rrs	sr^{-1}	double	satellite Remote Sensing Reflectance at band xx, corrected for BRDF.
satellite_WQSF	none	unint	Classification flags, quality and science flags for Marine and Inland Waters pixels

3.4.2 VERIFICATION

The verification of the wrapper shall be done first outside the SW-TOOL, by typing its calling sequence in a terminal:

```
wrapper_executable --ADF ADF_file --PDU PDU_file --lat lat_IS --lon lon_IS --outdir output_dir [option]
```

with all parameters being directly specified. Check that the output `MDB_L2.nc` is valid.

Then launch the SW-TOOL with the `main.py` code, e.g. by typing in a terminal:

```
python main.py
```

where python shall point to Python 3. Python will raise error in case of any missing packages on the machine (see section 3.2.2 Software configuration).

For testing in more details the SW-TOOL capabilities without installing an external Level-2 processor, user can follow step by step the Operations manual (section 3.5) by using directly the wrapper provided as example: `wrappers/AC_example/AC_example_wrapper.py`.

3.5 OPERATIONS MANUAL

3.5.1 GENERAL OPERATIONAL PRINCIPLES

3.5.1.1 GETTING STARTED

The software is launched by running the `main.py` Python script. The GUI presents the three tabs on top of the window. Although each tab is totally independent, a classical use follow this sequence: pre-process the Level-1 MDB (Figure 5), then compute individual gains on this MDB (Figure 6), then post-process the gains (Figure 7).

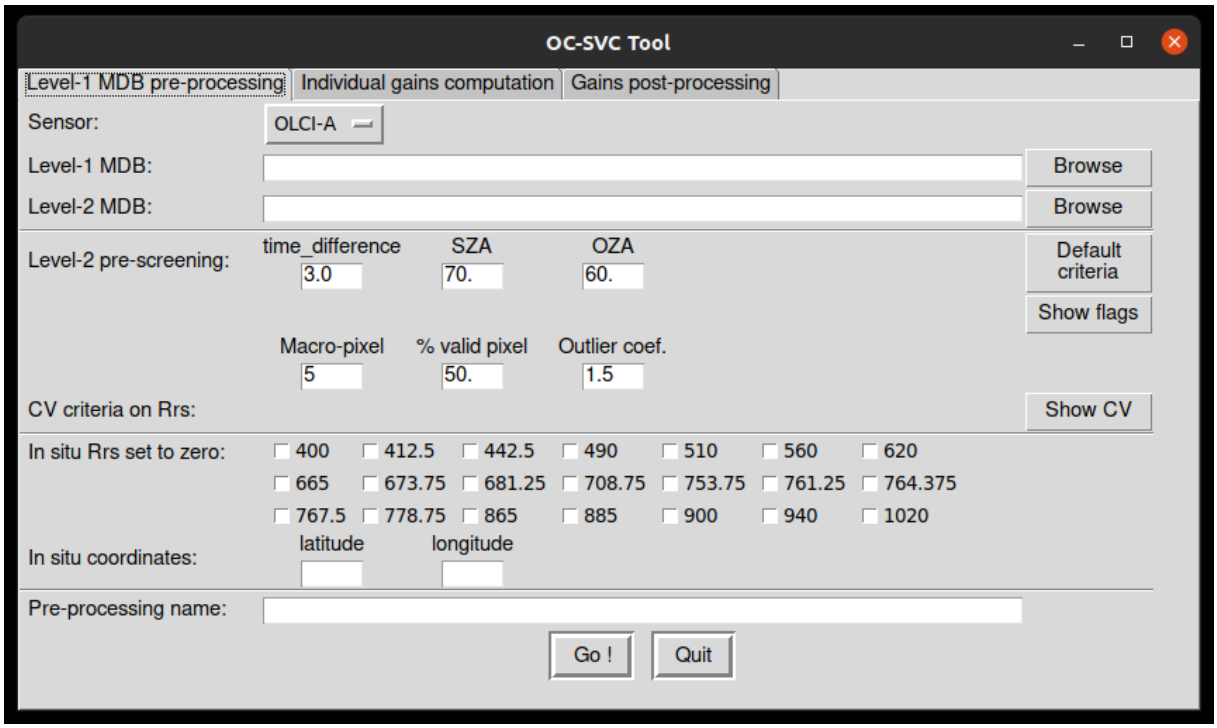

Figure 5 *Level-1 MDB pre-processing* tab of the GUI.

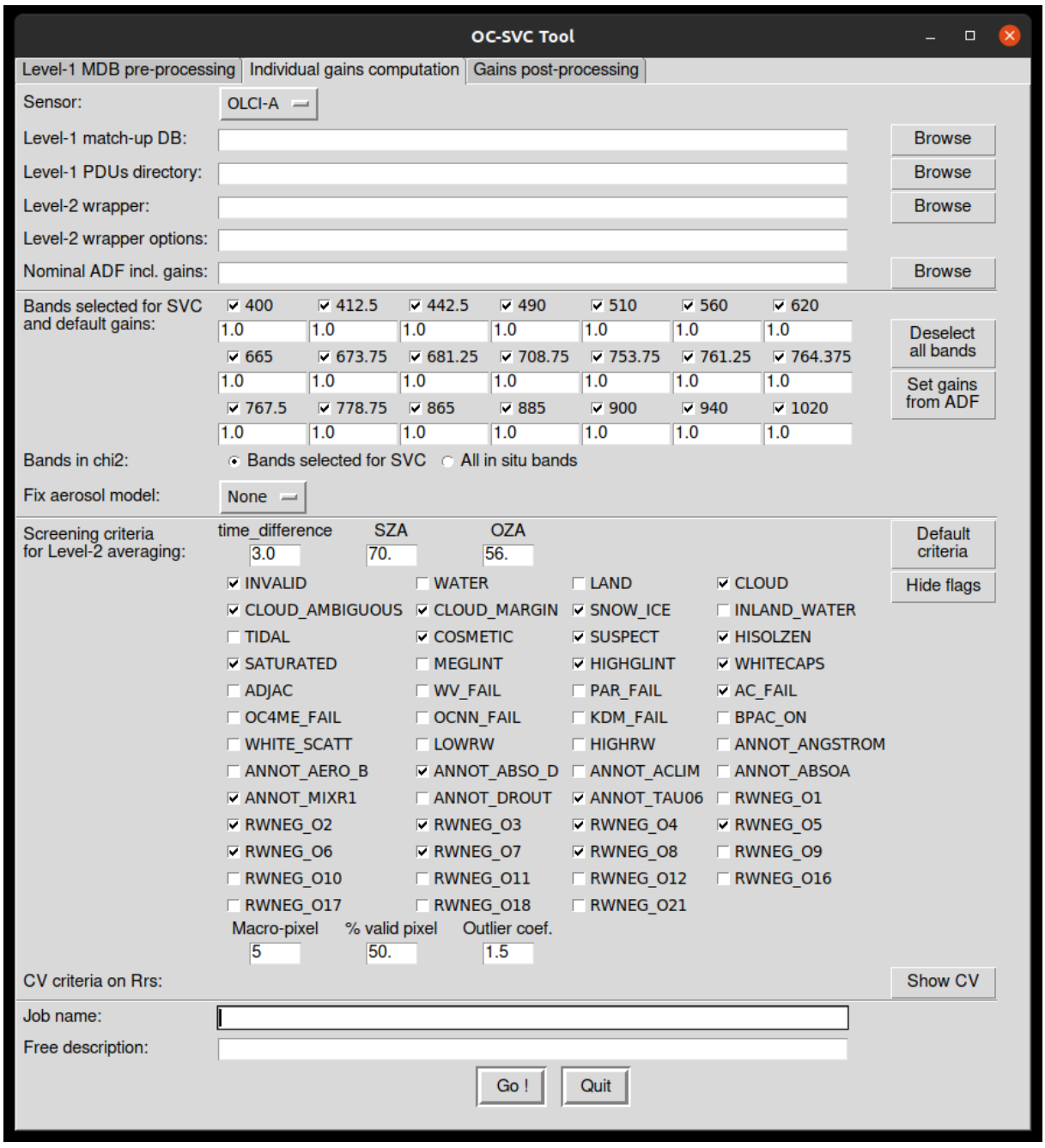

Figure 6 *Individual gains computation* tab of the GUI, with all flags displayed.

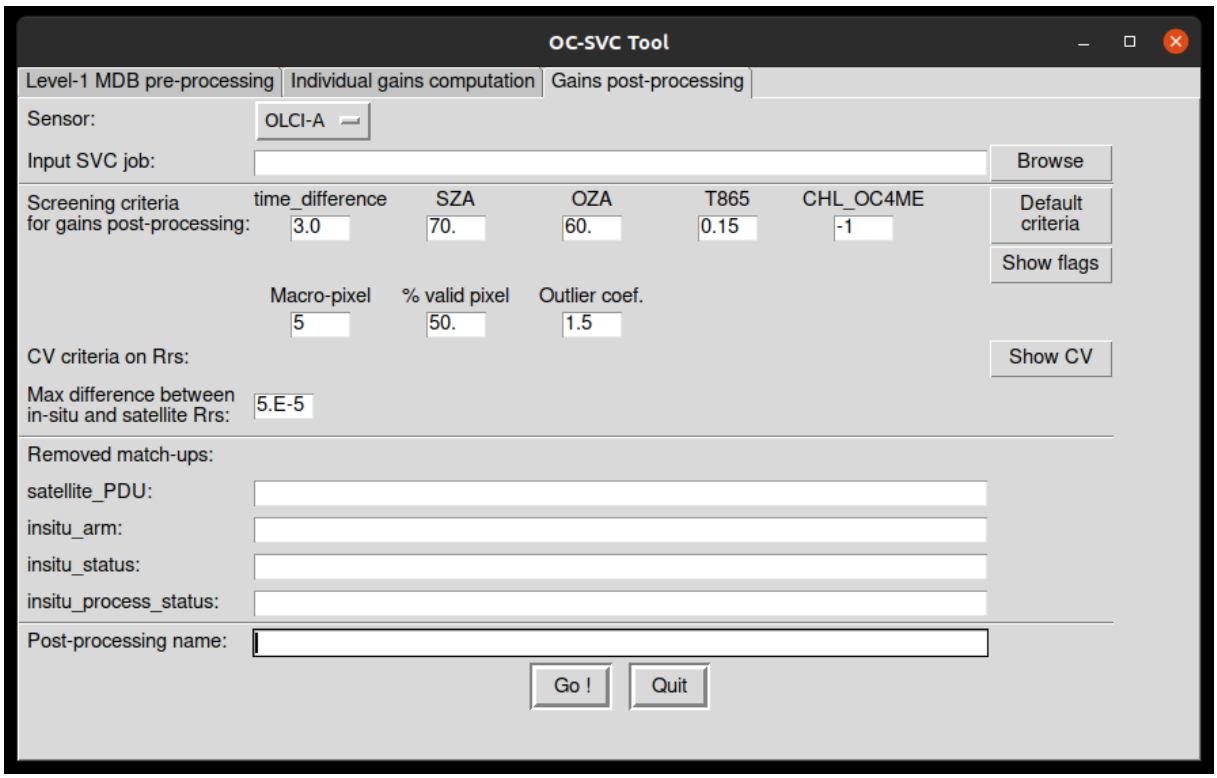

Figure 7 *Gains post-processing* tab of the GUI.

In the various tabs, some options dynamically change with the name of the sensor; for instance, bands, flags, aerosol models in the SVC tab.

To limit the size of the GUI window, some parameters are initially hidden and can be shown by the "*Show …*" buttons:

- Show flags
- Show CV

Clicking the "Go !" button will launch the process.

3.5.1.2 CONFIGURATION FILE

The `ocsvctool.cfg` configuration file is read by the software at each launch. This file can be duplicated and backed-up with other name, for instance to store different default paths on different environments (`[GLOBAL]` section). Some keys of this file refer to variables regularly changed by the user in the SVC process (typically the thresholds and the flags of the screening options), so that the `ocsvctool.cfg` file only contain default values that the user can further modify in the GUI. On the other hand, other options of the SW-TOOL are not expected to change regularly (typically the paths, facility description …) and their variables are only and definitely defined in this configuration file when the software is launched (see exhaustive list in the sections below). It is thus required to quit and relaunch the software any time these keys are changed in `ocsvctool.cfg`.

3.5.1.3 DEBUG PRINTING

Setting `debug = True` completes standard output by few more information about the SVC process (print of in situ and satellite Rrs, before and after SVC).

3.5.1.4 DELETING INDIVIDUAL ADF

Setting `delete_individual_ADF = True` (default option) deletes all ADFs containing individual gains of each match-up. All individual gains are stored in any case in the output file `MDB_svc.nc`. Keeping individual ADFs can be useful for test purpose, to see the impact of individual gains on a scene.

3.5.1.5 PARALLEL PROCESSING

Setting `parallel = True` (default option) computes for each match-up the Jacobian matrix by parallel launch of the Level-2 processor. This is useful when more than one band is calibrated. See section 3.2.3.2 for constraint on disk space.

3.5.1.6 PDU VS CSV PROCESSING MODE

Depending on the capability of the Level-2 processor, the Level-1 data can be ingested in two modes:

- Setting `proc_mode = PDU` (default option) makes the Level-2 processor (wrapper) ingest the Level-1 PDUs in native format, as stored on the disk with filenames recorded in the Level1-MDB.
- Setting `proc_mode = CSV` convert each Level-1 match-ups into temporary CSV files (with semi-colon as delimiter and limited to the macro-pixel chosen by the user) through function `generate_L1_CSV()` in `MDB_util.py` . The CSV file is then processed instead of the native PDU by the Level-2 processor. This option can be useful to save CPU time when the processor beneficiates from such capability. **Importantly, this processing mode ingest directly the Level-1 data stored in the MDB, and does not extract the native Level-1 PDUs. Hence it is the responsibility of the user to be sure that the data in the Level-1 MDB effectively correspond to the Level-1 PDUs on the disk.**

3.5.1.7 LIMIT NUMBER OF MATCH-UPS

The number of match-ups processed in the gain computation can be configured:

- Setting `nmatchup = 0` creates only the output job directory with the job configuration.
- Setting `nmatchup = N` runs the SVC computation over the N first match-ups of the Level-1 MDB (independently of their relevance regarding screening). This can be useful to test on a couple of match-ups a new wrapper or new options.
- Setting `nmatchup = -1` (default options) runs the SVC computation over the full MDB.

3.5.1.8 SCREENING OPTIONS

The list of variables used in the screening criteria of the three tabs (see Figure 5, Figure 6 and Figure 7) are dynamically generated in the GUI from the list `thresholds = …` given in `ocsvctool.cfg`. For instance, the default variables of section `[SVC]` are `thresholds = time_difference,SZA,OZA`, what creates three widgets in the GUI, to screen for fields time_difference, satellite_SZA and satellite_OZA. The screening relies only on **upper thresholds**. Then, for each of these variables, default values for these upper thresholds shall be further given:

- `time_difference = 3.0`
- `OZA = 56`
- `SZA = 70`

User can freely modify the list of **satellite** variables displayed in the GUI for screening, by:

i. Updating the key `thresholds = var1, var2, …`
ii. Adding a default threshold for each variable name, i.e. `var1 = default_threshold1`, `var2 = default_threshold2`, etc.
iii. Checking that the variables `satellite_var1`, `satellite_var2` … do exist in the MDB. Note that only `time_difference` does not include the `satellite_` prefix.
iv. Closing and relaunching the GUI to observe the modified widgets for screening.

In the SW-TOOL, only strictly positive upper thresholds are considered. Setting a threshold to e.g. 0 or -1 amounts to deactivating the screening on the selected variable.

3.5.2 NORMAL OPERATIONS

3.5.2.1 PRE-PROCESSING

MDB screening – The main purpose of the pre-processing module is to screen the Level-1 MDB further used for SVC. User must provide an existing Level-2 MDB, that shall be totally consistent with the Level-1 MDB (i.e. same match-ups). In the context of SVC, this screening is only relevant for Level-2 fields not impacted by the SVC, like classification flags. For OLCI, relevant for flags not impacted by SVC are: INVALID, WATER, LAND, CLOUD, CLOUD_AMBIGUOUS, CLOUD_MARGIN, SNOW_ICE, INLAND_WATER, TIDAL, COSMETIC, SUSPECT, HISOLZEN, SATURATED, MEGLINT, HIGHGLINT, WHITECAPS, ADJAC, WV_FAIL.

MDB completion – Additionally, for NIR SVC pre-processing, user can select bands to set in situ Rrs to zero, and add coordinates of the site. This option typically applies to the original MDB at SPG, which does not contain any in situ measurement; if not existing, the relevant fields are created (insitu_latitude, etc.).

3.5.2.2 INDIVIDUAL GAINS

Case study – Running a SVC job first needs to define the case study, in the first part of the GUI:

- Sensor name, impacting choice of flags, bands, etc.
- Level-1 PDUs directory containing all PDUs in the native format readable by the processor; the SW-TOOL will search recursively in the sub-folders.
- Level-2 wrapper (filepath of the executable script).
- Possibly any complementary options for the Level-2 wrapper, as would be given in command line.
- Nominal ADF containing nominal gains. See section 3.3.1.3 for more description on this ADF. Values of the gains can be modified in the GUI as described hereafter.

Bands for SVC and default gains – User shall first tick the l bands to be vicariously calibrated (we refer to section 2.2 for notation on the dimensionality of the SVC problem). For standard AC, a typical use is to select first the bands in the NIR except one, and then, for another SVC job, the bands in the VIS only (see Demonstration in section 4). Then, user shall specify the values of the nominal gains, **at all n bands**:

- By default, values are taken from the nominal ADF given above.
- User can then modify these gains in the GUI; in this case, a new ADF is created locally and used as the nominal ADF.
- To ease update of the gains with classical values, right button of the widget alternates between "*Set gains from ADF*" and "*Set gains to unity*".

While the computation of gains is generally limited to a subset of $l < n$ bands, it is important to define and check the values of default gains at all n bands, since they all impact the Level-2 processor. For instance, gains in the NIR have to be carefully fixed to some values while computing gains in the VIS.

Bands in χ^2 – This option defines the m bands used in the optimisation problem, as defined in section 2, Eq. (9). Two options are possible:

- Either χ^2 is built upon the same l bands as those chosen for SVC gains (default option). This case is relevant for standard AC, where the SVC optimisation amounts to a square linear problem with l unknown gains and $m = l$ inputs (R_{rs}^t). As demonstrated in section 2, choosing this option for a standard AC makes the SW-TOOL converge towards the standard SVC gains.
- Or all available in situ inputs are considered, whatever the required number of gains ($m \geq l$). This is an overdetermined problem. This case has to be considered for non-standard AC. The SW-TOOL detects automatically all in situ bands from the field names in the MDB.

For both options, the in situ spectrum has to be complete for the selected bands: any missing in situ measurement in this band set (*not a number* or masked data in the MDB) discards the match-ups.

Fix aerosol model – When relevant for the Level-2 processor, user can optionally fix the aerosol model to be used in the AC during the SVC process. This typically applies to SVC in the NIR. The list of all models is given once for all in the `ocsvctool.cfg` file, per sensor. By default, the option is set to

None, meaning that the SVC is launched with models existing in the nominal ADF, without any constraint.

Screening criteria – In the SVC tab, these criteria refer to the way the satellite R_{rs} is averaged and filtered on the macro-pixel, as required in the validation protocols (section 1.3.1). The screening is applied to all data generated during the SVC process: for nominal ADF and for all temporary gains used during the Jacobian matrix computation. If any of these data does not pass the criteria, the match-up is discarded, without any individual gain being computed.

Job name – This is the directory name where the SVC is running (temporary files) and where all outputs are stored, as detailed in section 3.3.2.2.

Free description – This optional free text is written in the bottom-right corner of all images generated during the SVC and its post-processing, to keep track of the user' case study.

Check individual gains – After individual gains have been generated, the user is encouraged to look at the scatter plots showing relevance of the SVC.

3.5.2.3 SVC JOB STOP AND RESTART

For external reasons the SVC job might be accidentally stopped (e.g. failure of the Level-2 processor, disk access problem, etc.) or even the Python process be deliberately interrupted by the user. All match-ups entirely processed, i.e. whose individual gains have been computed, are sequentially stored in the output MDBs:

- *OUT_dir*/job_name/nominal_run/MDB_nominal.nc
- *OUT_dir*/job_name/svc_run/MDB_svc.nc

Hence stopping the SVC job does not cancel the match-ups already processed. Furthermore, the user has the capability to restart the SVC job by relaunching the GUI and giving the **exact job name already existing**. In this case, this will pop up a warning message (Figure 8). **Importantly, restarting an existing job exactly takes the configuration stored in its `svc_job.cfg` file, whatever the options displayed in the GUI.** The SVC is then launched over all match-ups of the input Level-1 MDB not already stored in the output MDBs aforementioned. These MDBs are updated sequentially with the new match-ups passing the screening criteria.

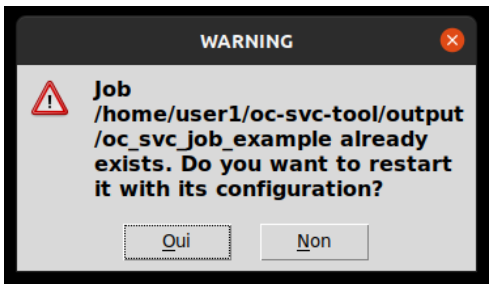

Figure 8. Warning message to restart an existing SVC job.

3.5.2.4 POST-PROCESSING

Case study – User shall first give the sensor and name of the SVC job to be post-processed. This SVC job is identified by its full path directory. Name of the sensor is required to display properly in the GUI the bands and flags; an error message occurs if this sensor does not match the one's of the SVC job.

Screening criteria – This option discards match-ups (hence individual gains) not passing the criteria. Generally, the output `MDB_post.nc` is thus a subset of the `MDB_svc.nc` generated during the SVC job, unless the criteria between the two modules are exactly equal. As a reminder, the list of variables to be considered for thresholding can be tuned in the `ocsvctool.cfg` file, section `[POSTPROCESSING]`, key `thresholds`.

One criterion is specific to the post-processing tab: maximum difference between in situ and satellite Rrs (key `max_rrs_diff` in `ocsvctool.cfg`). This test compares the in situ and satellite Rrs, after the individual SVC. For standard AC, the SVC is expected to make the Level-2 processor exactly match the in situ data; however small differences may exist due to numerical rounding (e.g. digitization of Level-2 data) or non-linearities in non-standard AC. If the difference is higher than the threshold **at any band where gains have been computed** (not full spectrum), the match-up is discarded.

Manual match-up screening – Optionally, user can give manually a list of match-ups to be removed. These match-ups are identified through:

i. Selected variables existing in the MDB. Typically, this can refer to in situ variables. Similarly to the variables used for thresholding, this list is given in the `ocsvctool.cfg` file, section `[POSTPROCESSING]`, key `manual_screening`. The default list provided in the SW-TOOL was made relevant for the MOBY MDB with `manual_screening = satellite_PDU, insitu_arm, insitu_status, insitu_process_status, insitu_Deploy`.
ii. For each of these variables, a list of values manually given in the GUI (comma separated), that shall discard the match-up. Because the manual screening may apply to alphanumeric characters, these values are read by the SW-TOOL as string. **It is the responsibility of the user to check how the variables are stored in the MDB (which types) and whether their conversion in string is correct.** For instance, in the MOBY MDB, the deployment number `insitu_Deploy` is stored as float instead of integer so that removing all match-ups for deployment 261 actually needs to specify in the GUI `insitu_Deploy: 261.0`.

Importantly, the output `MDB_post.nc` contains all match-ups that have passed the criteria, **before the MSIQR statistical filtering**. MSIQR is only seen as a robust final averaging, which indirectly consider all valid data to select the semi-interquartile range.

Post-processing name – This refer to the subdirectory that will be created, inside the directory of the selected SVC job, and containing all post-processing outputs (see section 3.3.2.3).

Visualisation – User can analyse the individual and average gains through the various plots generated in the post-processing directory. In these figures, all individual match-ups passing the post-processing screening are plotted (see for instance a time-series on Figure 13):

- Grey points have passed the criteria but are outside the semi-interquartile range;
- Green points have passed the criteria and are inside the semi-interquartile range, hence used for the final averaging (MSIQR).

Again, the number of match-up displayed in the legend of plots correspond to the total number of valid match-ups, before MSIQR.

3.5.3 ADDING A NEW SENSOR

While most parts of the SW-TOOL are generic, a few low-level routines are required to handle the specific format of the sensor. In the current version, only OLCI-A and OLCI-B are fully implemented. MODIS-Aqua is given in the `ocsvctool.cfg` file only to illustrate the dynamic widgets of the GUI. Adding a new sensor in the SW-TOOL requires the following steps:

1. In file `ocsvctool.cfg`, create a new section with name of the sensor, like `[NEW_SENSOR]`. Then define all keys related to this sensor, i.e.:
    a. `bands_sat`: complete list of Level-1 wavelengths, as existing in the Level-1 MDB and Level-1 PDUs. The exact wavelengths (float numbers) are not used per se in the SVC computation, but are displayed in the GUI and in the post-processing plots and output files. What matters for SVC is to have the proper number of bands in the Level-1 input. As a reminder, bands in the MDB are referred by their index (`Oaxx`).
    b. `level1_flags`: complete list of Level-1 flags names, as defined in the Level-1 MDB.
    c. `level2_flags`: complete list of Level-2 flags names, as defined in the output Level-2 MDB.
    d. `ADF_filter`: pattern to check the correct name of the ADF when selected in the GUI, following the Python conventions on regular expression operations (package *re*, see https://docs.python.org/3/library/re.html).
    e. `pre_flags`: list of flags ticked by default in the pre-processing GUI, among Level-1 and Level-2 flags.
    f. `val_flags`: list of Level-2 flags ticked by default in the SVC computation GUI; as a reminder this refers to the flags used in the macro-pixel averaging, following the validation protocols in ocean colour.

g. `cal_flags`: list of Level-2 flags ticked by default in the post-processing GUI; as a reminder this refers to the flags used to screen the individual gains.
h. `aer_models`: complete list of aerosol models to be listed in the SVC processing GUI, for optional aerosol selection. The list has to match the aerosols effectively implemented in the ADF, either directly by their name or indirectly by their indices.

2. Define the format of the ADF to be used by the SW-TOOL for the sensor. The simplest case is to take the format actually used by the Level-2 processor, but this requires to have both the vicarious gains and aerosol models in it (see requirements on this ADF in section 3.3.1.3). If not possible, any format can be used (e.g. copy OLCI format) and then the wrapper will have to interface between this ADF and the Level-2 processor.
3. Update the various I/O routines impacted by the sensor in module `utils.py`, to handle the product and ADF formats:
   a. `get_ADF_filetype()`: define the filetype of the ADF, either a file or a directory.
   b. `set_ADF_name()`: define the name of the output ADF, from options of the SVC job. By default the same name as input ADF is kept; for OLCI, the name includes date and time of generation, processing center.
   c. `read_SVC_gain()`: read vicarious gains in the ADF.
   d. `write_SVC_gain()`: write vicarious gains in the ADF.
   e. `fix_aer_model()`: deactivate all aerosol models except one in the ADF; the selected aerosol is identified by its index starting from zero in the list `aer_models` of the configuration file.
   f. `get_PDU_L1_pattern()`: from the name of a Level-1 PDU stored in the Level-1 MDB, return the unambiguous pattern of the corresponding PDU that can be found on the disk. Differences may come due to the date of generation of the PDUs.
   g. `get_PDU_L2_pattern()`: from the name of a Level-1 PDU stored in the Level-1 MDB, return the unambiguous pattern of the corresponding Level-2 PDU stored in the Level-2 MDB (required for the pre-processing).

3.5.4 ERROR CONDITIONS

Standard outputs of the SW-TOOL are redirected to stdout, while error and warning messages are redirected to stderr. Most of the I/O sequences are controlled (missing file, invalid data, etc.). However, in case some would not be checked, the SW-TOOL may crash with a Python error such as RuntimeError.

3.6 RECOVERY OPERATIONS

Since the software is delivered in source code, any alteration or loss can be repaired by reinstalling the software from scratch (see section 3.4.1 Set up and initialisation).

4 DEMONSTRATION AND EVALUATION

4.1 DIAGNOSTIC DATASET

4.1.1 DATASET RELEVANT FOR SVC IN THE NIR

Gains in the NIR are computed over the South Pacific Gyre (SPG). OLCI data in Full Resolution are extracted over 15x15 pixels around the central point (-27°N, -134° E). This constitutes the raw MDB provided by EUMETAST. The MDB is further pre-processed by the SW-TOOL to add the targeted R_{rs}^{t}, set to zero at 708.75, 753.75, 778.75, 865, 885 and 1020 nm, add artificial time difference of zero, and screen the match-ups upon these criteria:

- Macro-pixel size: 5x5
- Percentage of valid pixel: 100%
- Thresholds: SZA < 70°, OZA < 56°.
- Flags to be rejected: INVALID, CLOUD, CLOUD_AMBIGUOUS, CLOUD_MARGIN, SNOW_ICE, COSMETIC, SUSPECT, HISOLZEN, SATURATED, HIGHGLINT, WHITECAPS

The other filtering (CV on R_{rs}) are de-activated since SVC is not yet computed.

4.1.2 DATASET RELEVANT FOR SVC IN THE VIS

Gains in the VIS are computed at the MOBY site (Clark et al., 2003). The MOBY measurements gathered in EUMETSAT in situ database have been completely reviewed at this occasion. Hyperspectral data provided by the MOBY team (https://www.star.nesdis.noaa.gov/socd/moby/filtered_spec) have been spectrally integrated over OLCI-A and OLCI-B spectral response functions (SRF). Various sets of measurements exist, depending on:

- The combined arms used to propagate the marine radiance at sea surface (top, middle, bottom).
- The modelling of the depth propagation, based either on direct measurement of diffuse attenuation at the two depths or the model of Voss et al. (2017) accounting for Raman scattering. This latter only affects the radiance after 575 nm.

The various possibilities are given in Table 3. A prioritization logic has been implemented to select a single measurement per acquisition in the EUMETSAT database:

Lw21 > Lw22 > Lw1 > Lw2

Hence, Lw7 and Lw27 are never used. In practice, as can be seen on Figure 9, most of the data relevant for the OLCI-A and OLCI-B timeframe correspond to measurement Lw21; measurements Lw22 exist for deployments M261 and M267, without any obvious difference with the other measurements, and are kept in order to keep as much possible the seasonal pattern and, for M267, extend overlap between OLCI-A and OLCI-B. The average in situ reflectance shown in Figure 9 in the blue is actually slightly

different over the OLCI-A and OLCI-B match-ups, due to the data acquired before Sentinel-3B launch in April 2018 (higher in situ reflectance in 2017). This is a limitation of the current in situ database, lacking in particular data of the M265 deployments due to MOBY issues.

Table 3 Sets of MOBY radiometric measurements

Arms / Propagation	Top-middle	Top-Bottom	Middle-Bottom
Measured Kl	Lw1	Lw2	Lw7
Modeled Kl	Lw21	Lw22	*not provided*

The MOBY status, which is a combination of data inspection, including consistency check of the diffuse attenuation coefficients at various arms, is most of the time “Good”, and “Questionable” data have been kept for same reasons as Lw22. Clearly, a trade-off is made between the ideal quality of in situ data and the number of match-ups required to get meaningful mission-average SVC gains.

Regarding calibration, only MOBY data reprocessed with post-deployment calibration are considered.

MOBY MDB with OLCI is then pre-processed by the SW-TOOL to screen match-ups upon these criteria:

- Macro-pixel size: 5x5
- Percentage of valid pixel: 50%
- Thresholds: time difference < 3 hours, SZA < 70°, OZA < 56°.
- Flags to be rejected: INVALID, CLOUD, CLOUD_AMBIGUOUS, CLOUD_MARGIN, SNOW_ICE, COSMETIC, SUSPECT, HISOLZEN, SATURATED, HIGHGLINT, WHITECAPS

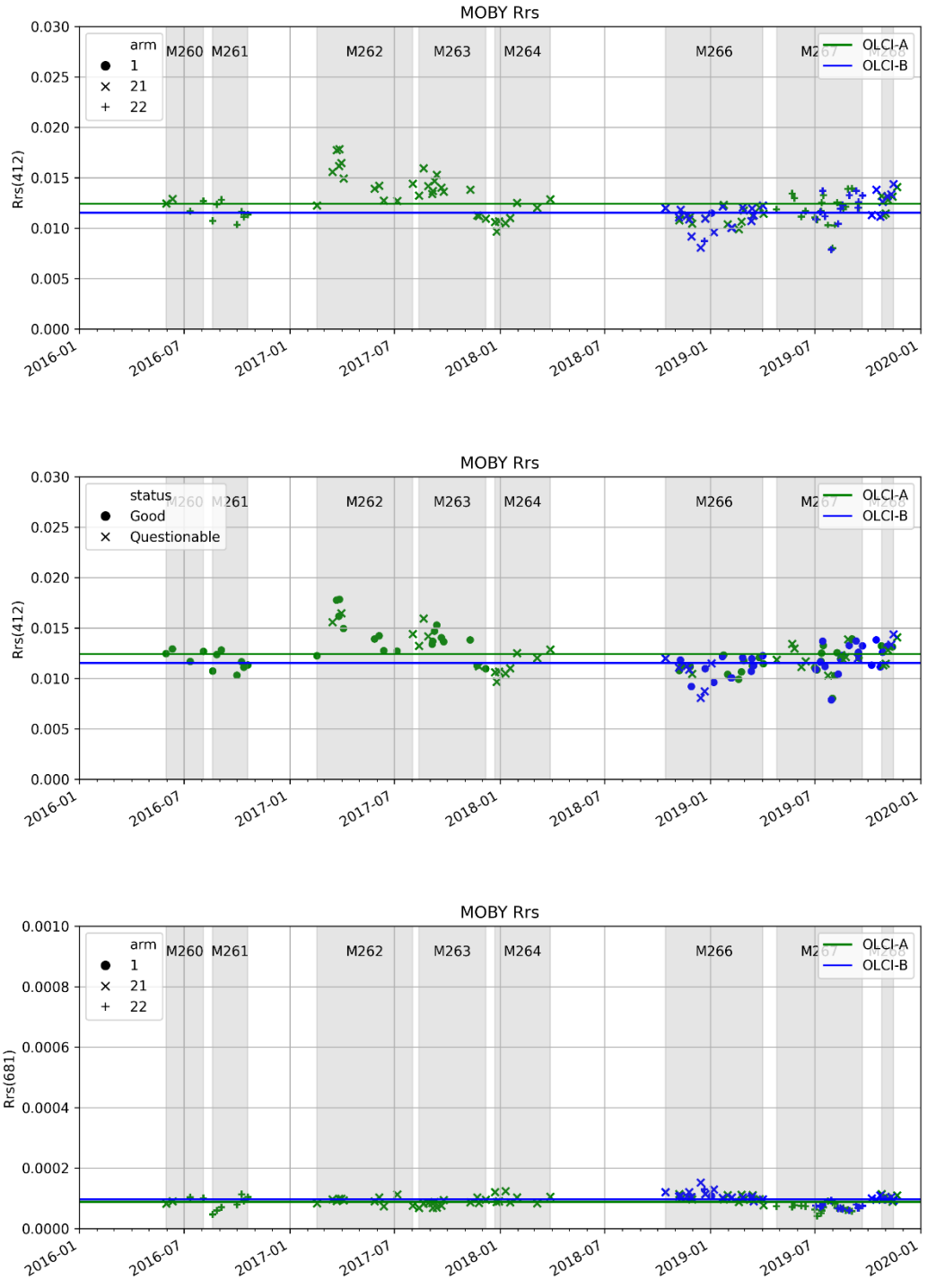

Figure 9 Time-series of in situ MOBY Rrs at 412 nm (top and middle) and 681 nm (bottom) matching OLCI-A (green) and OLCI-B (blue) acquisitions. Deployments are given on top of the shaded areas. Ticks refer to either depth propagation (top and bottom) or status (middle), as given in the top-left corner. Horizontal lines are the temporal average of in-situ data over the match-ups, for each sensor. Data are limited to match-ups effectively selected in the SVC gain post-processing.

4.1.3 DATASET FOR SVC EVALUATION

The MDB for SVC evaluation is that available at EUMETSAT for the routine validation of S3A and S3B. This MDB consists of in situ data at various AERONET-OC sites matched-up with satellite remote sensing reflectance from Sentinel-3A and Sentinel-3B, both with BRDF correction applied. From the available matchups, a selection of the best considered matchups has been done, following the recommendations given by EUMETSAT documents on protocols (EUM/SEN3/DOC/19/1092968):

- Time difference between in situ and satellite overpass has been reduced to $\pm$ 3 hours.
- The spatial window for extraction has been on the 5 x5 central pixels of the initial 25 x 25 macropixel.
- The filtering criteria has followed the established protocols for flag and outlier filtering.
- The matchups statistics extracted are:
    - Mean Absolute Difference (MAD) to investigate dispersion and Mean Difference (MD) to investigate bias for each band.
    - Mean Absolute Percentage Difference (MAPD) to investigate dispersion and Mean Percentage Difference (MPD) to investigate bias.
    - SAM (Spectral Angle Mapper) or χ2 can be calculated along visible and NIR wavelengths.

4.2 OLCI IPF CONFIGURATION FOR SVC

4.2.1 NIR GAINS

The purpose of the NIR SVC is to calibrate bands used by the CWAC for the aerosol detection, under three assumptions:

1. The marine signal in the NIR is zero: $R_{rs}^{t}(\lambda) = 0$ or equivalently $\rho_w(\lambda) = 0$, for $\lambda \geq 708.75$. This is achieved over the SPG oligotrophic site;
2. The gain of the farthest band used by the CWAC is known, here g(865);
3. The aerosol model is fixed.

These assumptions totally determine the path reflectance, $\rho_{path}(\lambda)$, by application of the full AC, which for OLCI IPF is made by BPC + CWAC. The input of the CWAC at 779 and 865 nm is impacted by the residual signal found by BPC, $t\rho_{wC2}$; with an aerosol model fixed, $\rho_{path}(779)$ is not used as input of the CWAC and BPC impacts only 865 nm:

$$\rho_{path}(865) = g(865) * \rho_{gc}(865) - t\rho_{wC2}(865) \quad (18)$$

For all other bands, $\rho_{path}(\lambda)$ is deduced by the AOT computed at 865 nm and the fixed aerosol model. Then ρ_w is computed at all bands by the CWAC by:

$$\rho_w(\lambda) = \frac{g(\lambda) * \rho_{gc}(\lambda) - \rho_{path}(\lambda)}{t(\lambda)} \quad (19)$$

The NIR gain $g(\lambda)$ are such that $\rho_w(\lambda)$ should be zero for $\lambda \geq 708.75$. The analytic solution is

$$g(\lambda) = \frac{\rho_{path}(\lambda)}{\rho_{gc}(\lambda)} \quad (20)$$

This solution is theoretically found by our generic SVC formulation by making Eq. (19) converge to zero (in fact, Eq. (15) expressed in term of R_{rs}). Because the NIR marine reflectance provided by the IPF in the Level-2 products is by default that from BPC, $\rho_{wC2}(\lambda)$, it is important to access $\rho_w(\lambda)$ as if it would be effectively computed by the CWAC, i.e. by Eq. (19). This is achieved by an option of the IPF (`--RHOW_NIR_CWAC`). If not, the SVC procedure may not work since BPC is a non-linear inversion over six bands and SVC gains may never make $\rho_{wC2}(\lambda)$ strictly converge to zero.

Further to option `--RHOW_NIR_CWAC`, activating or not of the BPC has an impact on the NIR gains. NASA choice is to deactivate the NIR-VIS iteration (whose purpose is similar to BPC) and thus compute each gain in the NIR independently, band per band. The same choice has been made here, by using the IPF option `--BPC_OFF`, to avoid a spectrally-coupled problem and solve the SVC optimisation in an exact manner. Deactivating BPC amounts to have $t\rho_{wC2}(865) = 0$ in Eq. (18), and thus $\rho_w(865) = 0$ from Eq. (19), whatever the calibration at 865 nm. This can be seen on Figure 10 and Figure 11 of next sections for OLCI-A, and similarly Figure 27 and Figure 28 for OLCI-B.

The values of the fixed gain at 865 nm was chosen on the best knowledge of the Level-1 calibration performance, and the consistency between OLCI-A and OLCI-B. The NIR band is supposed to be perfectly calibrated for OLCI-B. The value for OLCI-A is based on the Level-1 intercomparison of the two sensors done by Lamquin et al. (2020) during the tandem phase of Sentinel-3A and 3B (from 6 June to 16 October 2018). The average inter-calibration coefficient between B and A at 865 nm over all detectors and cameras is about -1.375% (their Figure 16), what translates into a SVC gain of 0.986 for OLCI-A, under the assumption of unit gain for OLCI-B.

Individual NIR gains are generated with following configuration:

- The Level-1 MDB is that at SPG, pre-processed to have zero insitu Rrs at the six bands below.
- The Level-2 wrapper shall launch the OLCI IPF configured to provide marine reflectance in the NIR from the CWAC and deactivate BPC (option `--RHOW_NIR_CWAC --BPC_OFF`).
- SVC gains are computed at following bands: 708.75, 753.75, 778.75, 885, 1020 nm.
- Default gains are set to unity at all bands, except g(865) = 0.986 for OLCI-A.
- Bands in the chi2 are the bands selected for SVC.
- The aerosol model is fixed to MAR-90.
- Screening criteria in the Rrs averaging per match-up are those from S3VT Validation Protocols, except that flags impacted by the aerosol detection in the NIR are not considered (i.e. AC_FAIL, ANNOT_TAU06, ANNOT_MIXR1 raised when fixing an aerosol model, ANNOT_ABSO_D although it cannot be raised with MAR-90, and all RWNEG from RWNEG_O2 to RWNEG_O8):
    - Thresholds: time difference < 3 hours, SZA < 70°, OZA < 56°.

- Flags to be rejected: CLOUD, CLOUD_AMBIGUOUS, CLOUD_MARGIN, INVALID, COSMETIC, SATURATED, SUSPECT, HISOLZEN, HIGHGLINT, SNOW_ICE, WHITECAPS
- Macro-pixel size: 5x5
- Percentage of valid pixel: 100%
- Outlier coefficient: 1.5
- CV criteria at 560 nm: 0.2

The post-processing to compute average NIR gains applies the EUMETSAT criteria for SVC, except that CHL is not considered because VIS gains are not applied yet, CV criteria is slightly relaxed, ANNOT_MIXR1 is not considered at SPG, RWNEG as well for similar reasons as previously and MEGLINT is added:

- T865 < 0.15
- Macro-pixel size: 5x5
- Percentage of valid pixel: 100%
- Outlier coefficient: 1.5
- CV from bands Oa02 to Oa06 < 0.2
- Flags to be rejected are: CLOUD, CLOUD_AMBIGUOUS, CLOUD_MARGIN, INVALID, COSMETIC, SATURATED, SUSPECT, HISOLZEN, MEGLINT, HIGHGLINT, SNOW_ICE, WHITECAPS, ANNOT_ABSO_D, ANNOT_TAU06

Note that AC_FAIL is not included here, cf. EUMETSAT SVC protocols.

4.2.2 VIS GAINS

Individual VIS gains are generated with following configuration

- The Level-1 MDB is that at MOBY.
- The Level-2 wrapper shall launch the OLCI IPF in standard mode.
- SVC gains are computed at following bands in the VIS: 400, 412.5, 442.5, 490, 510, 560, 620, 665, 673.75, 681.25 nm.
- Default gains are set to unity at all bands in the VIS (note this has no impact, as demonstrated in section 2.4), and to the average value computed by SVC in the NIR for the 6 NIR bands (see Table 4 and Table 6 for OLCI-A and OLCI-B, respectively).
- Bands in the chi2 are the bands selected for SVC.
- No aerosol model fixed.
- Screening criteria in the Rrs averaging per match-up are those from S3VT Validation Protocols, except that RWNEG is not considered (reflectance at MOBY can be slightly negative before SVC in the red bands, and won't be negative in the blue bands):
  - Thresholds: time difference < 3 hours, SZA < 70°, OZA < 56°.
  - Flags to be rejected: CLOUD, CLOUD_AMBIGUOUS, CLOUD_MARGIN, INVALID, COSMETIC, SATURATED, SUSPECT, HISOLZEN, HIGHGLINT, SNOW_ICE, AC_FAIL, WHITECAPS, ANNOT_ABSO_D, ANNOT_MIXR1, ANNOT_TAU06

- Macro-pixel size: 5x5
- Percentage of valid pixel: 100%
- Outlier coefficient: 1.5
- CV criteria at 560 nm: 0.2

The post-processing to compute average VIS gains applies these criteria:

- CHL_OC4ME < 0.2 mg/m3
- T865 < 0.15
- CV from bands Oa02 to Oa06 < 0.15
- Flags to be rejected are: CLOUD, CLOUD_AMBIGUOUS, CLOUD_MARGIN, INVALID, COSMETIC, SATURATED, SUSPECT, HISOLZEN, MEGLINT, HIGHGLINT, SNOW_ICE, WHITECAPS, ANNOT_ABSO_D, ANNOT_MIXR1, ANNOT_TAU06

4.3 OLCI-A GAINS

4.3.1 GAINS IN THE NIR

The comparison between the targeted R_{rs}^{t} (fixed to zero) and satellite R_{rs} in the NIR is shown on Figure 10 and Figure 11 for respectively the default gains (unity except 0.986 at 865 nm) and the computed gains per match-up. A nearly perfect retrieval is achieved after applying the individual gains, considering the very low level of the signal (see scale on the figures). Possibly the digitization of the marine reflectance by the IPF in the Level-2 products induces some small errors in the Jacobian matrix computation, visible when the signal is very small such as at 1020 nm at SPG.

The averaged NIR gains (Table 4 and Figure 12) show a nearly flat shape from 709 to 885 nm of about -1.4% adjustment, and about -9% at 1020 nm, consistent with the known overbrightness of the Level-1 OLCI-A radiometry. On 55 good match-ups (27 for the MSIQR) acquired in about 3 years, the gains present an excellent temporal stability (Figure 13 and Figure 14) and no trend with respect to the geometry or detectors is observed either (Figure 15 to Figure 17).

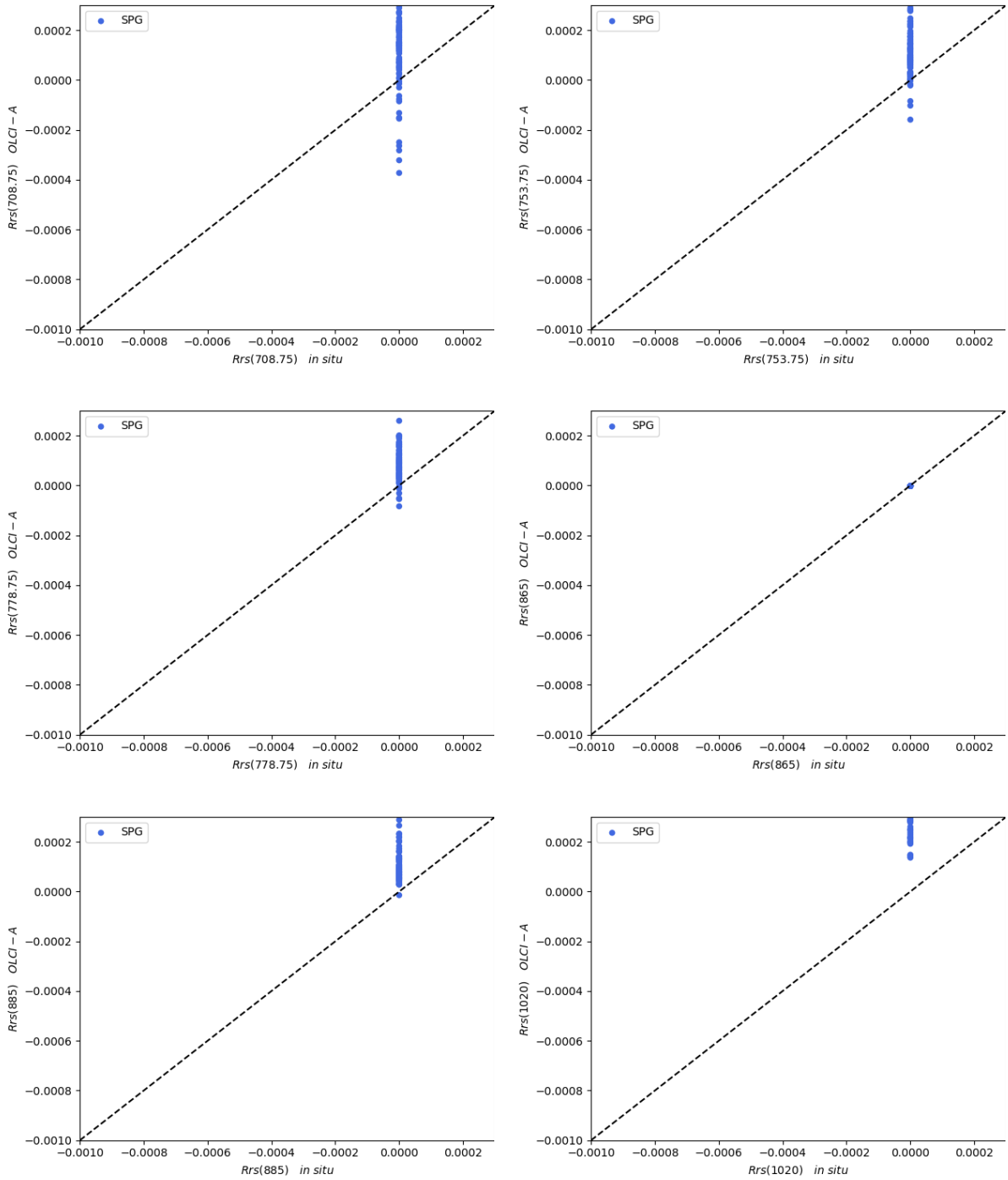

Figure 10 Validation of OLCI-A R_{rs} at SPG with nominal gains (see text) at 708.75, 753.75, 778.75, 865, 885 and 1020 nm.

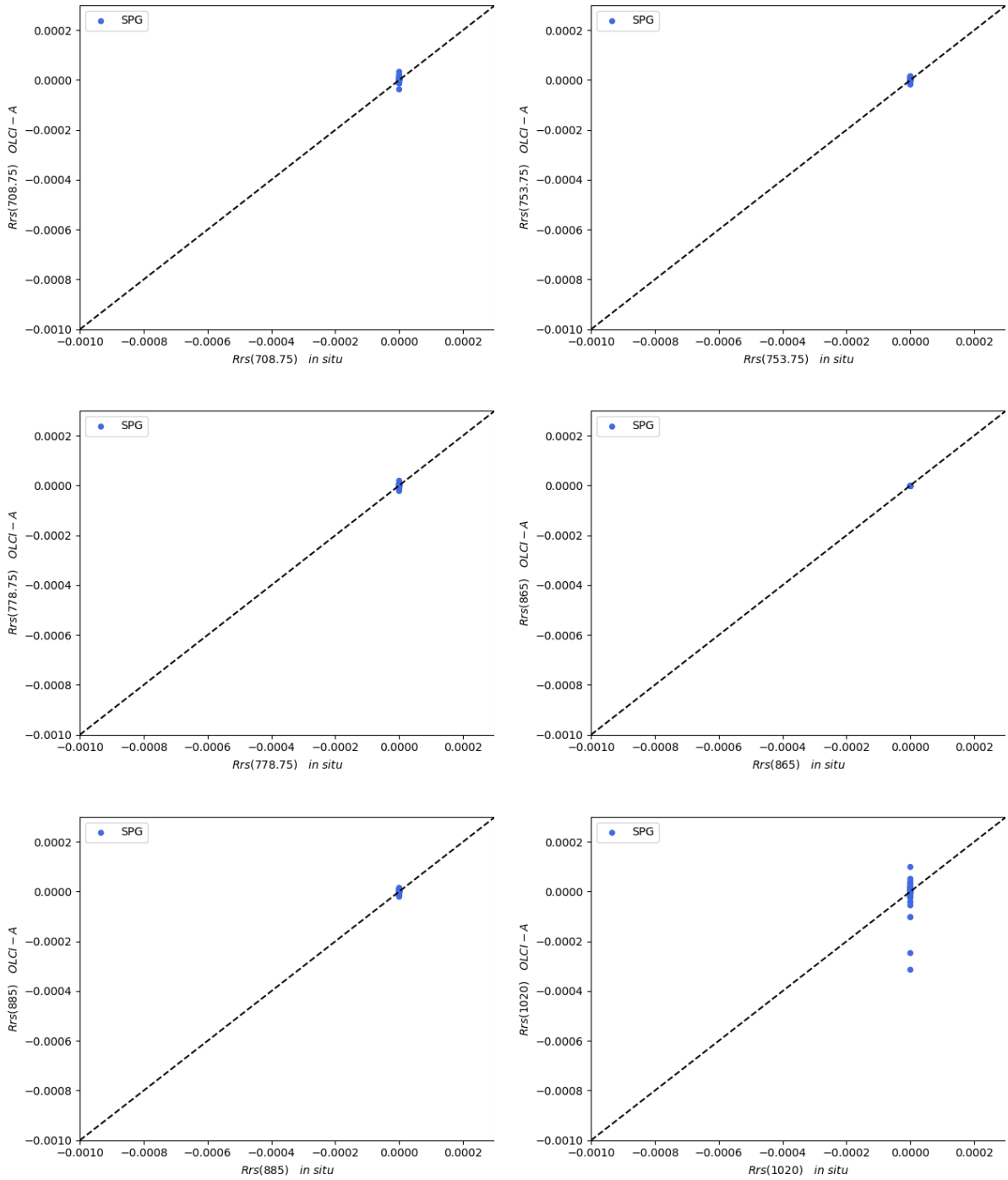

Figure 11 Validation of OLCI-A R_{rs} at SPG after calibration by individual gains (see text) at 708.75, 753.75, 778.75, 865, 885 and 1020 nm.

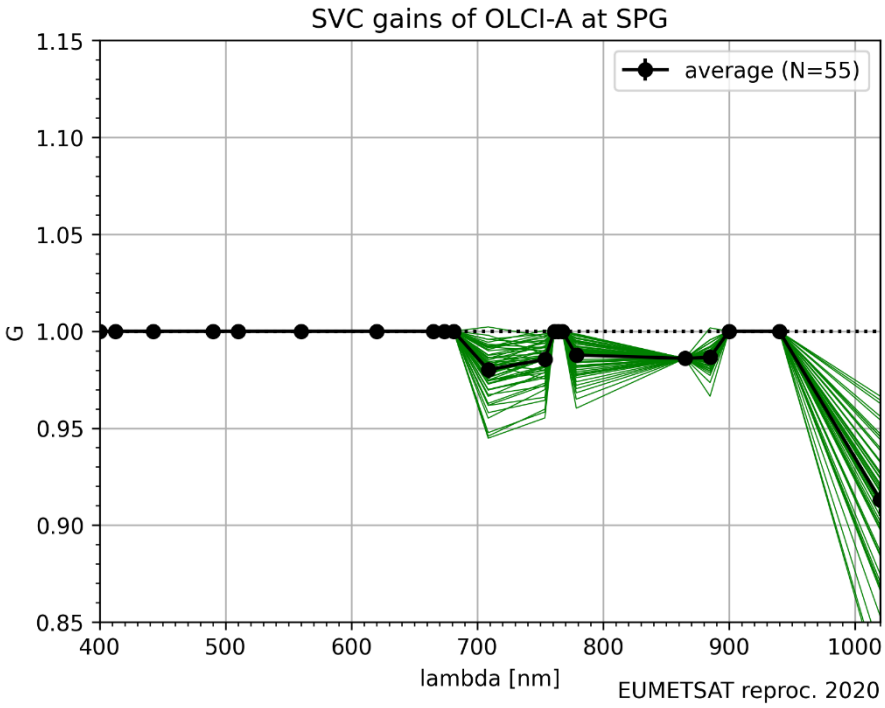

Figure 12 Individual spectral gains of OLCI-A at SPG, before MSIQR screening.

Table 4 Statistics of OLCI-A averaged gains at SPG, after MSIQR filtering

Wavelength	Number	Average gain	Standard-deviation
708.75	27	0.980135	0.004555
753.75	27	0.985516	0.003723
778.75	27	0.987718	0.00352
865		0.986	
885	27	0.986569	0.00176
1020	27	0.913161	0.008537

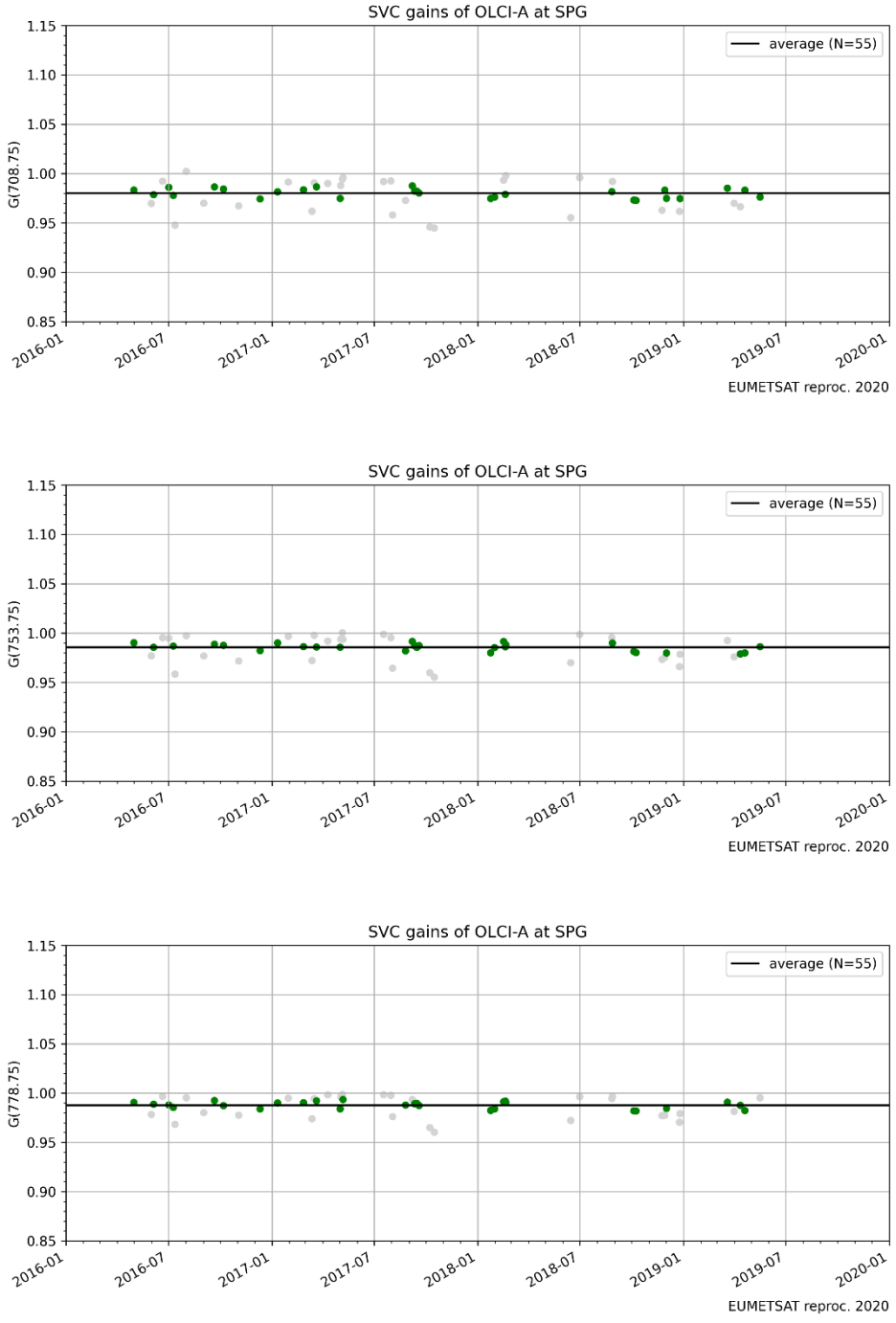

Figure 13 Time-series of OLCI-A gains at SPG at 708.75, 753.75 and 778.75 nm. Gains in green fall within the semi-interquartile range used in final averaging.

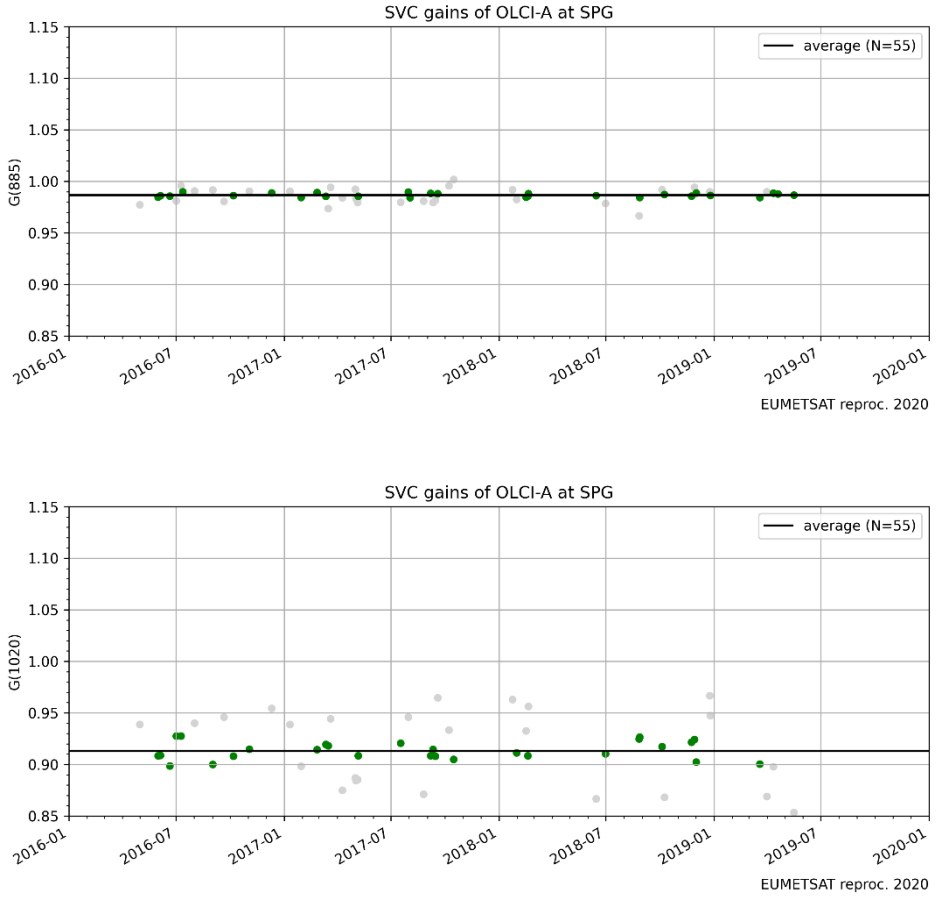

Figure 14 Time-series of OLCI-A gains at SPG at 885 and 1020 nm. Gains in green fall within the semi-interquartile range used in final averaging.

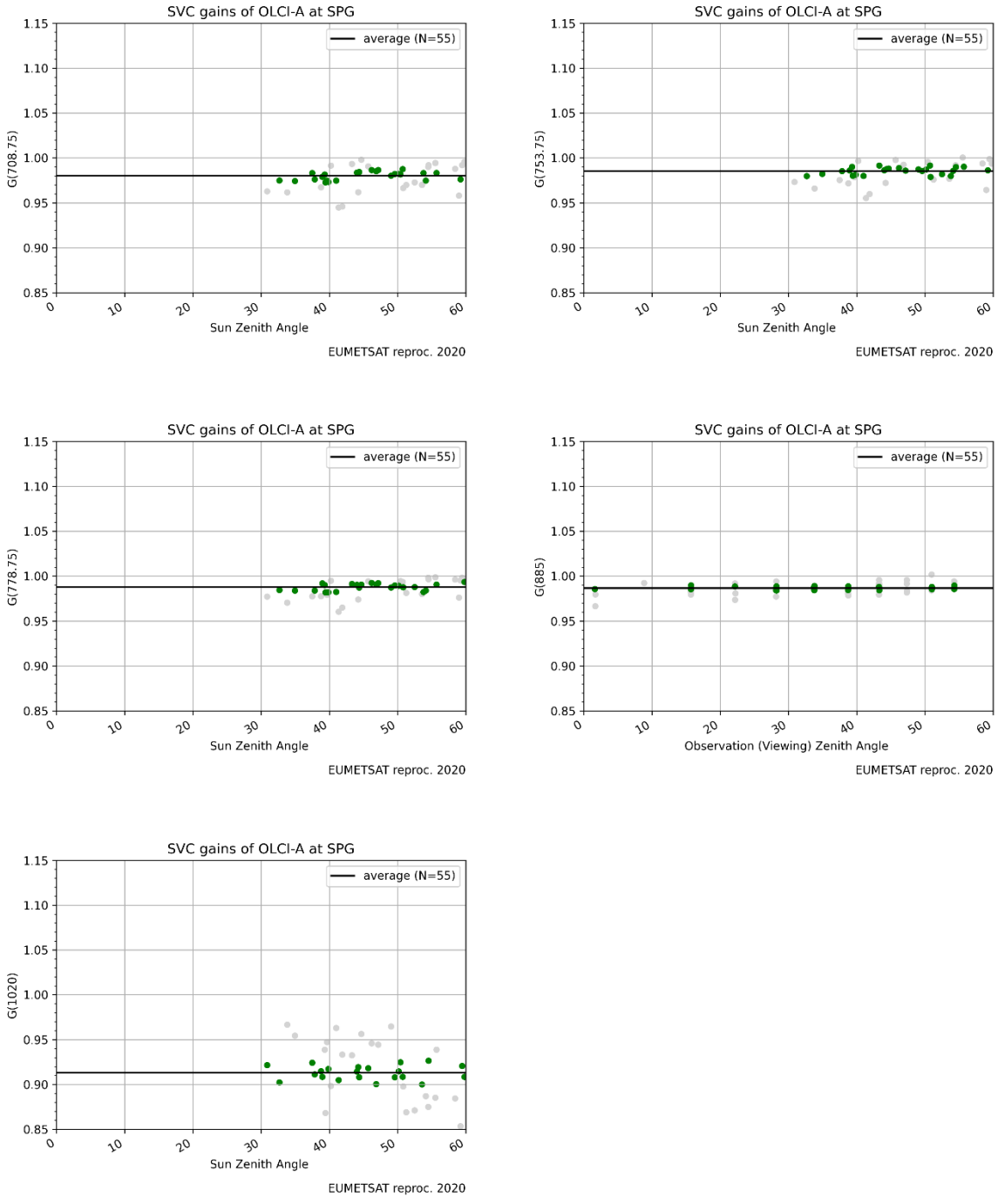

Figure 15 OLCI-A gains at SPG at 708.75, 753.75, 778.75, 885 and 1020 nm as a function of sun zenith angle. Gains in green fall within the semi-interquartile range used in final averaging.

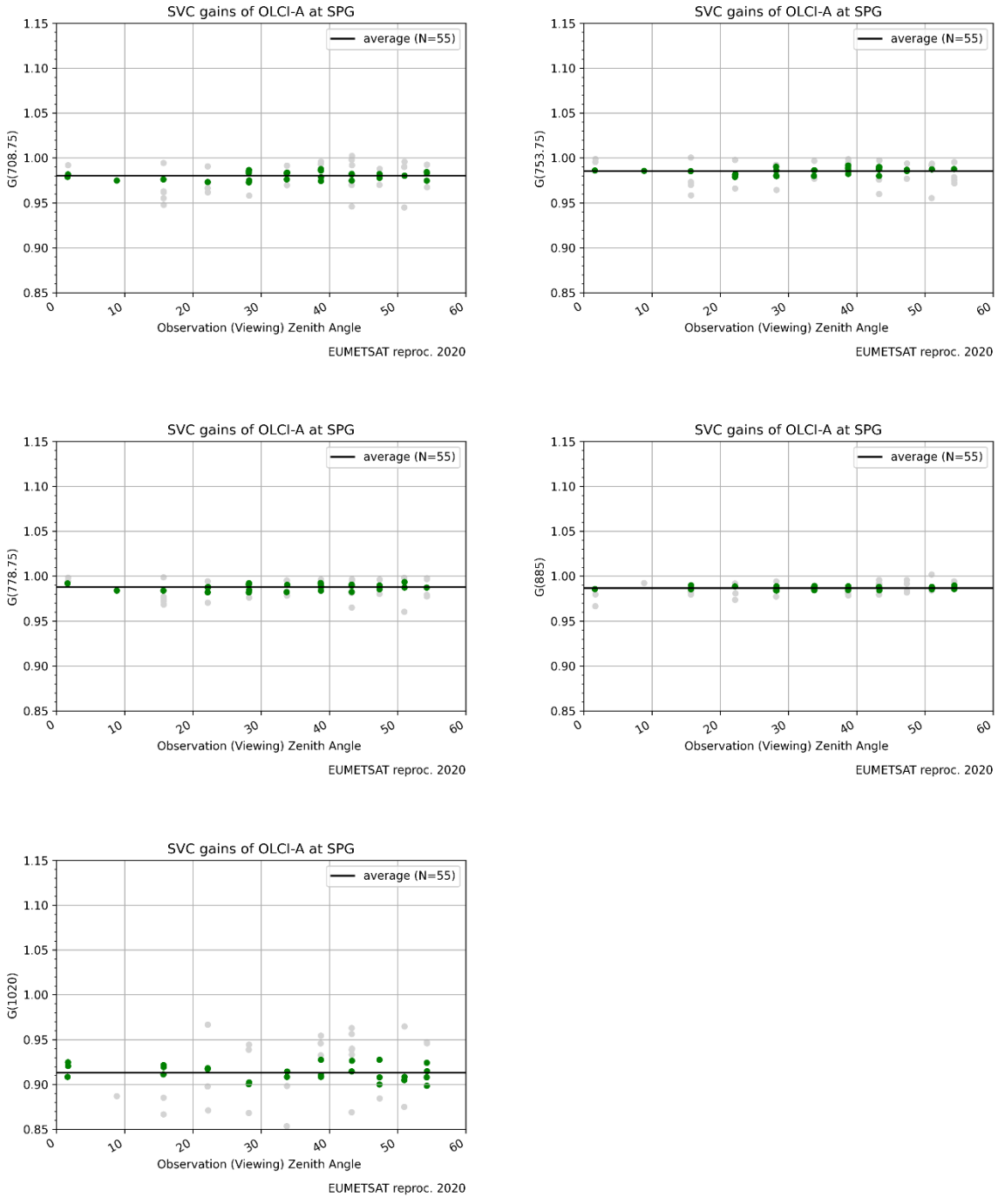

Figure 16 OLCI-A gains at SPG at 708.75, 753.75, 778.75, 885 and 1020 nm as a function of view zenith angle. Gains in green fall within the semi-interquartile range used in final averaging.

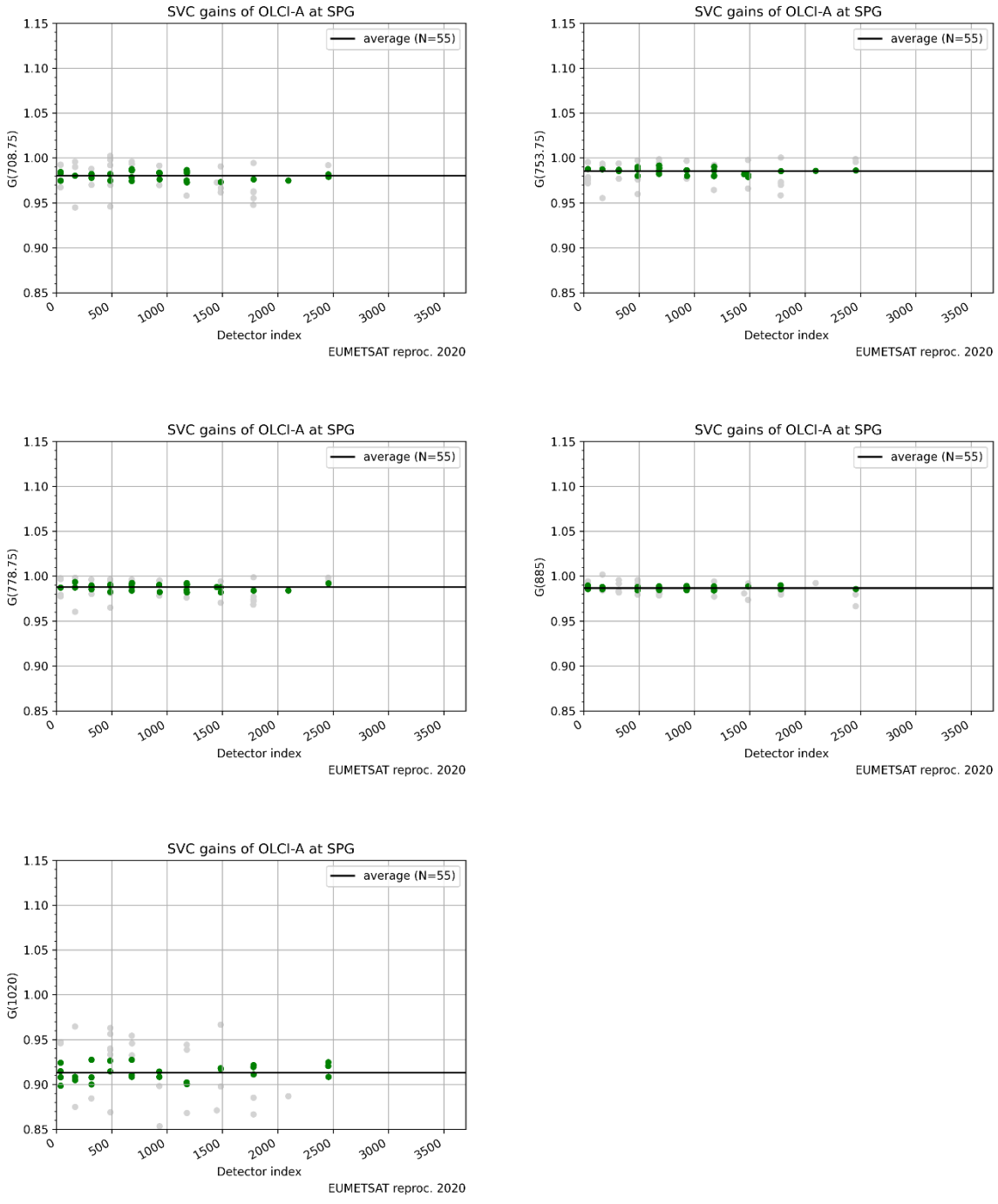

Figure 17 OLCI-A gains at SPG at 708.75, 753.75, 778.75, 885 and 1020 nm as a function of detector index. Gains in green fall within the semi-interquartile range used in final averaging.

4.3.2 GAINS IN THE VIS

The comparison between the MOBY R_{rs}^{t} and satellite R_{rs} in the VIS is shown on Figure 18 and Figure 19 for respectively the default gains (unit gain in the VIS, new gains in the NIR) and the computed VIS gains per match-up. This demonstrates the relevance of the individual gains.

The averaged gains (Table 5 and Figure 20) decreases slightly from the NIR to the green band, and stabilises in the blue, over an amplitude of about -2.5% which is consistent with the known performance of OLCI-A Level-1 calibration. Temporal stability seems very good at all bands (Figure 21 to Figure 23), with variation in the blue bands likely linked to the seasonal variation of the actual in situ measurement at this bands where the signal is the strongest (see Figure 9, top, at 412 nm). Gains in the VIS are robust to geometry and detectors (Figure 24 to Figure 26). Values of RSEM, scalded over a decade (Table 5) reach closely the requirements, being as low as 0.05% in the blue and nearly 0.025% at 560 nm; they decrease in the red toward 0.01%, however without reaching the target of 0.005% that seems unachievable over clear waters (see Zibordi et al., 2015).

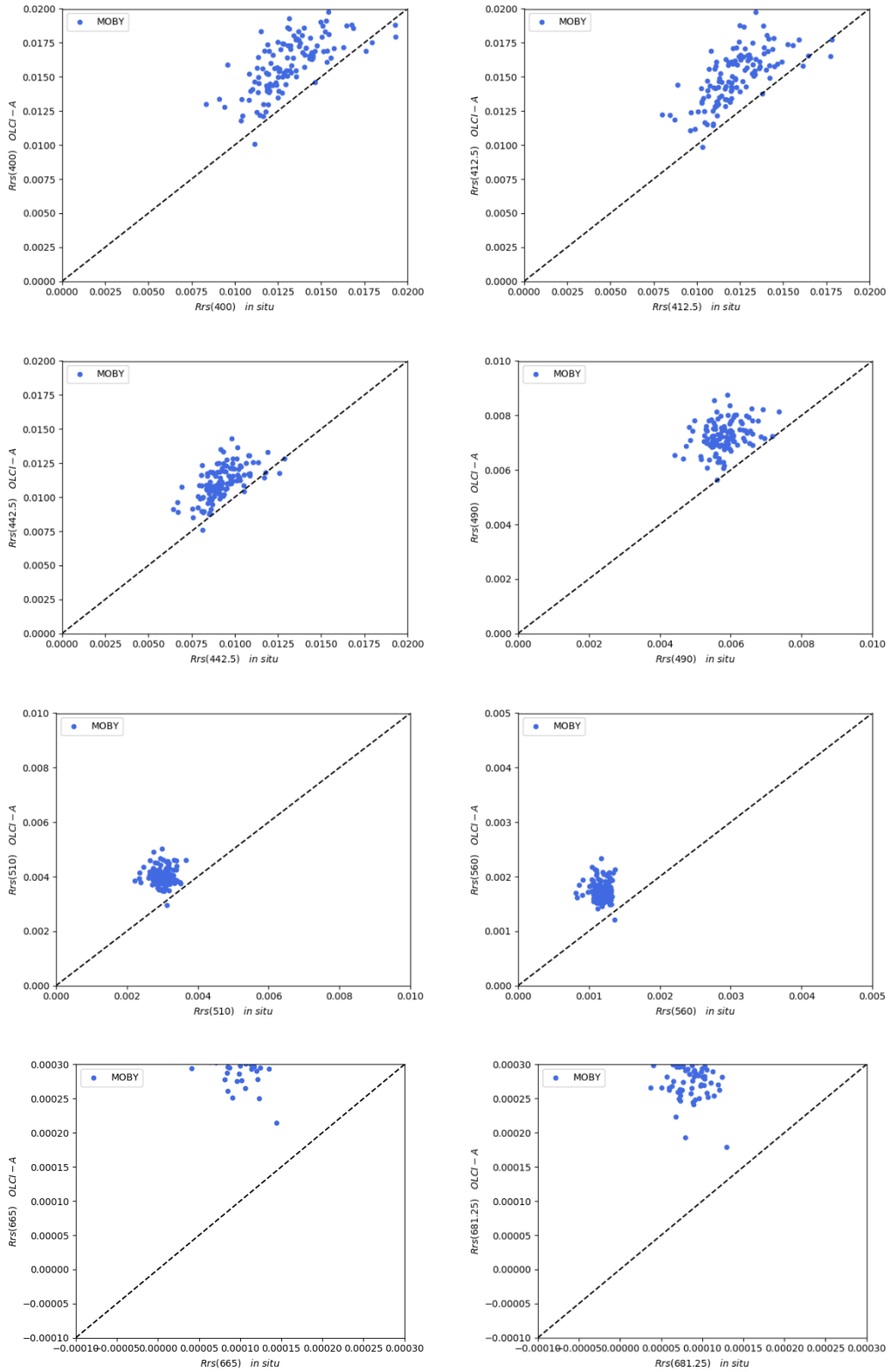

Figure 18 Validation of OLCI-A R_{rs} at MOBY with nominal gains (see text) at 400, 412.5, 442.5, 490, 510, 560, 665 and 681.25 nm.

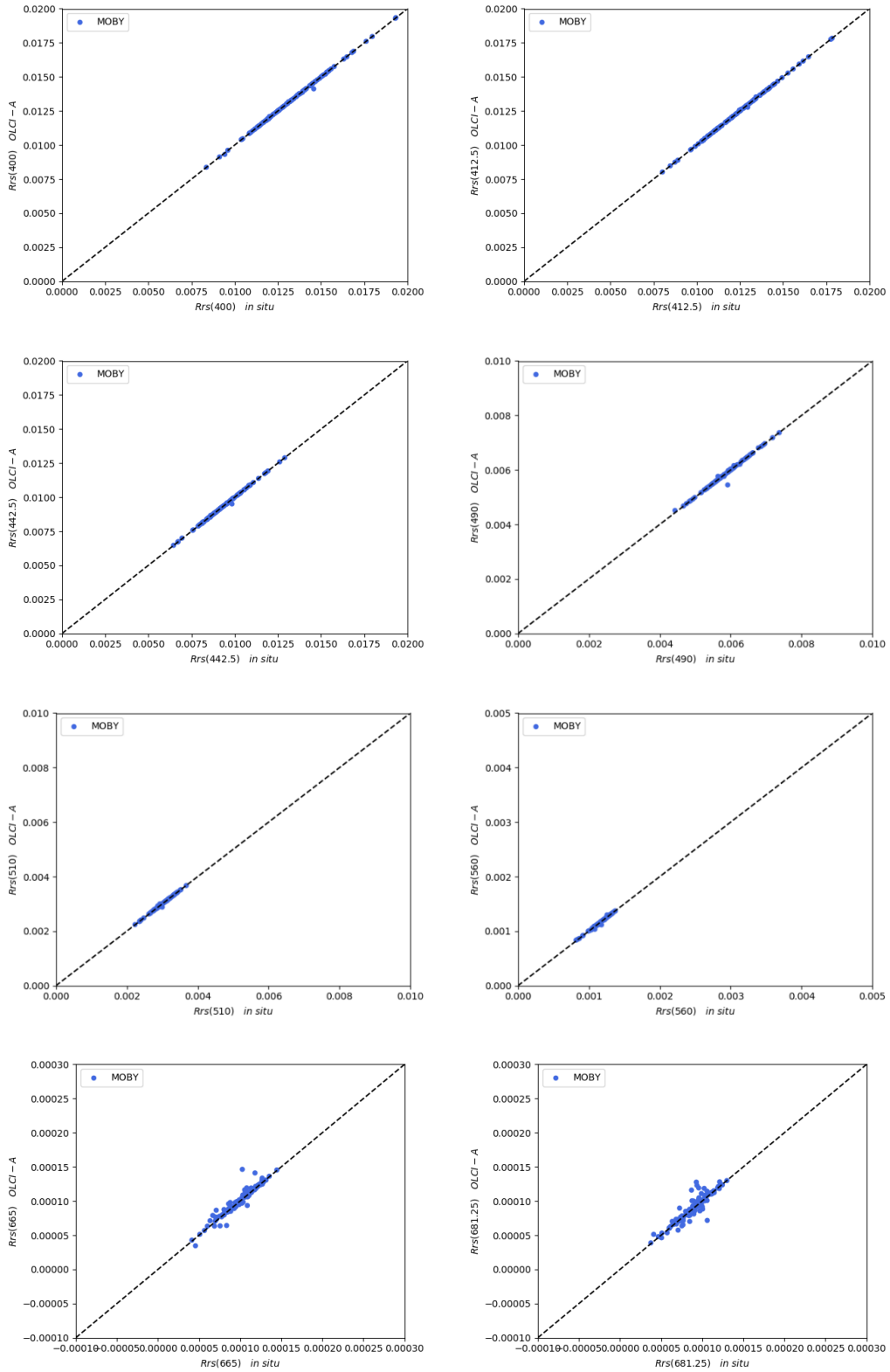

Figure 19 Validation of OLCI-A R_{rs} at MOBY after calibration by individual gains (see text) at 400, 412.5, 442.5, 490, 510, 560, 665 and 681.25 nm.

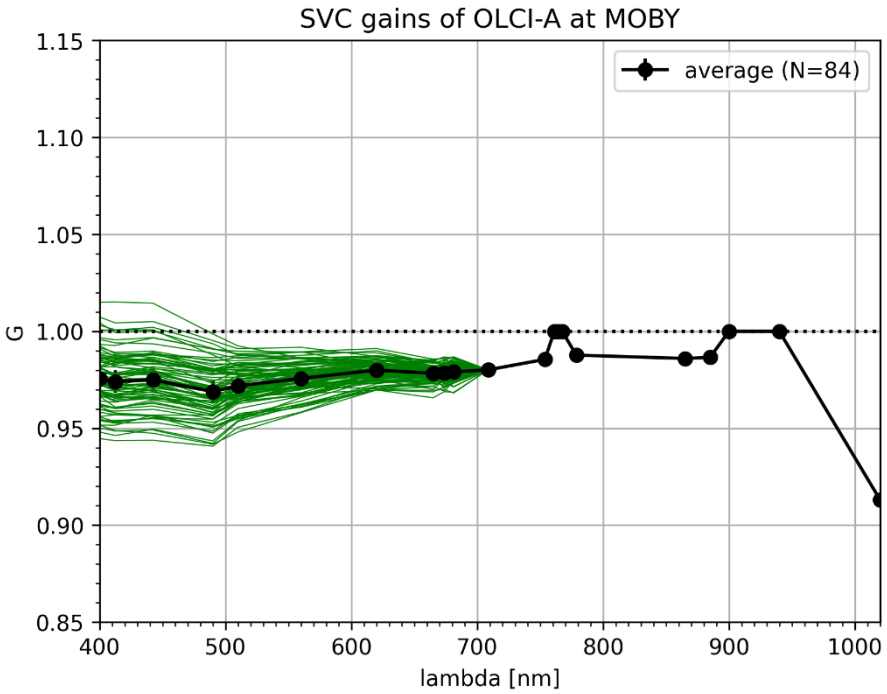

Figure 20 Individual spectral gains of OLCI-A at MOBY, before MSIQR screening.

Table 5 Statistics of OLCI-A averaged gains at MOBY, after MSIQR filtering

Wavelength	Number	Average gain	Standard-deviation	RSEM [%]
400	42	0.975458	0.005544	0.0517
412.5	42	0.974061	0.005897	0.0551
442.5	42	0.974919	0.005435	0.0507
490	42	0.968897	0.005645	0.053
510	42	0.971844	0.004139	0.0388
560	42	0.975705	0.003086	0.0288
620	42	0.980013	0.002107	0.0196
665	42	0.978339	0.001412	0.0131
673.75	42	0.978597	0.002128	0.0198
681.25	42	0.979083	0.001504	0.014

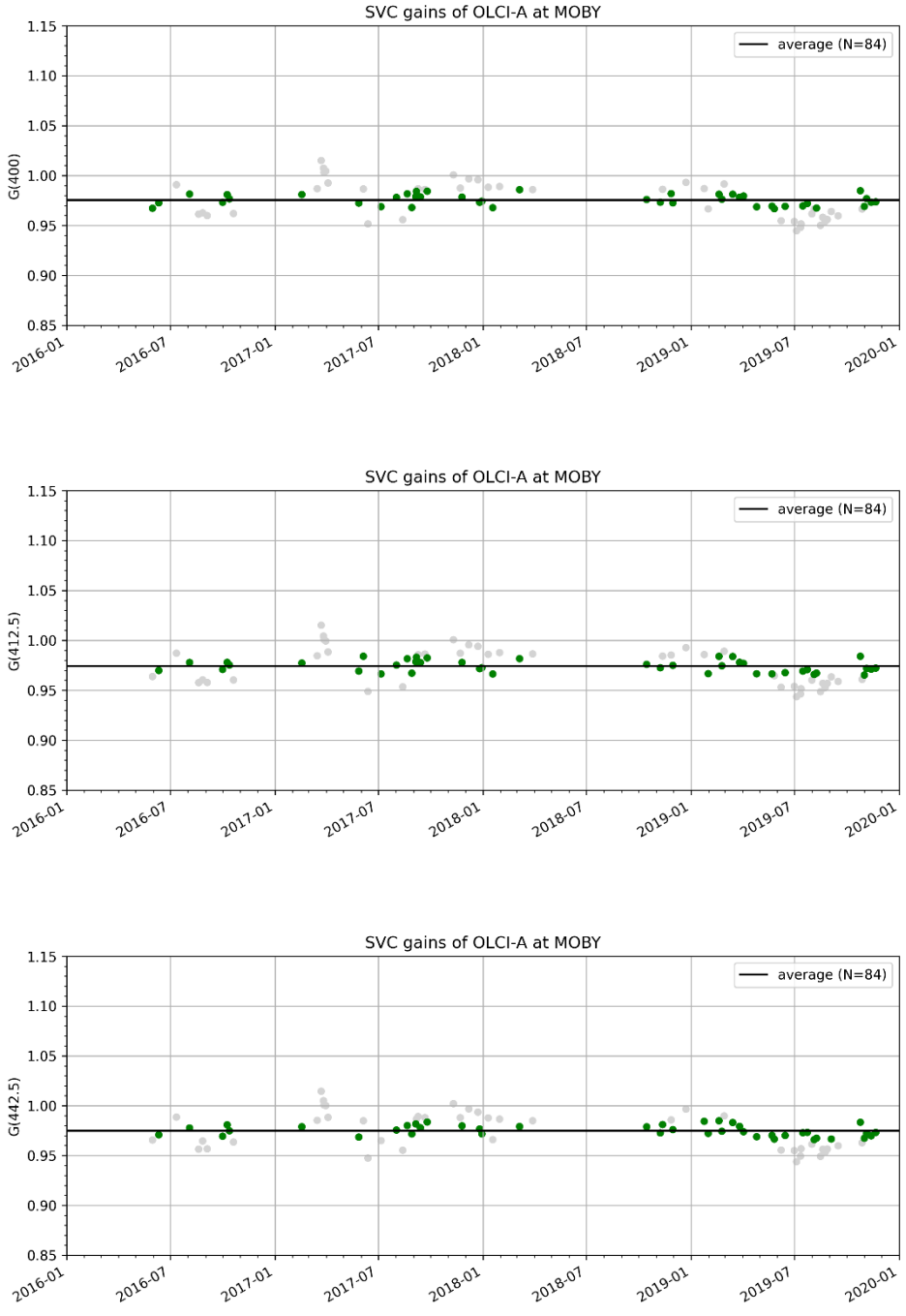

Figure 21 Time-series of OLCI-A gains at MOBY at 400, 412.5 and 442.5 nm. Gains in green fall within the semi-interquartile range used in final averaging.

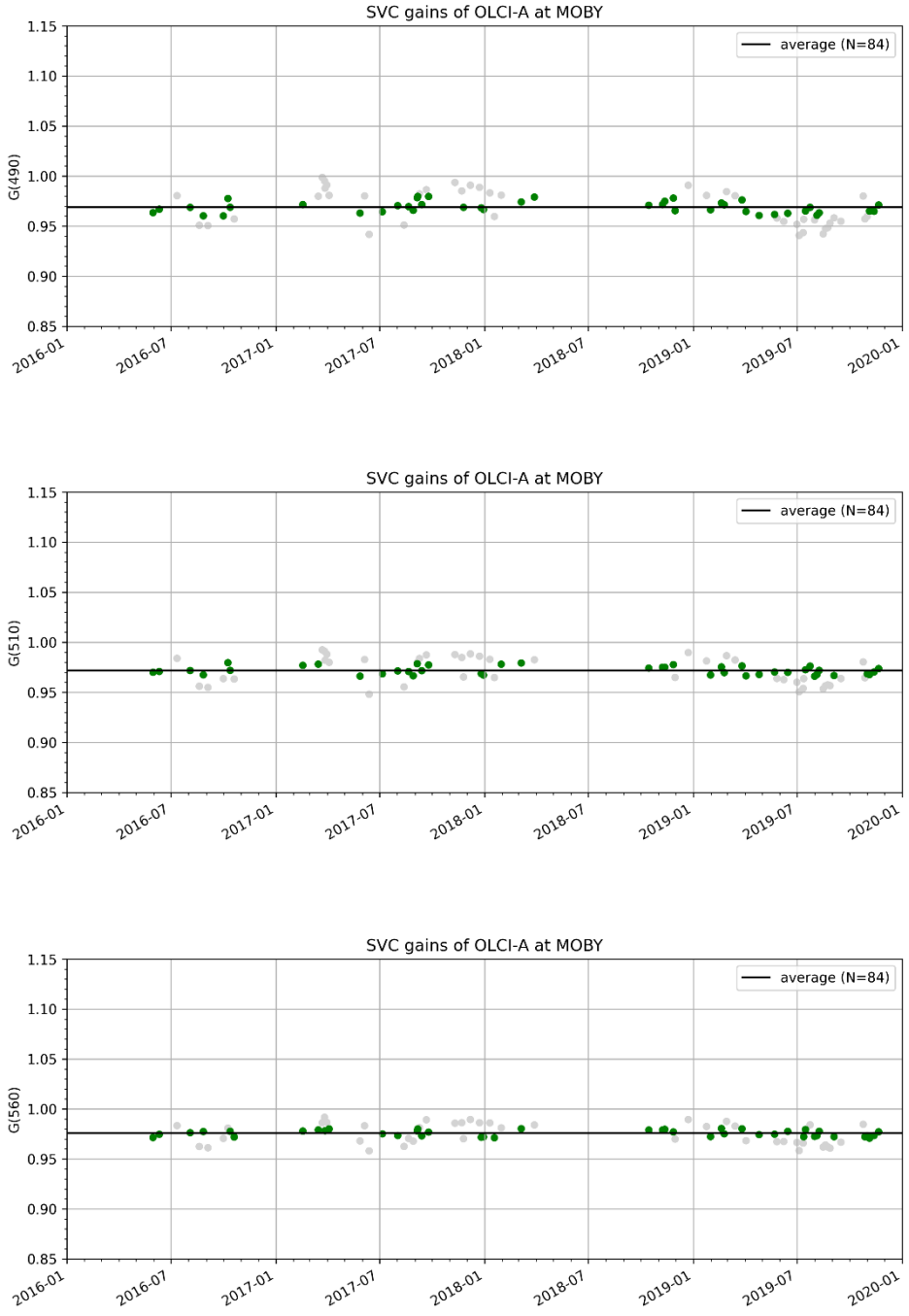

Figure 22 Time-series of OLCI-A gains at MOBY at 490, 510 and 560 nm. Gains in green fall within the semi-interquartile range used in final averaging.

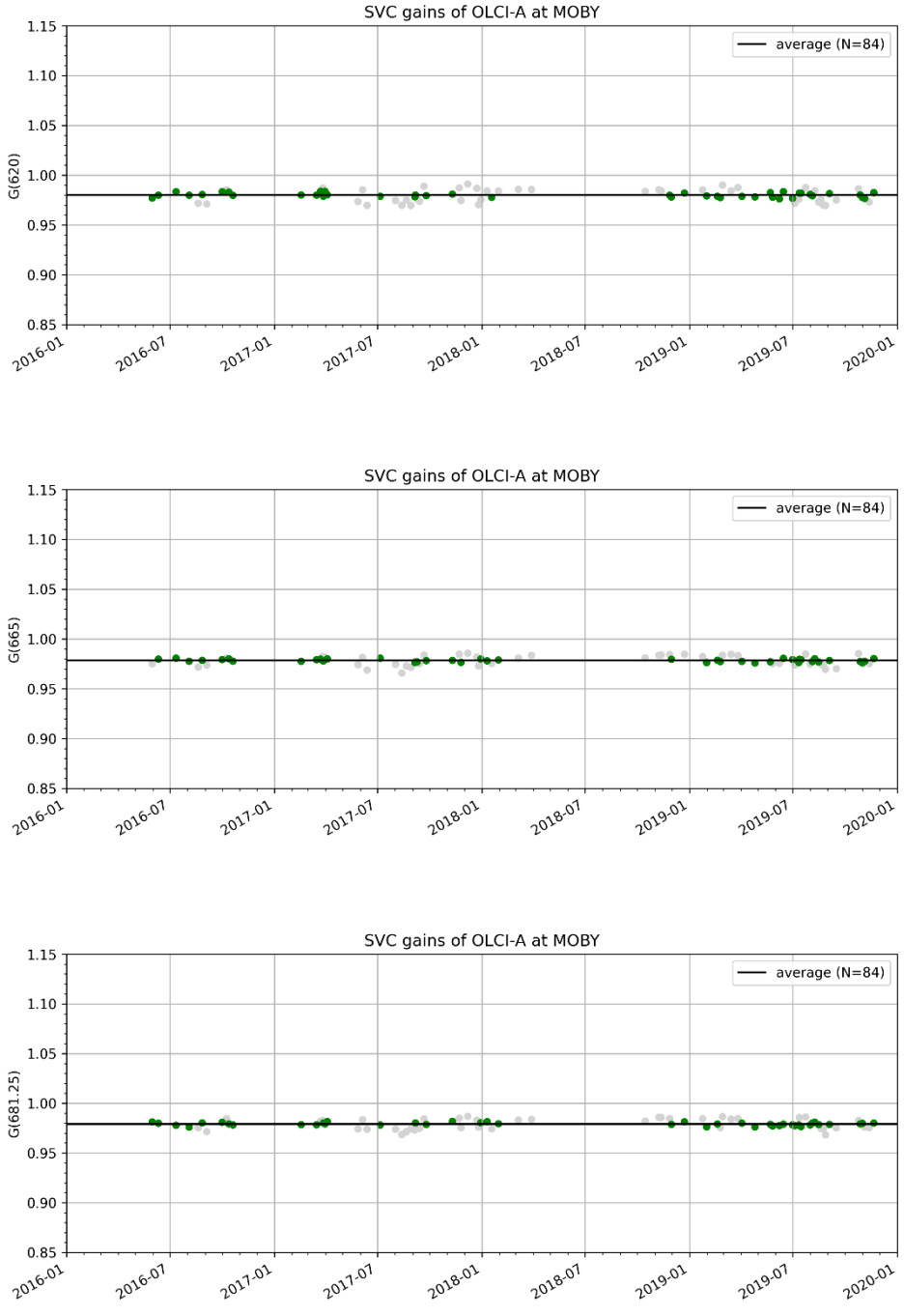

Figure 23 Time-series of OLCI-A gains at MOBY at 620, 665 and 681.25 nm. Gains in green fall within the semi-interquartile range used in final averaging.

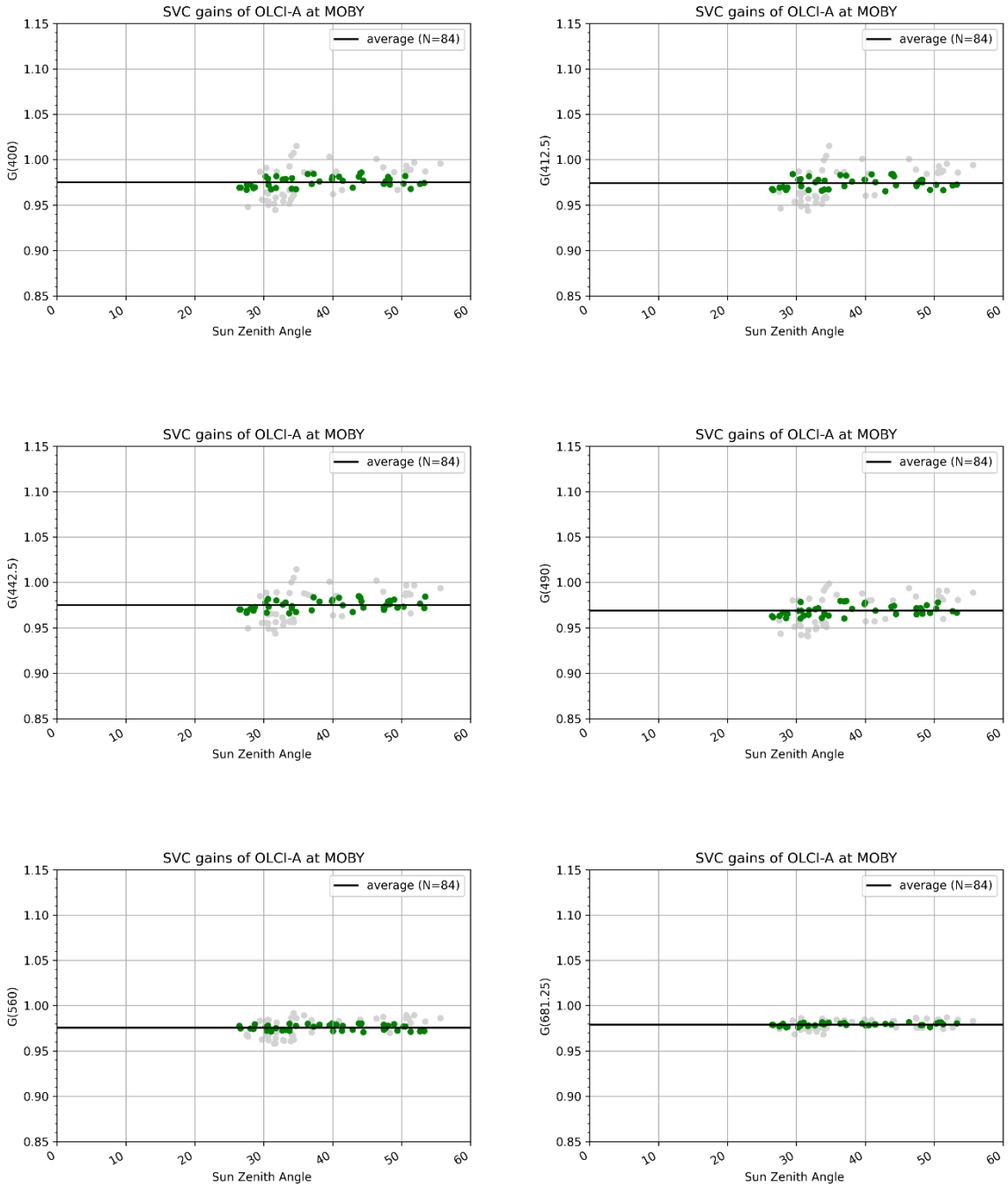

Figure 24 OLCI-A gains at MOBY at 400, 412.5, 442.5, 490, 560 and 681.25 nm as a function of sun zenith angle. Gains in green fall within the semi-interquartile range used in final averaging.

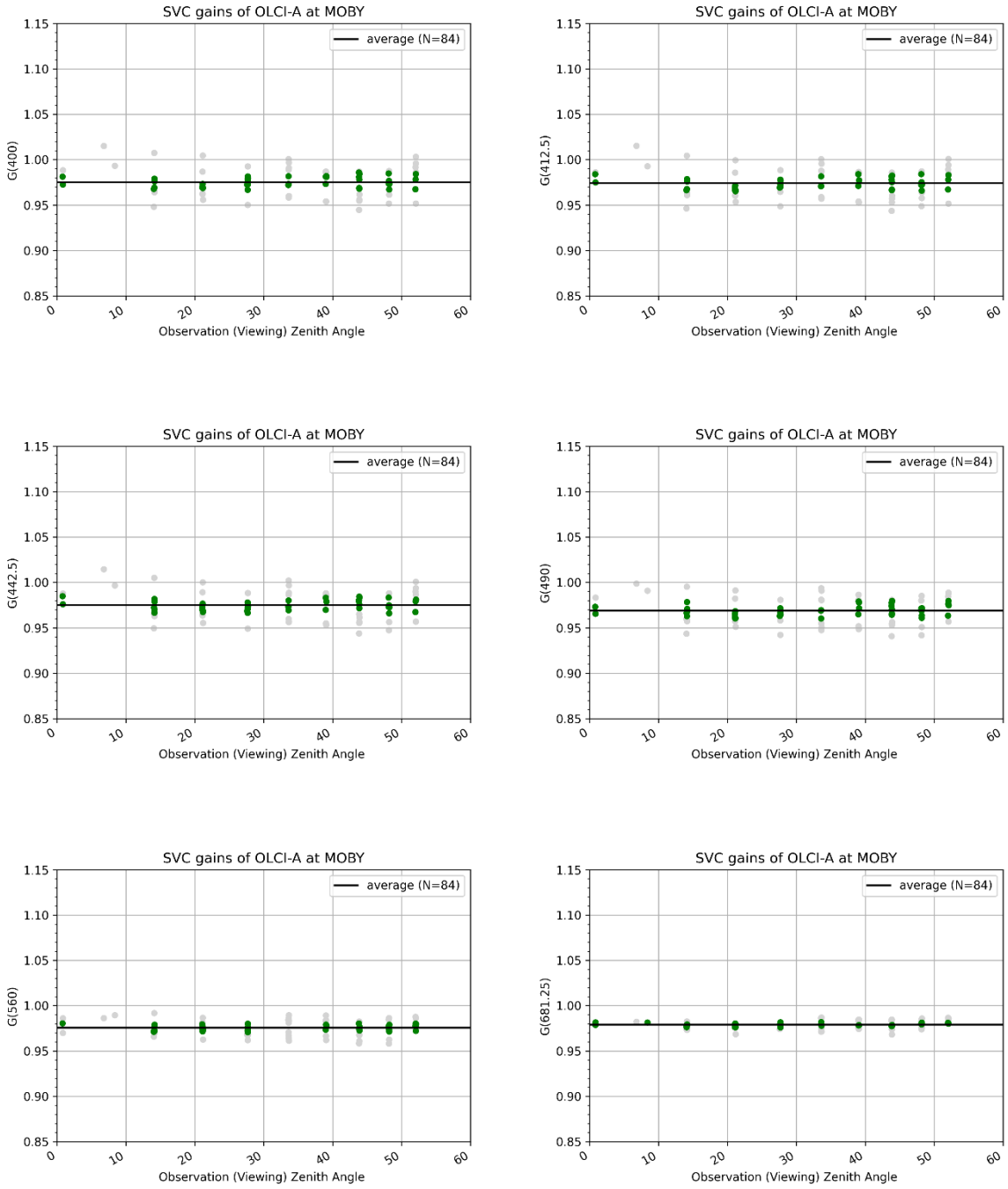

Figure 25 OLCI-A gains at MOBY at 400, 412.5, 442.5, 490, 560 and 681.25 nm as a function of view zenith angle. Gains in green fall within the semi-interquartile range used in final averaging.

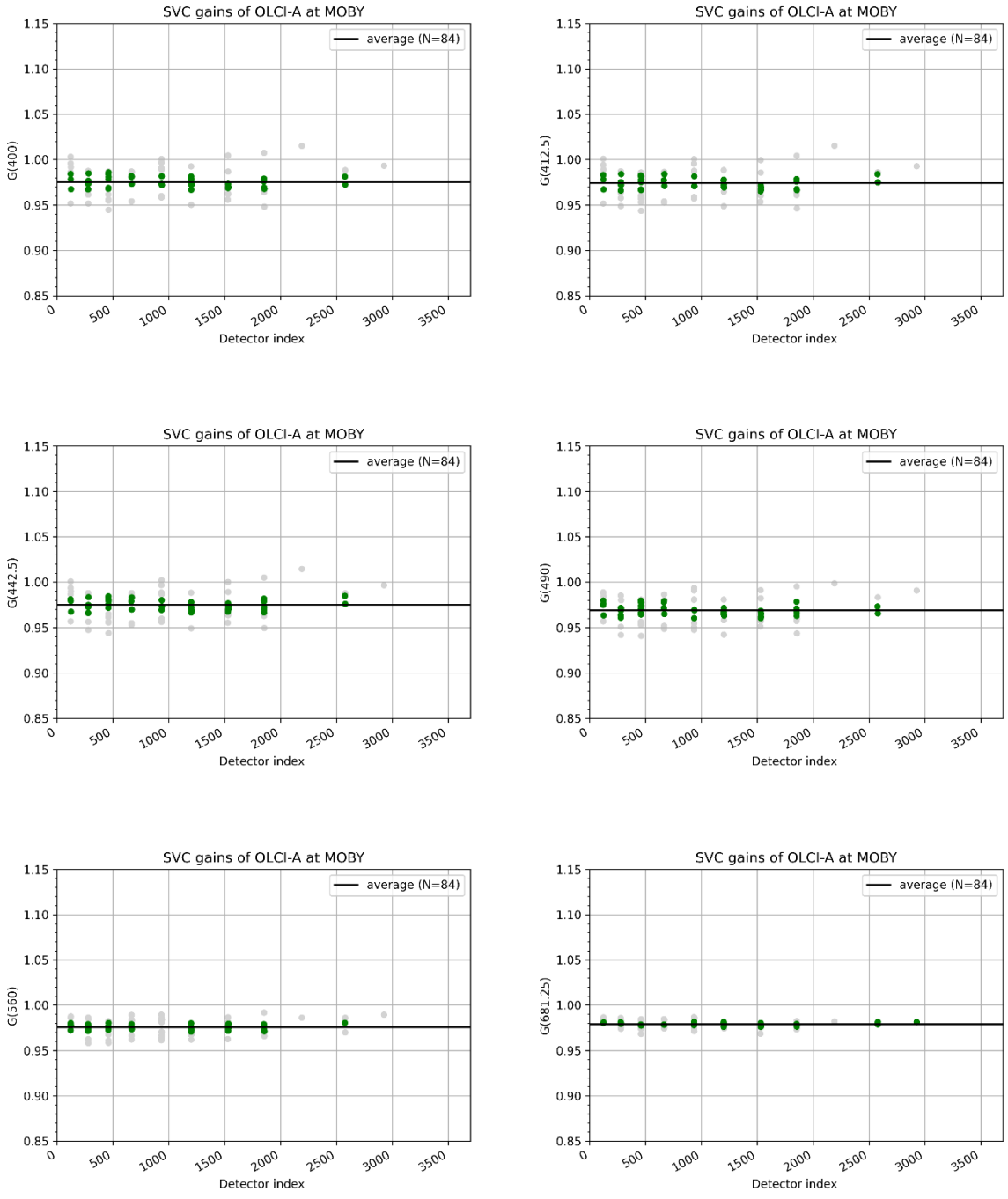

Figure 26 OLCI-A gains at MOBY at 400, 412.5, 442.5, 490, 560 and 681.25 nm as a function of detector index. Gains in green fall within the semi-interquartile range used in final averaging.

4.4 OLCI-B GAINS

4.4.1 GAINS IN THE NIR

The comparison between the targeted R_{rs}^{t} (fixed to zero) and satellite R_{rs} in the NIR is shown on Figure 27 and Figure 28 for respectively the default gains (unity) and the computed gains per match-up. Similarly to OLCI-A, a nearly perfect retrieval is achieved after applying the individual gains, considering the very low level of the signal (see scale on the figures).

The averaged NIR gains (Table 6 and Figure 29) are extremely close to unity from 709 to 885 nm, confirming the excellent relative Level-1 calibration of the sensor at these bands, and of about -6% at 1020 nm. Despite a quite limited temporal coverage (30 good match-ups, about one year), there is no obvious temporal trend nor dependence on the acquisition geometry (Figure 30 to Figure 34).

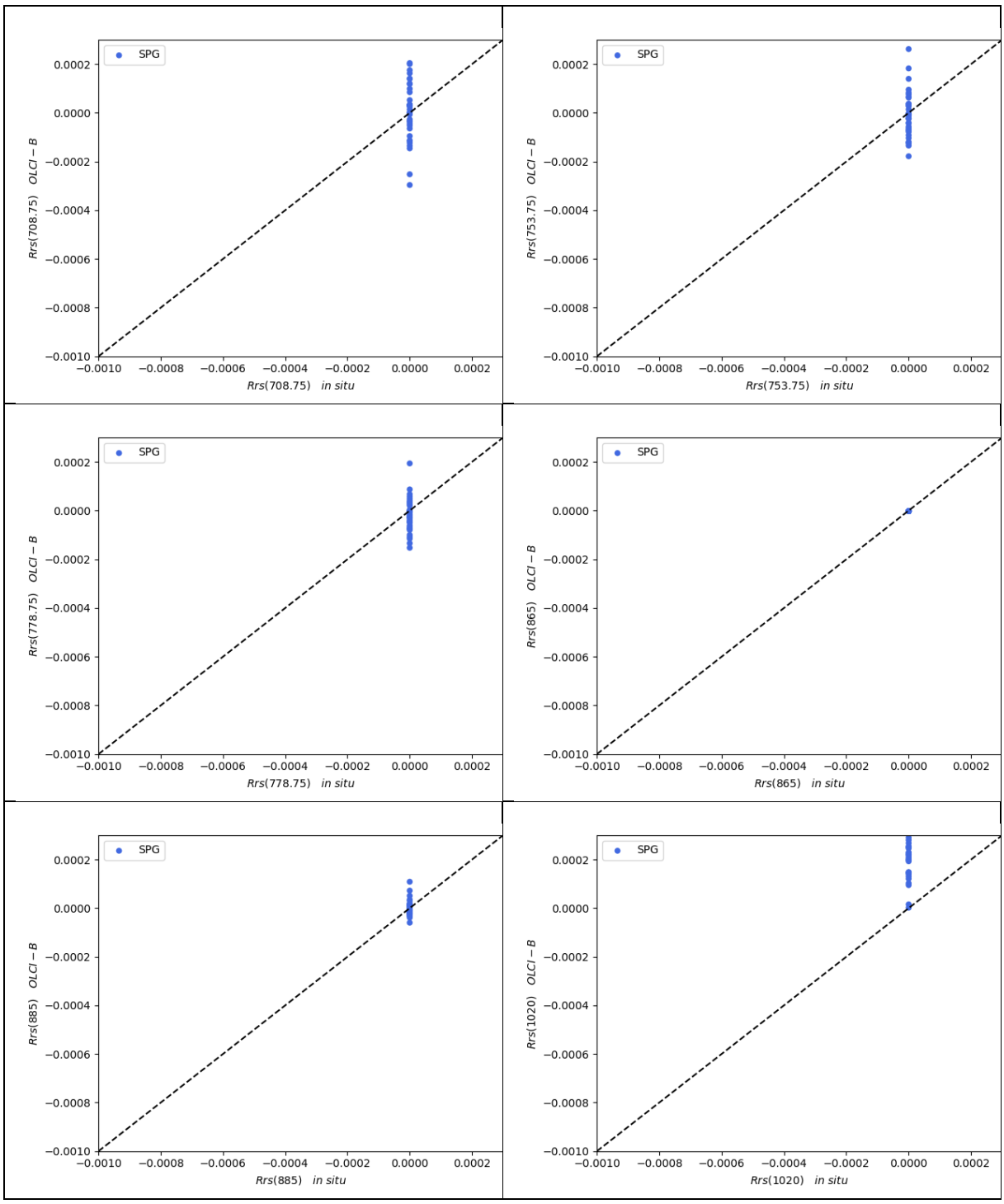

Figure 27 Validation of OLCI-B R_{rs} at SPG with nominal gains (see text) at 708.75, 753.75, 778.75, 865, 885 and 1020 nm.

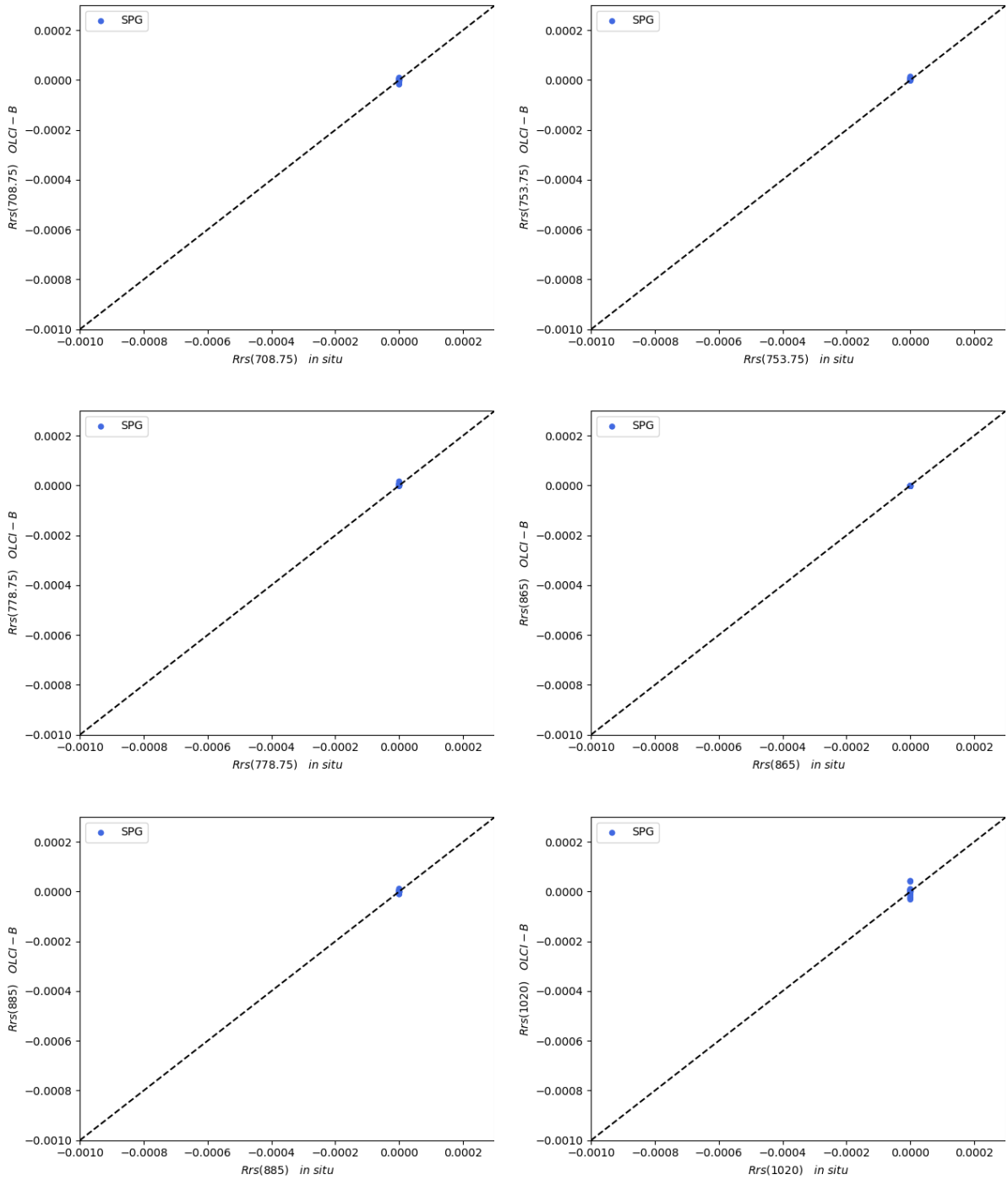

Figure 28 Validation of OLCI-B R_{rs} at SPG after calibration by individual gains (see text) at 708.75, 753.75, 778.75, 865, 885 and 1020 nm.

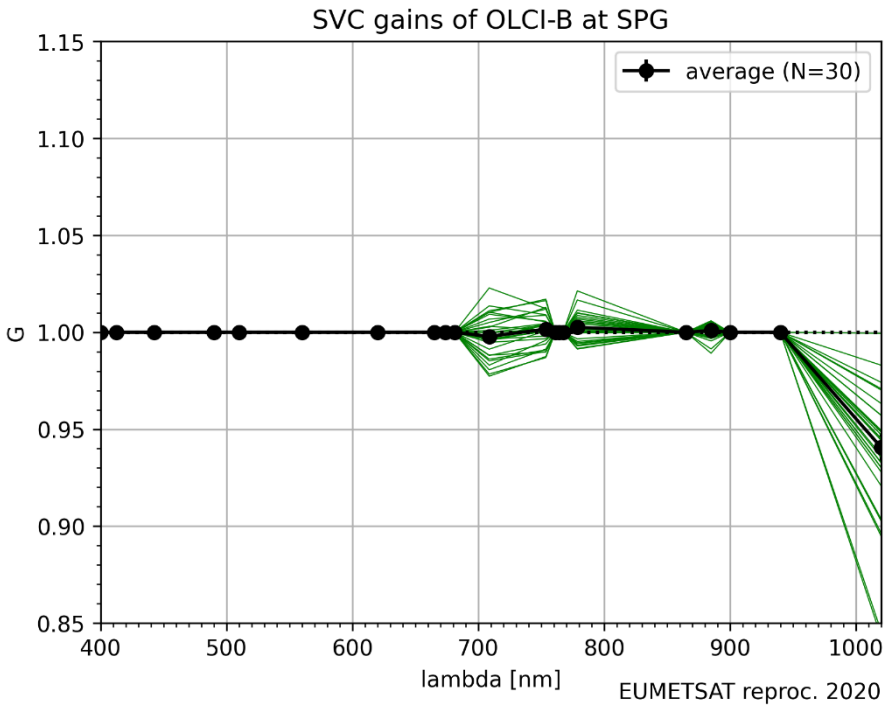

Figure 29 Individual spectral gains of OLCI-B at SPG, before MSIQR screening.

Table 6 Statistics of OLCI-B averaged gains at SPG, after MSIQR filtering

Wavelength	Number	Average gain	Standard-deviation
708.75	14	0.997824	0.003089
753.75	14	1.001631	0.002391
778.75	14	1.002586	0.002176
865		1	
885	14	1.000891	0.001693
1020	14	0.940641	0.007011

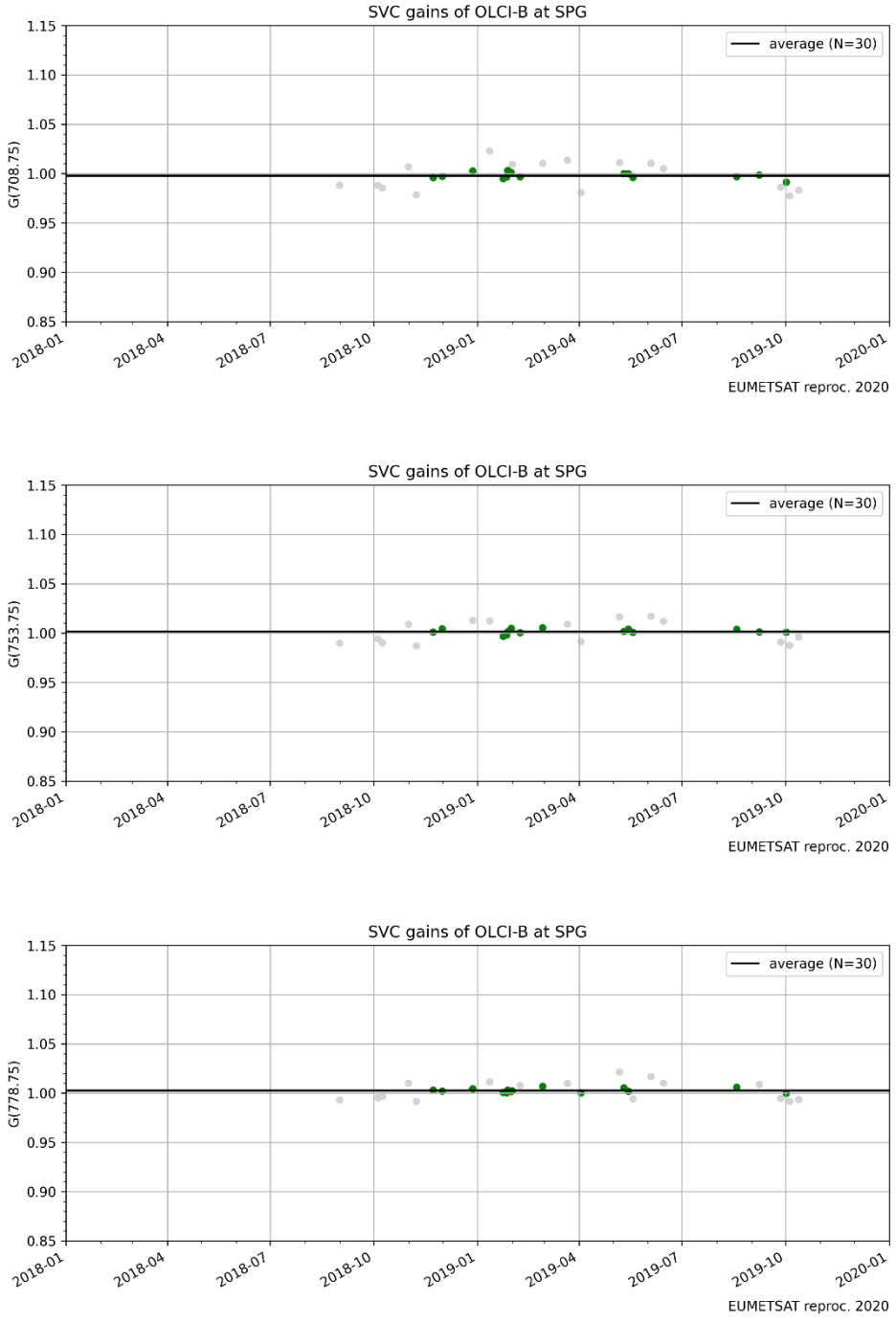

Figure 30 Time-series of OLCI-B gains at SPG at 708.75, 753.75 and 778.75 nm. Gains in green fall within the semi-interquartile range used in final averaging.

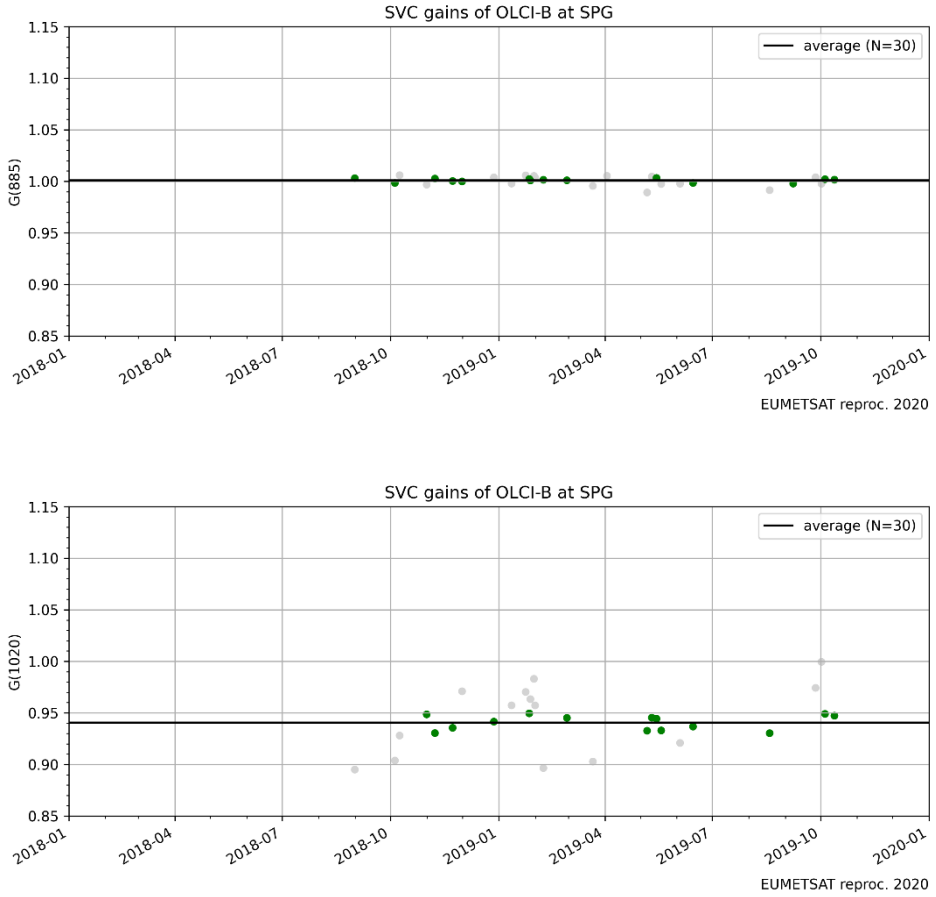

Figure 31 Time-series of OLCI-B gains at SPG at 885 and 1020 nm. Gains in green fall within the semi-interquartile range used in final averaging.

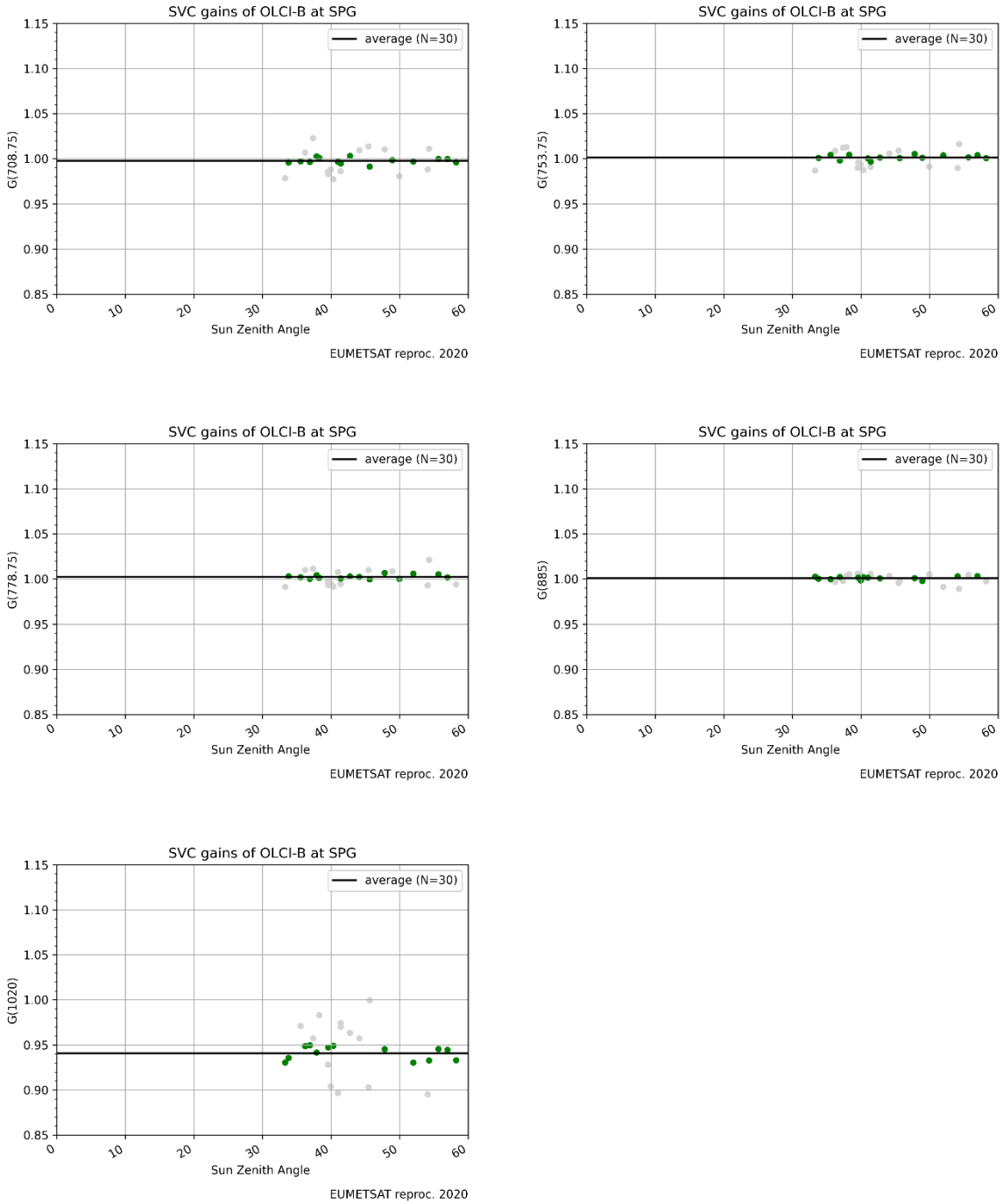

Figure 32 OLCI-B gains at SPG at 708.75, 753.75, 778.75, 885 and 1020 nm as a function of sun zenith angle. Gains in green fall within the semi-interquartile range used in final averaging.

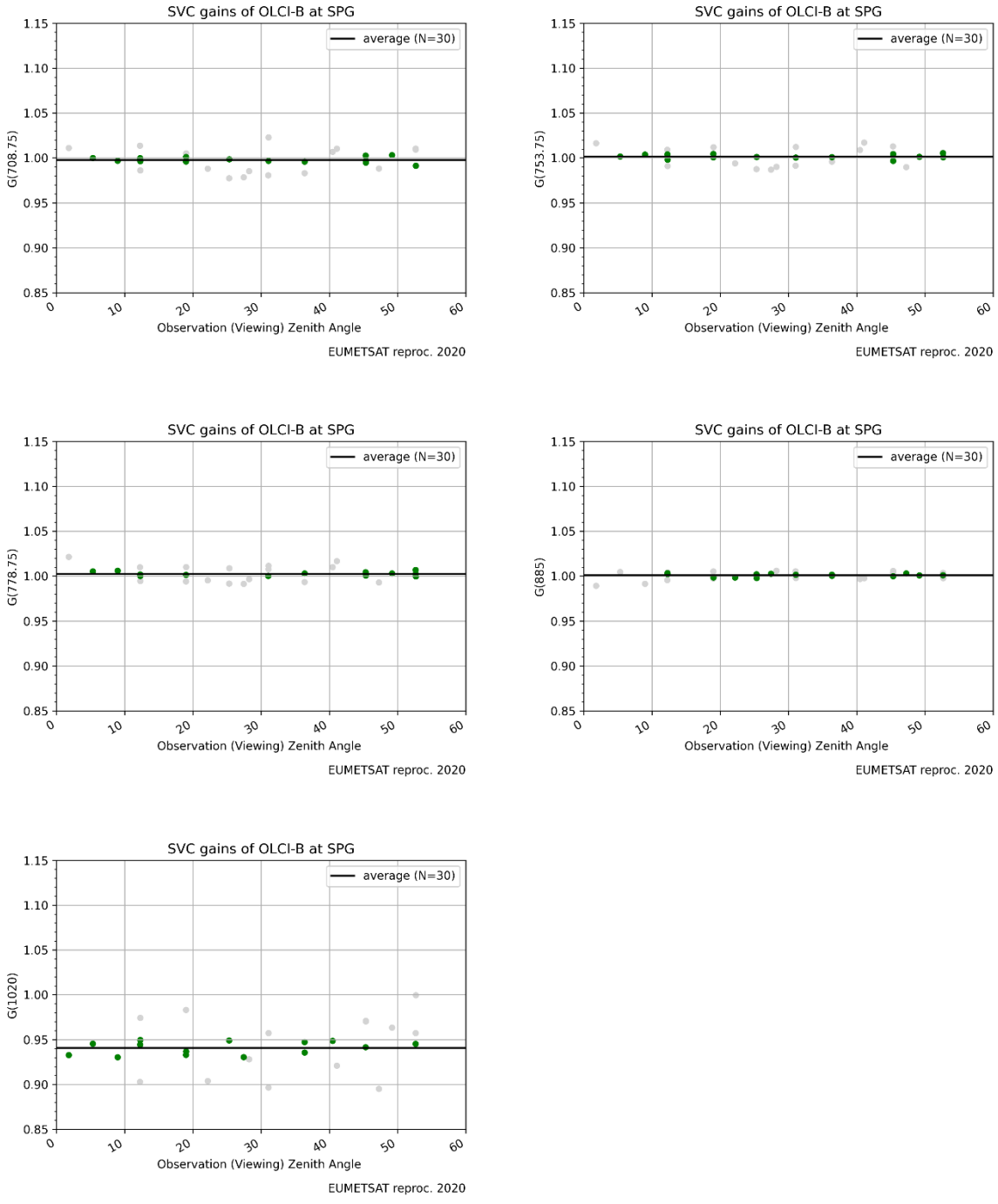

Figure 33 OLCI-B gains at SPG at 708.75, 753.75, 778.75, 885 and 1020 nm as a function of view zenith angle. Gains in green fall within the semi-interquartile range used in final averaging.

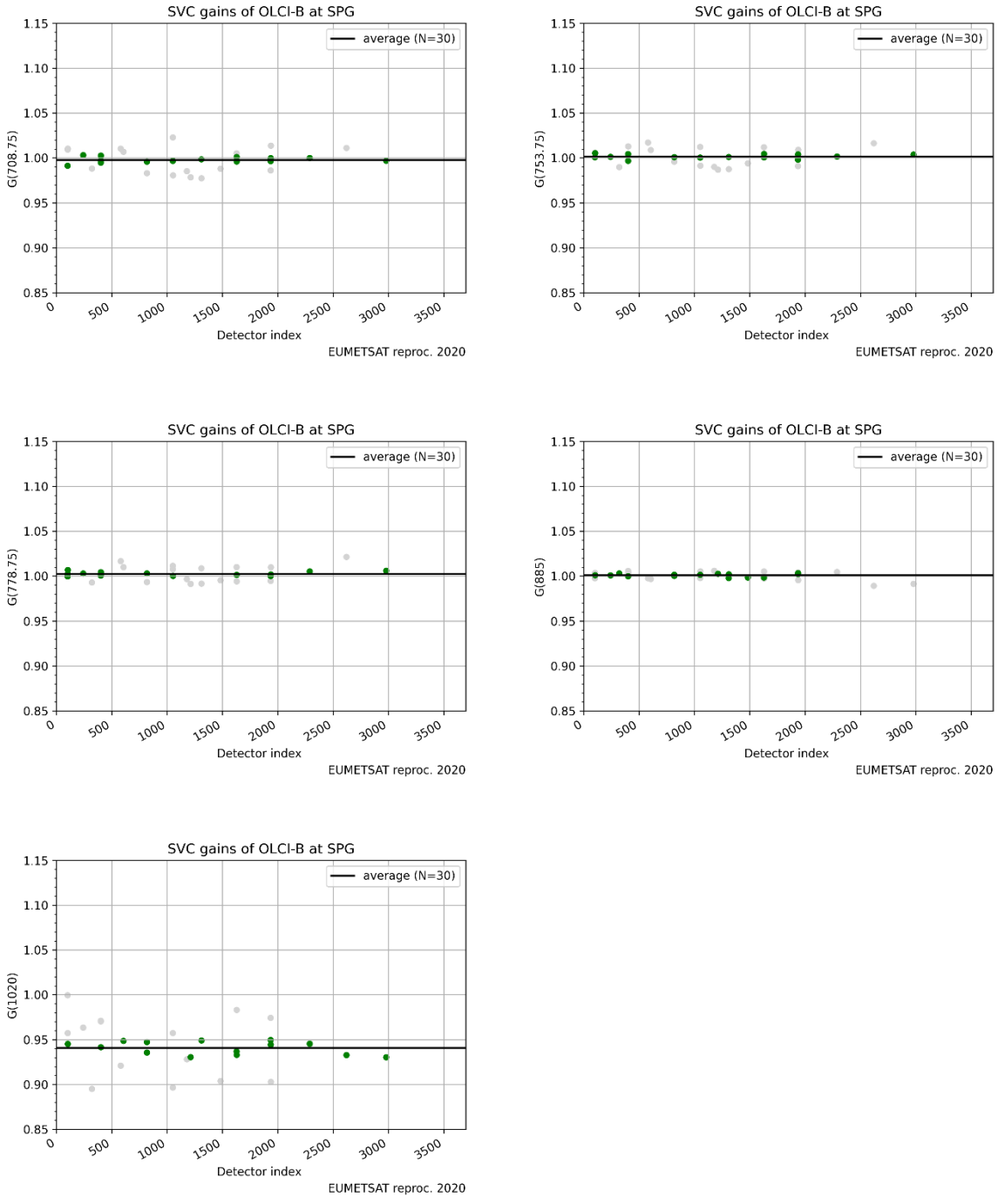

Figure 34 OLCI-B gains at SPG at 708.75, 753.75, 778.75, 885 and 1020 nm as a function of detector index. Gains in green fall within the semi-interquartile range used in final averaging.

4.4.2 GAINS IN THE VIS

The comparison between the MOBY R_{rs}^{t} and satellite R_{rs} in the VIS is shown on Figure 35 and Figure 36 for respectively the default gains (unit gain in the VIS, new gains in the NIR) and the computed VIS gains per match-up. This demonstrates once more time the relevance of the individual gains.

A total of 39 OLCI-B match-ups are kept (19 in MSIQR), yielding an average adjustment of about -1% in the visible, variable among wavelengths (Table 7 and Figure 37). The difference with the NIR assumption (0% at 865 nm) could be questioned; it may be that OLCI-B could require a small adjustment at this NIR band (less than -1%), that would decrease the overall amplitude of gains in the VIS. In any case, the individual gains are remarkably stable, with RSEM even lower than that of OLCI-A (0.03% in the blue).

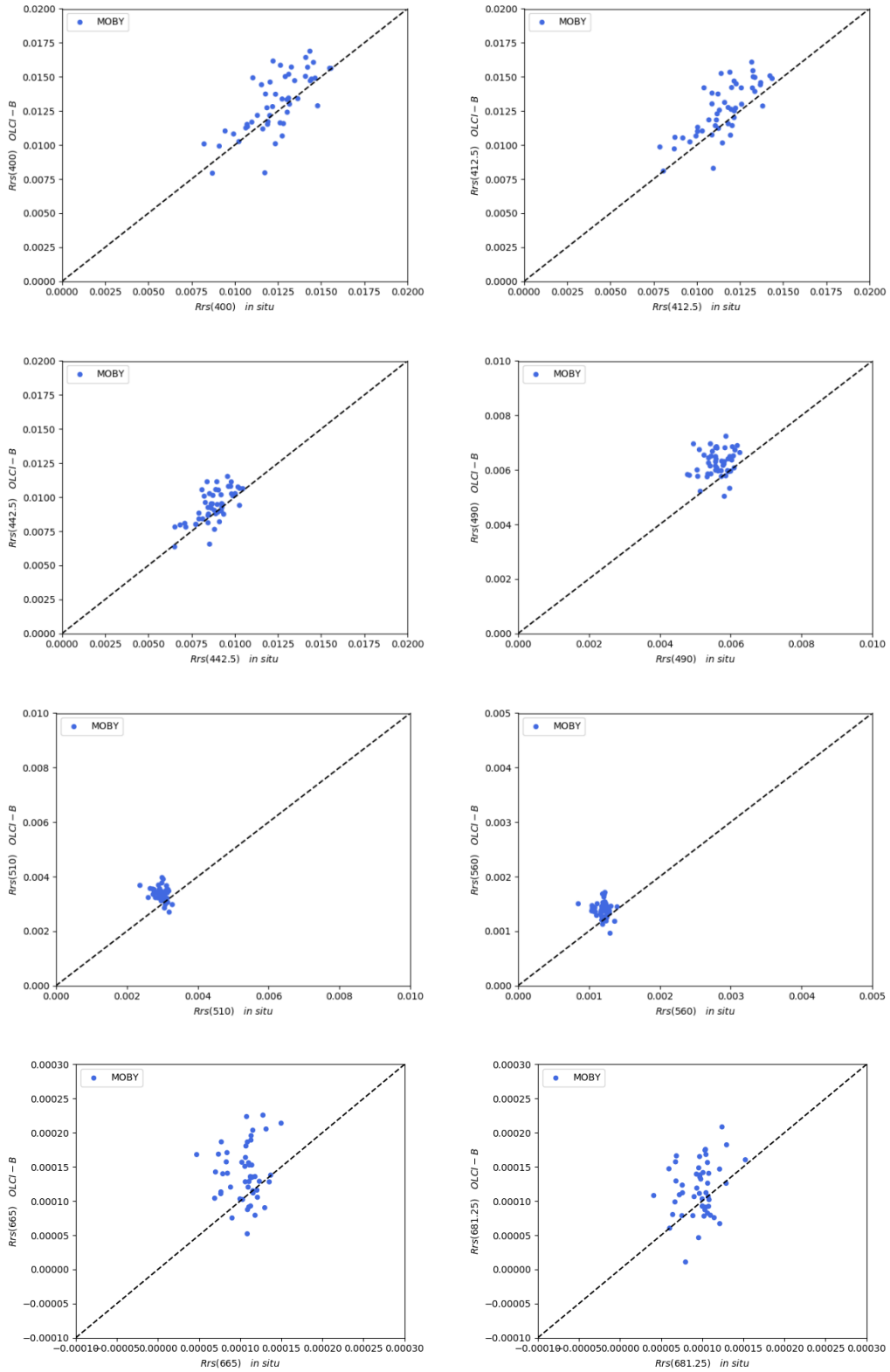

Figure 35 Validation of OLCI-B R_{rs} at MOBY with nominal gains (see text) at 400, 412.5, 442.5, 490, 510, 560, 665 and 681.25 nm.

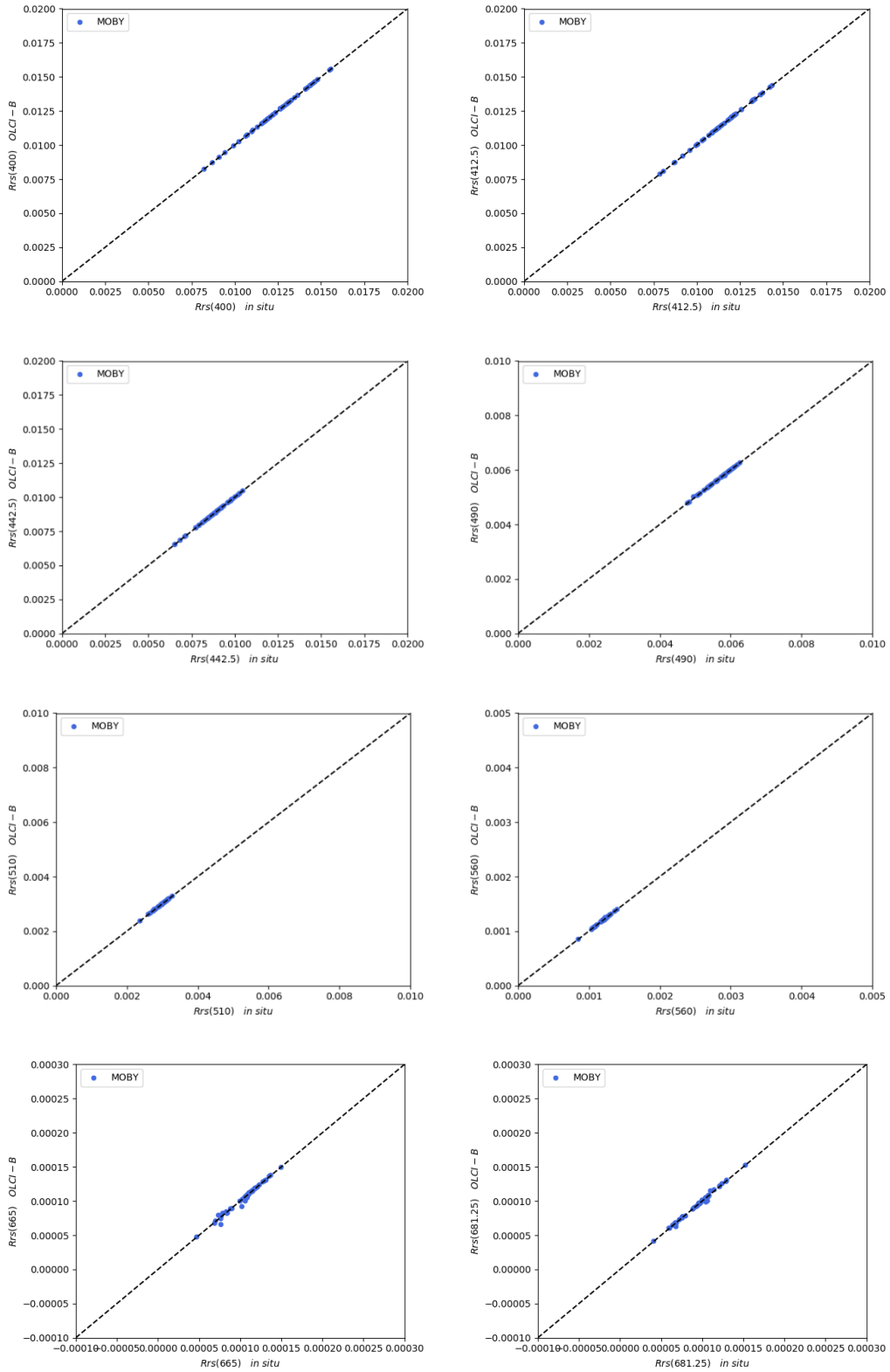

Figure 36 Validation of OLCI-B R_{rs} at MOBY after calibration by individual gains (see text) at 400, 412.5, 442.5, 490, 510, 560, 665 and 681.25 nm.

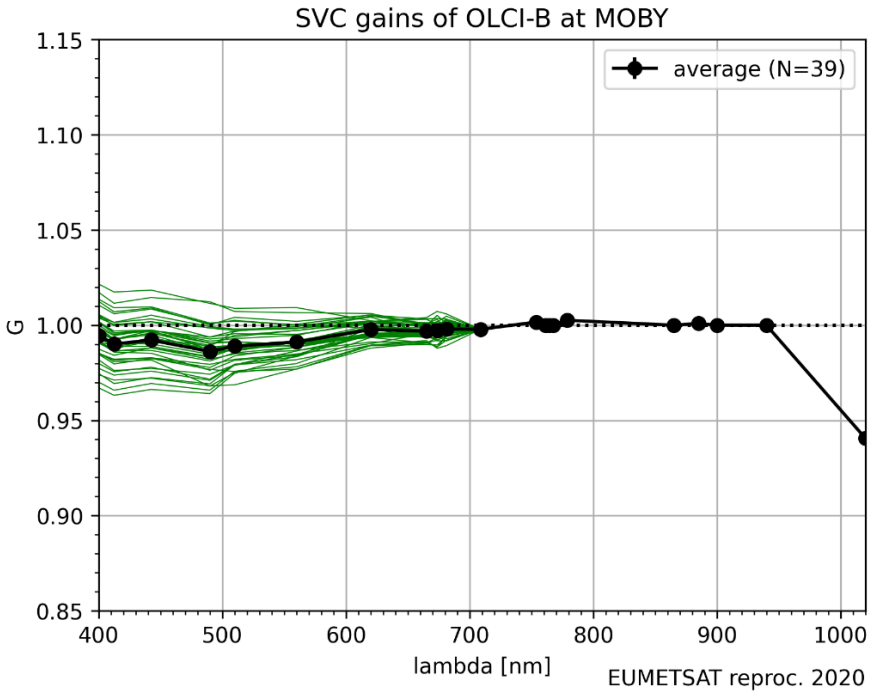

Figure 37 Individual spectral gains of OLCI-B at MOBY, before MSIQR screening.

Table 7 Statistics of OLCI-B averaged gains at MOBY, after MSIQR filtering

Wavelength	Number	Average gain	Standard-deviation	RSEM [%]
400	19	0.994584	0.004464	0.0339
412.5	19	0.9901	0.003902	0.0297
442.5	19	0.992215	0.004418	0.0336
490	19	0.986199	0.004067	0.0311
510	19	0.988985	0.003604	0.0275
560	19	0.99114	0.003021	0.023
620	19	0.997689	0.002244	0.017
665	19	0.996837	0.001841	0.0139
673.75	19	0.997165	0.001695	0.0128
681.25	19	0.998016	0.001902	0.0144

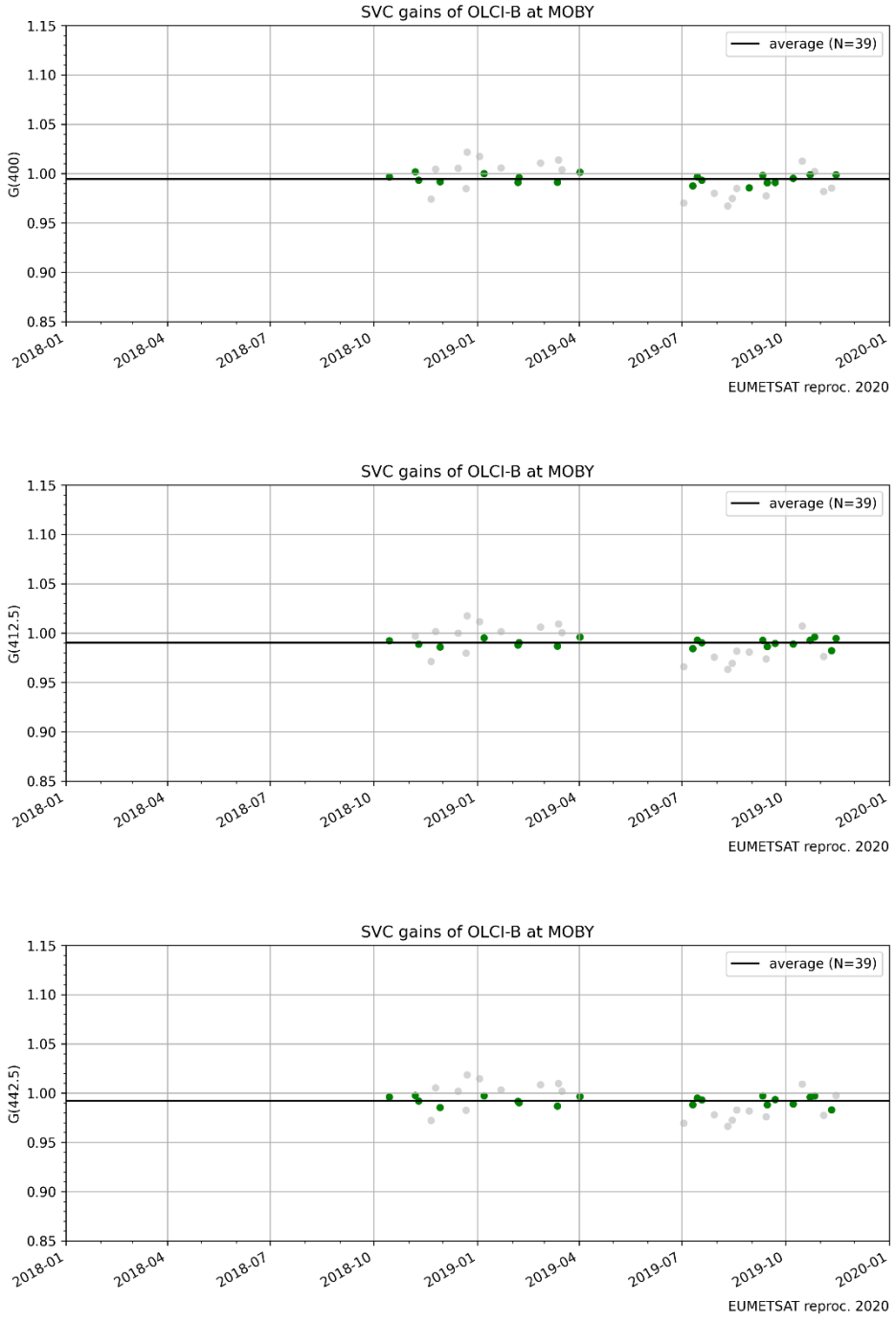

Figure 38 Time-series of OLCI-B gains at MOBY at 400, 412.5 and 442.5 nm. Gains in green fall within the semi-interquartile range used in final averaging.

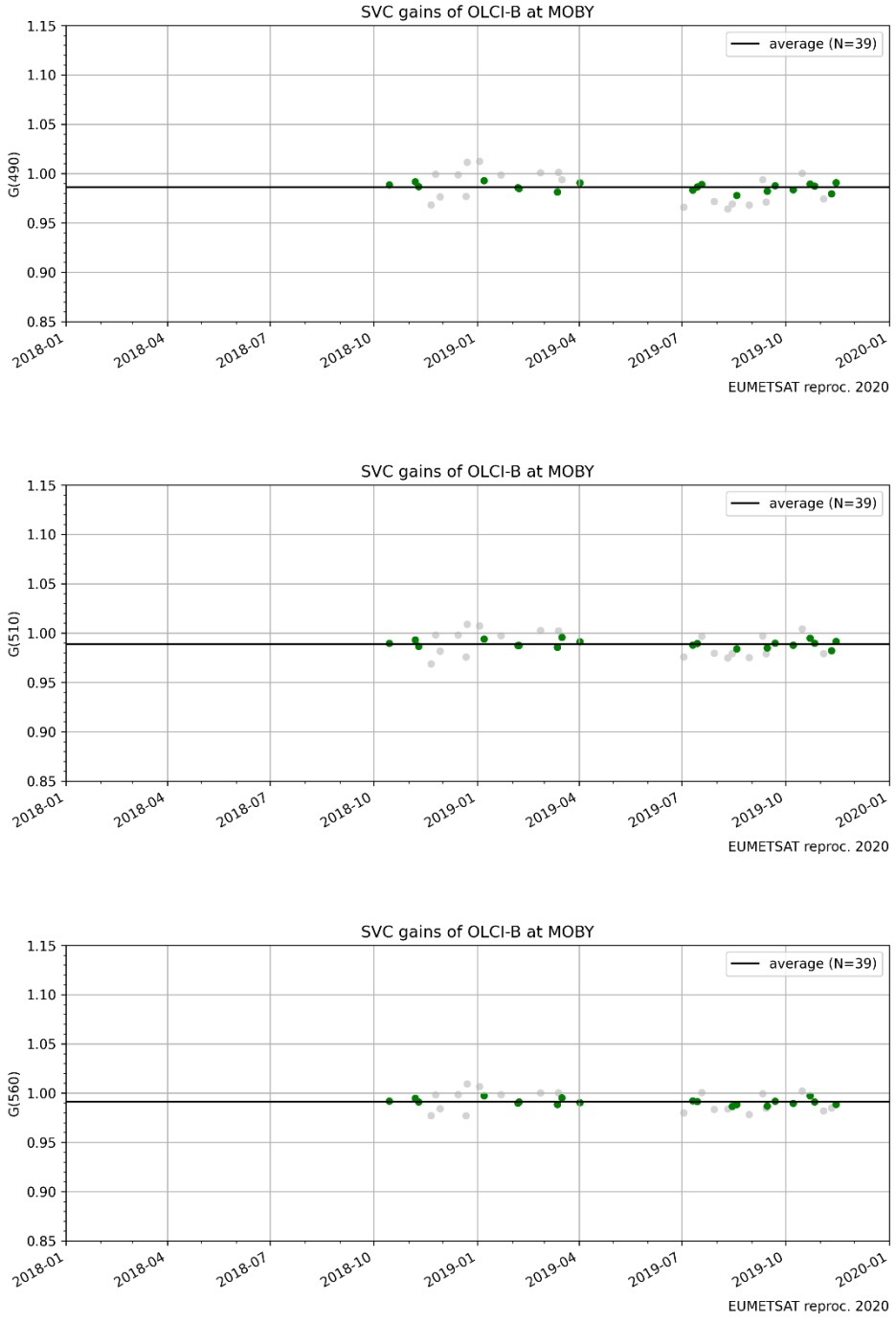

Figure 39 Time-series of OLCI-B gains at MOBY at 490, 510 and 560 nm. Gains in green fall within the semi-interquartile range used in final averaging.

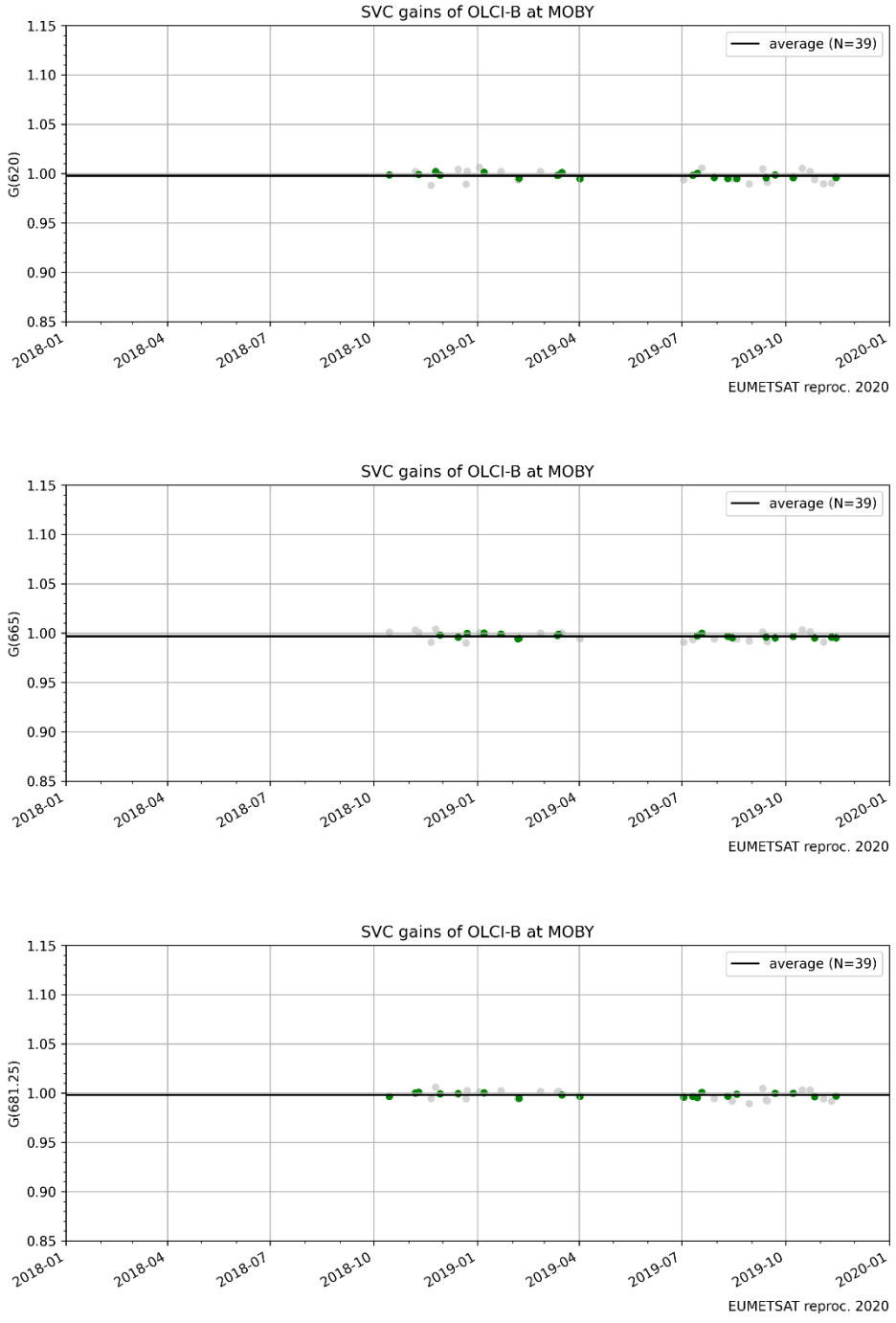

Figure 40 Time-series of OLCI-B gains at MOBY at 620, 665 and 681.25 nm. Gains in green fall within the semi-interquartile range used in final averaging.

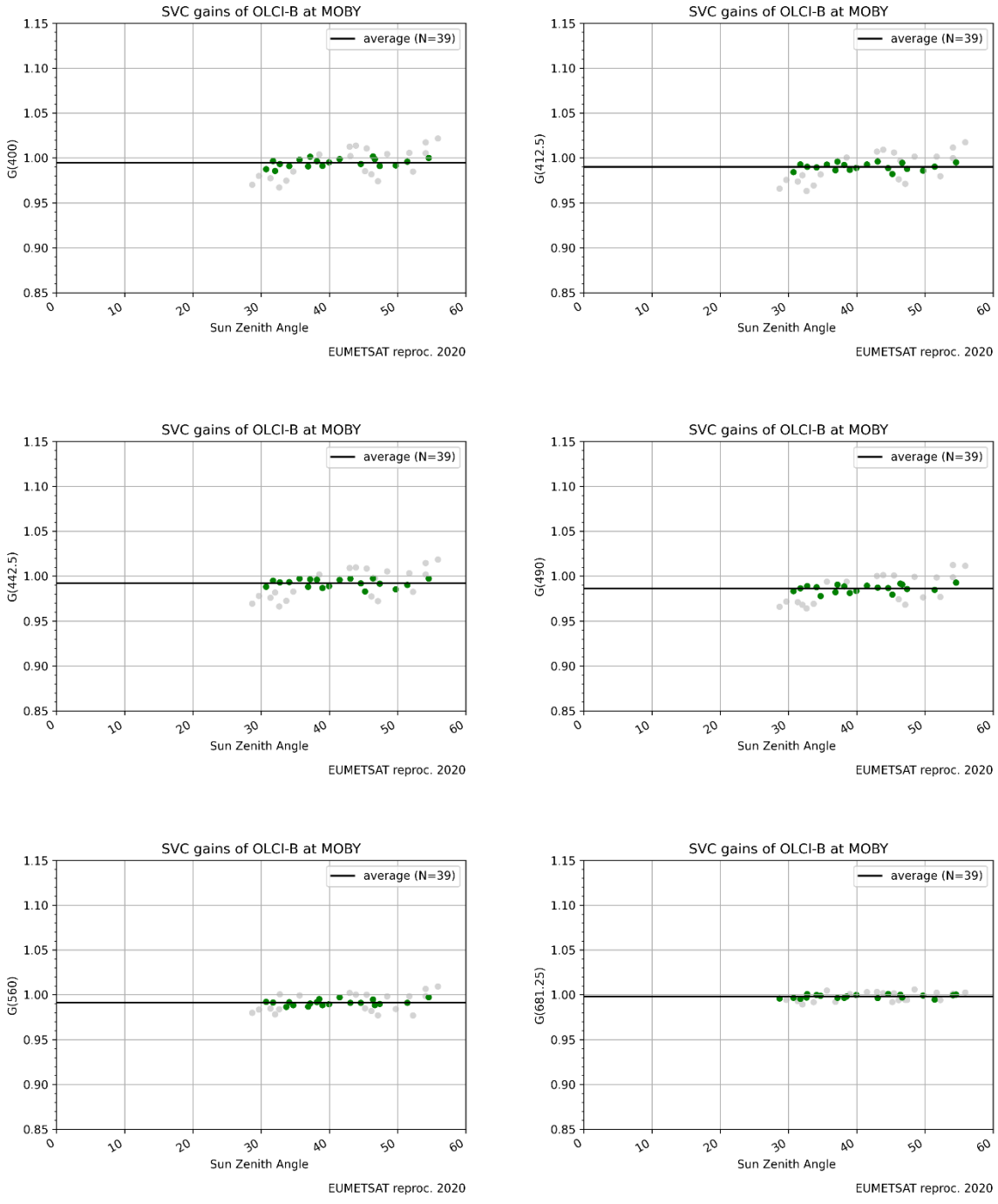

Figure 41 OLCI-B gains at MOBY at 400, 412.5, 442.5, 490, 560 and 681.25 nm as a function of sun zenith angle. Gains in green fall within the semi-interquartile range used in final averaging.

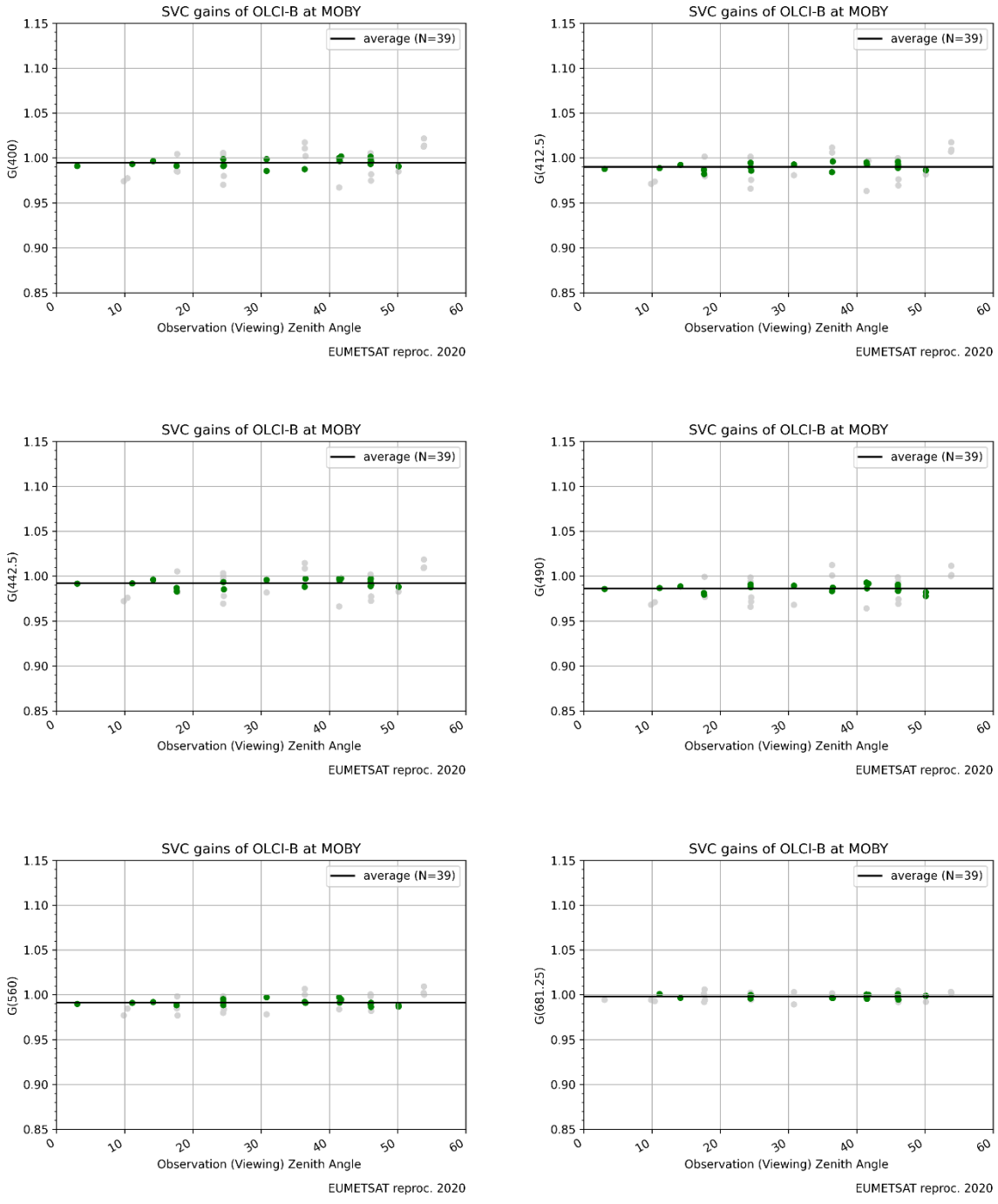

Figure 42 OLCI-B gains at MOBY at 400, 412.5, 442.5, 490, 560 and 681.25 nm as a function of view zenith angle. Gains in green fall within the semi-interquartile range used in final averaging.

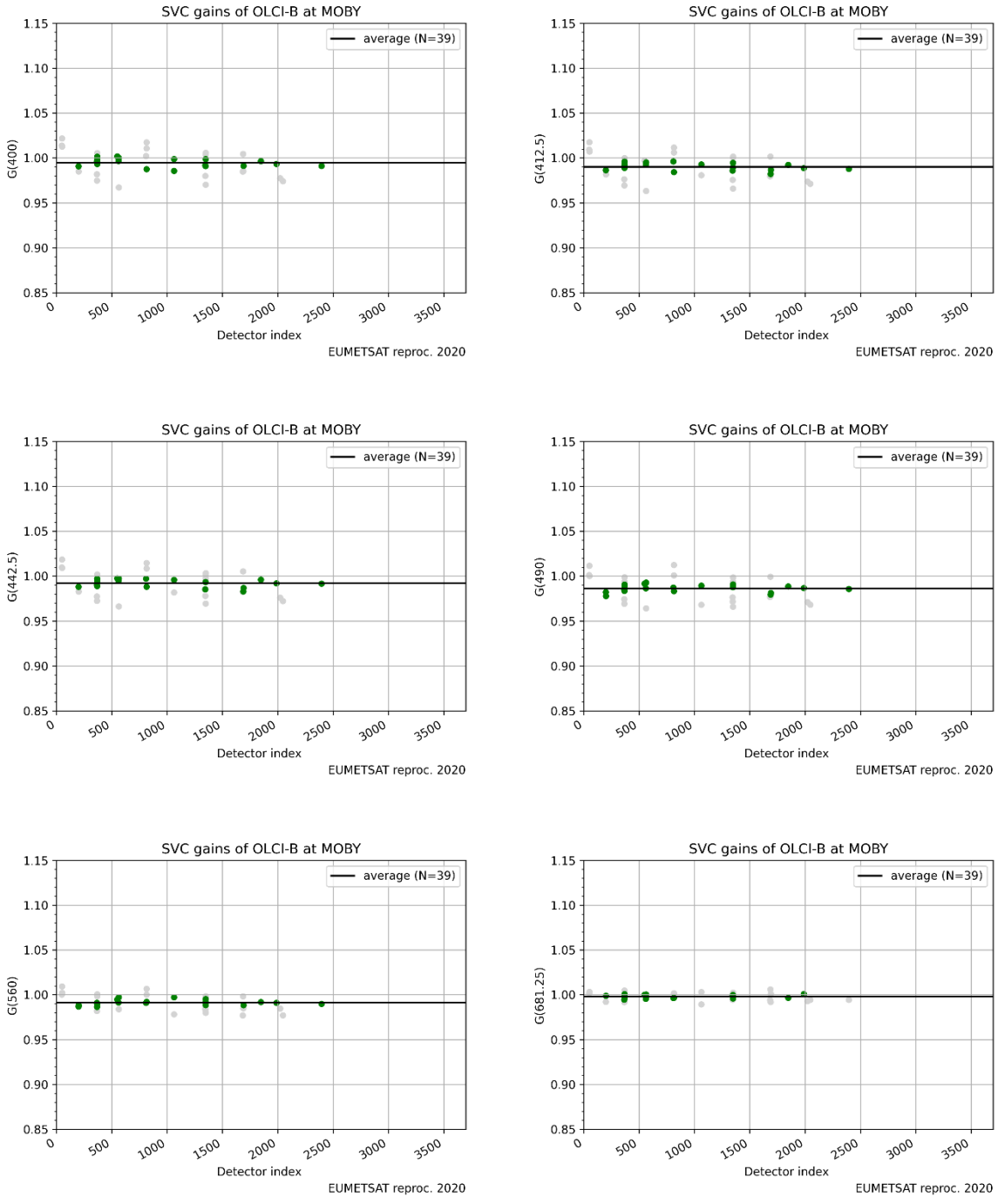

Figure 43 OLCI-B gains at MOBY at 400, 412.5, 442.5, 490, 560 and 681.25 nm as a function of detector index. Gains in green fall within the semi-interquartile range used in final averaging.

4.5 IMPACT ASSESSMENT OF SVC

Warning: The analysis hereafter goes beyond the OC-SVC-TOOL purpose. Plots in this chapter are not generated by the SW-TOOL. They illustrate the analysis that should be conducted after generating new SVC gains. Data referred to as "OC-SVC-TOOL" were generated by a version of the OLCI IPF that may be different from the EUMETSAT 2021's reprocessing.

4.5.1 IMPACT ON OLCI-A MATCH-UPS

The analysis has been made on a 5 x 5 macropixel centered in the central pixel of each site. EUMETSAT protocols have been applied for the match-up definition, filtering and median averaging.

Results are presented using scatterplots (band-individual or several bands in one plot) and line plots for summarizing the statistics. The colour scale adjacent to the scatter plot shows the standard deviation of the final macropixel averaged as a measure of uncertainty.

The sites analysed are: Venice Tower (AAOT), Bahía Blanca (BBL), Casablanca Platform (CSP), Galata Platform (GAL), Gustav Dalen Tower (GDT), Gloria (GLO), Helsinki Light House (HLH), Lake Eire (LER), LISCO (LIS), Palgrunden (PAL), Section 7 Platform (S7P), South Greenbay (SGB), USC SeaPRISM (USC), Zeebrugge (ZRB). These sites are representative of several water types, from more or less clear waters (AAOT) to highly turbid cases (BBL, HLH, GDT).

Because some changes in the flags were introduced in the recent IPF, only common cases for nominal (PB2.23) and OC-SVC-TOOL match-ups have been taken into account.

Venice Tower (AAOT)

Band-individual scatter plots are shown for this site from band B2 (412.5 nm) to B9 (673.75 nm) except for B7 (620 nm) where there was not good in situ data. Number of matchups is almost the same, since we only analysed common matchups for both the PB 2.23 and the OC-SCV-TOOL configurations. Coefficient of determination is in general lower for the OC-SVC gains results, but errors (all statistics) decrease as well or are kept very close to the PB 2.23 configuration.

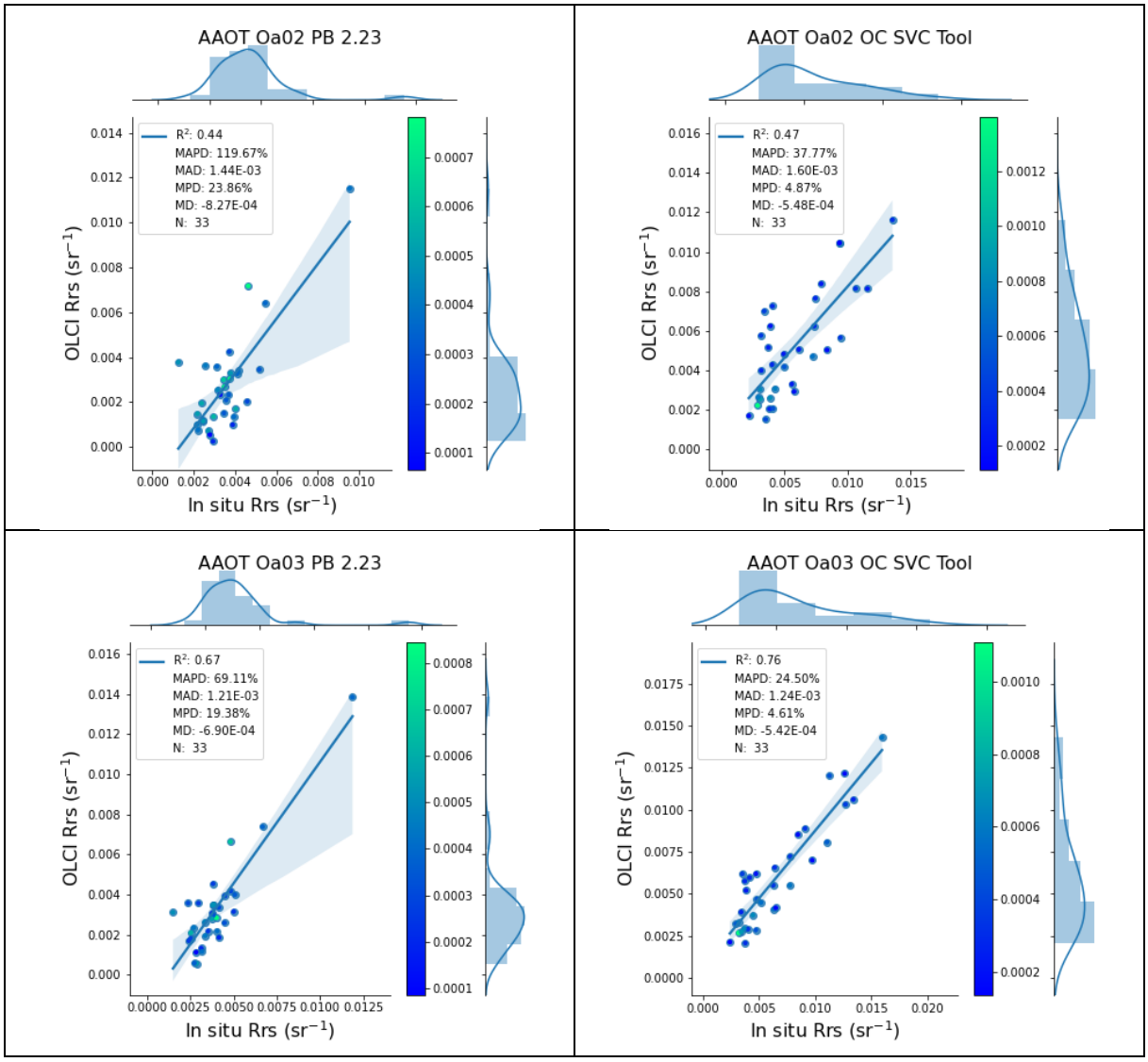

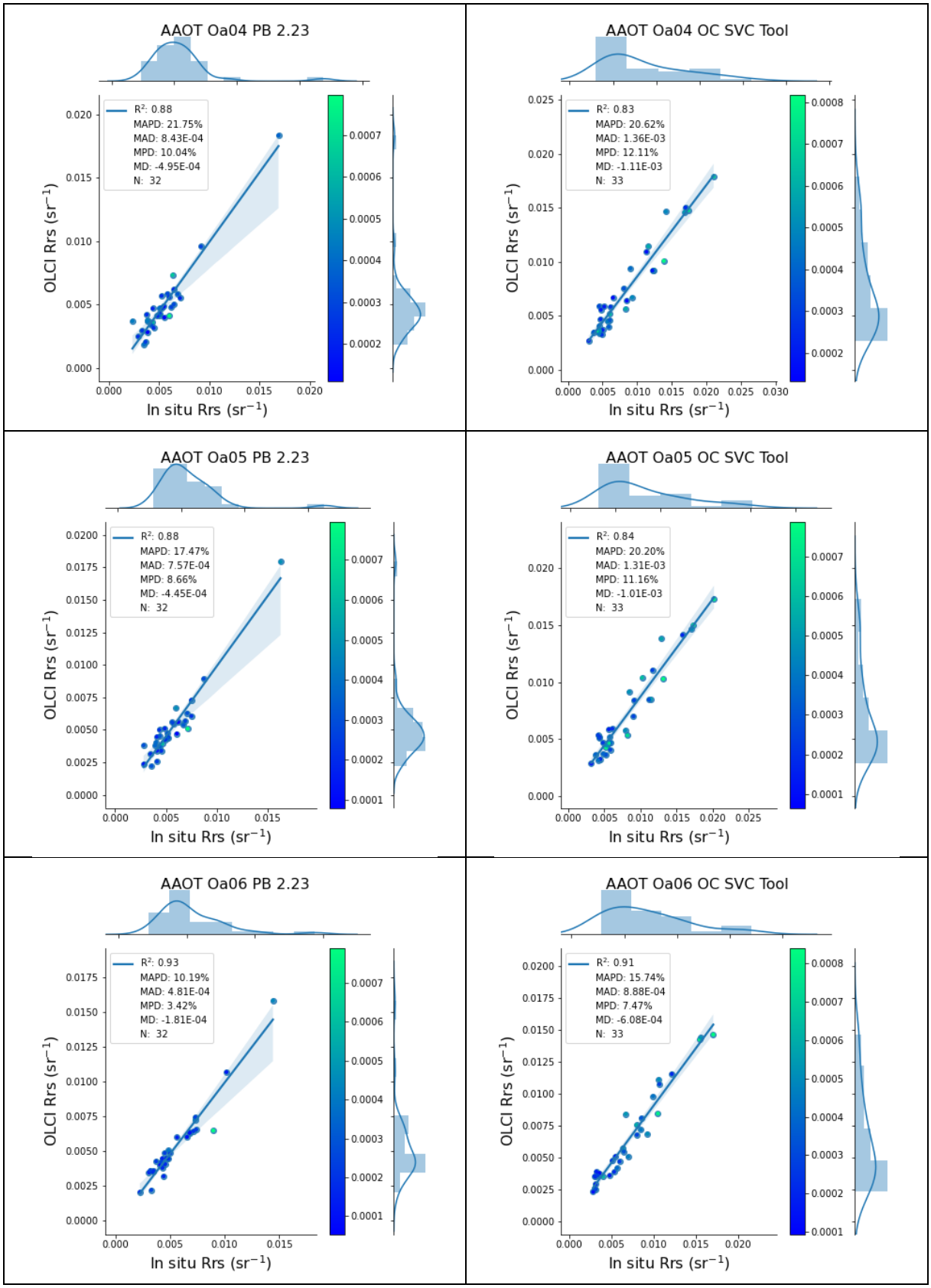
AAOT Oa04 PB 2.23
R²: 0.88
MAPD: 21.75%
MAD: 8.43E-04
MPD: 10.04%
MD: -4.95E-04
N: 32
OLCI Rrs (sr⁻¹)
In situ Rrs (sr⁻¹)
AAOT Oa04 OC SVC Tool
R²: 0.83
MAPD: 20.62%
MAD: 1.36E-03
MPD: 12.11%
MD: -1.11E-03
N: 33
OLCI Rrs (sr⁻¹)
In situ Rrs (sr⁻¹)
AAOT Oa05 PB 2.23
R²: 0.88
MAPD: 17.47%
MAD: 7.57E-04
MPD: 8.66%
MD: -4.45E-04
N: 32
OLCI Rrs (sr⁻¹)
In situ Rrs (sr⁻¹)
AAOT Oa05 OC SVC Tool
R²: 0.84
MAPD: 20.20%
MAD: 1.31E-03
MPD: 11.16%
MD: -1.01E-03
N: 33
OLCI Rrs (sr⁻¹)
In situ Rrs (sr⁻¹)
AAOT Oa06 PB 2.23
R²: 0.93
MAPD: 10.19%
MAD: 4.81E-04
MPD: 3.42%
MD: -1.81E-04
N: 32
OLCI Rrs (sr⁻¹)
In situ Rrs (sr⁻¹)
AAOT Oa06 OC SVC Tool
R²: 0.91
MAPD: 15.74%
MAD: 8.88E-04
MPD: 7.47%
MD: -6.08E-04
N: 33
OLCI Rrs (sr⁻¹)
In situ Rrs (sr⁻¹)

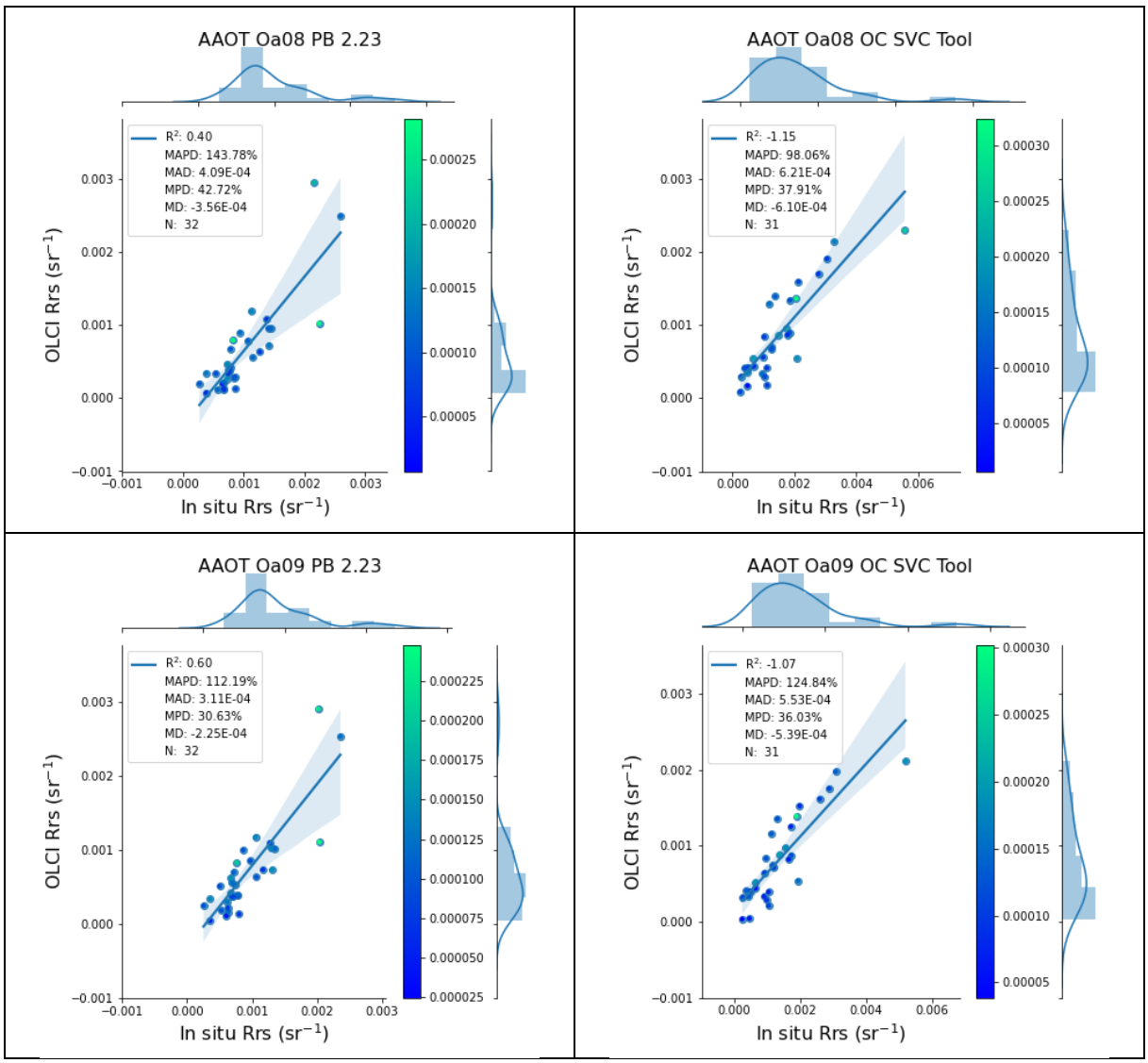

Figure 44. AAOT band individual scatterplots and associated statistics (common match-ups)

GLORIA

GLORIA (GLO) site shows a decrease of the coefficient of determination in the blue bands using the OC-SVC gains, and a maintenance of accuracy from wavelength 510 nm on (B5).

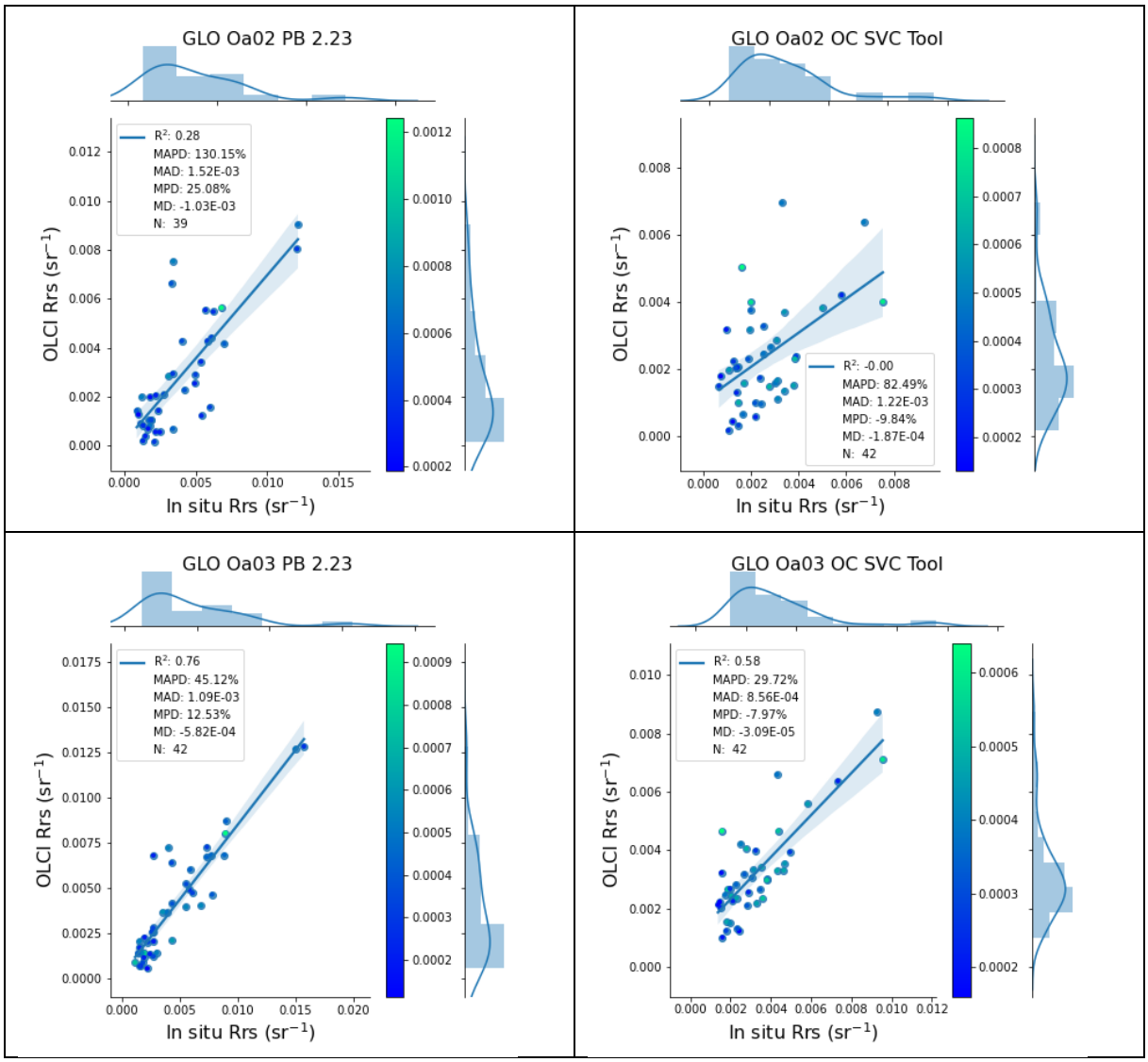

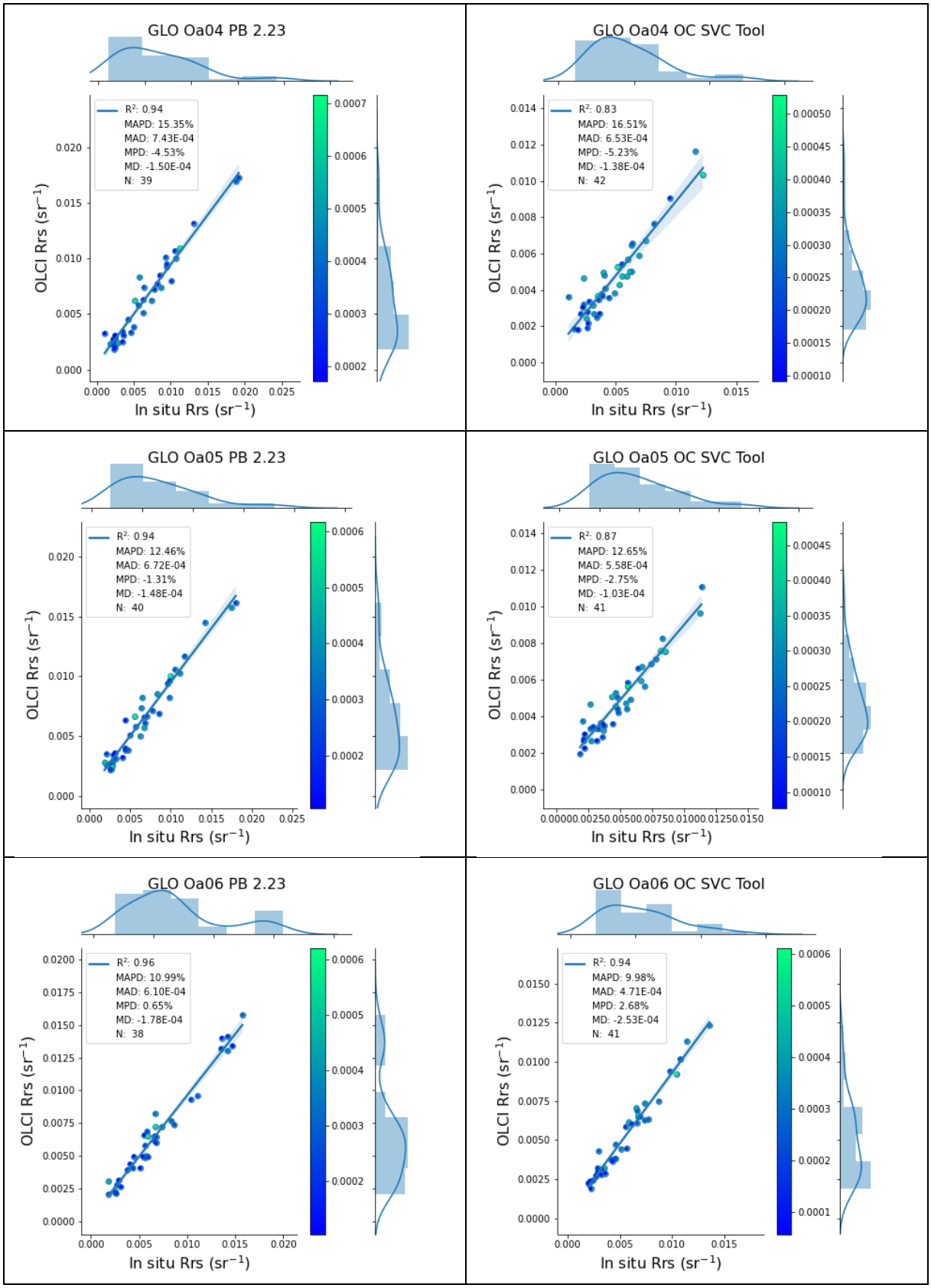
GLO Oa04 PB 2.23
R²: 0.94
MAPD: 15.35%
MAD: 7.43E-04
MPD: -4.53%
MD: -1.50E-04
N: 39
OLCI Rrs (sr⁻¹)
In situ Rrs (sr⁻¹)
GLO Oa04 OC SVC Tool
R²: 0.83
MAPD: 16.51%
MAD: 6.53E-04
MPD: -5.23%
MD: -1.38E-04
N: 42
OLCI Rrs (sr⁻¹)
In situ Rrs (sr⁻¹)
GLO Oa05 PB 2.23
R²: 0.94
MAPD: 12.46%
MAD: 6.72E-04
MPD: -1.31%
MD: -1.48E-04
N: 40
OLCI Rrs (sr⁻¹)
In situ Rrs (sr⁻¹)
GLO Oa05 OC SVC Tool
R²: 0.87
MAPD: 12.65%
MAD: 5.58E-04
MPD: -2.75%
MD: -1.03E-04
N: 41
OLCI Rrs (sr⁻¹)
In situ Rrs (sr⁻¹)
GLO Oa06 PB 2.23
R²: 0.96
MAPD: 10.99%
MAD: 6.10E-04
MPD: 0.65%
MD: -1.78E-04
N: 38
OLCI Rrs (sr⁻¹)
In situ Rrs (sr⁻¹)
GLO Oa06 OC SVC Tool
R²: 0.94
MAPD: 9.98%
MAD: 4.71E-04
MPD: 2.68%
MD: -2.53E-04
N: 41
OLCI Rrs (sr⁻¹)
In situ Rrs (sr⁻¹)

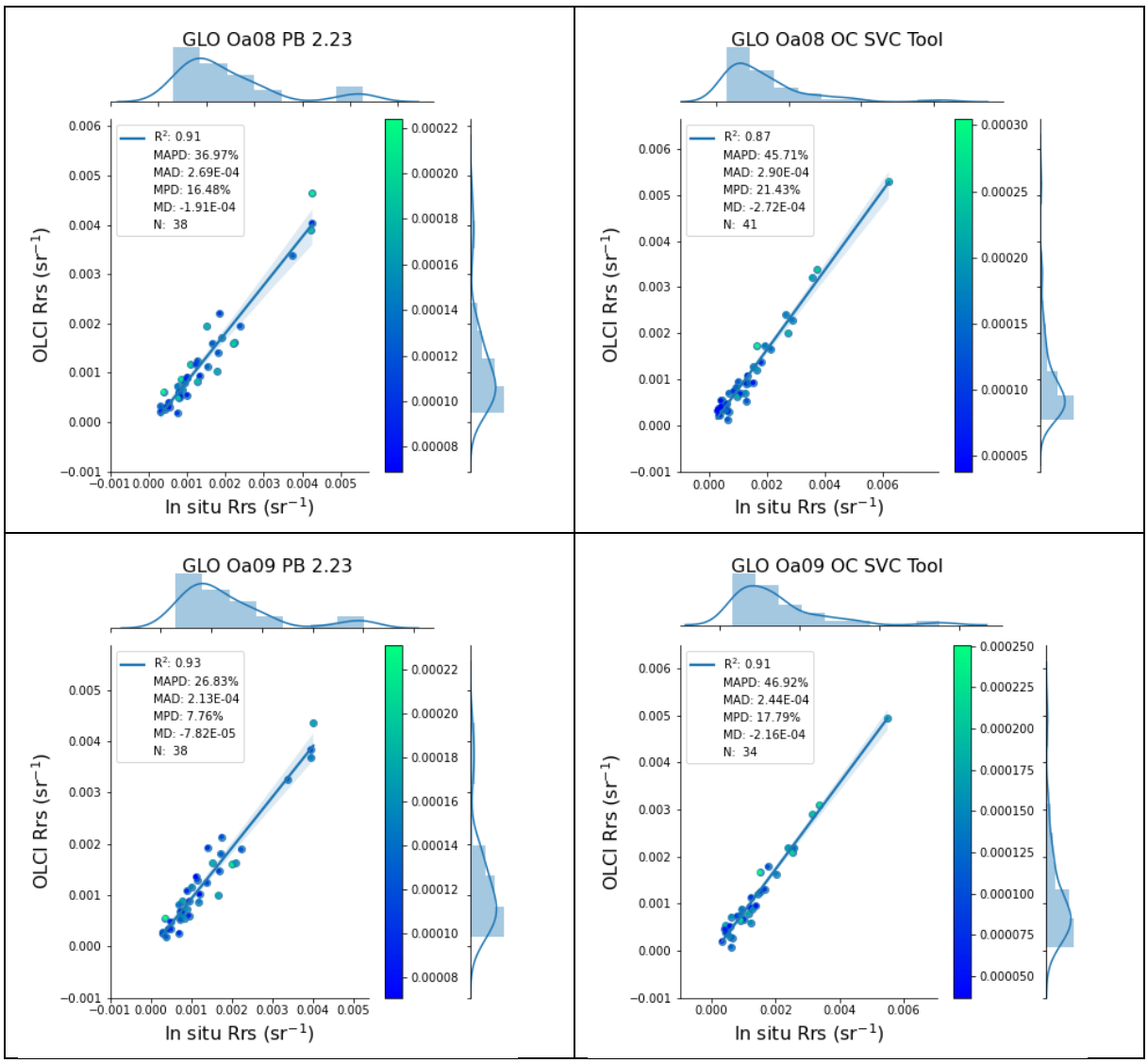

Figure 45. Gloria band individual scatterplots and associated statistics (common match_ups)

Other sites

For other sites, scatter plots using all bands together, and their associated statistics are shown in Figure 46. In some sites the number of matchups seems to increase because there are more bands with data on the SVC cases (GAL, PAL). There are some sites showing a clear improvement of coefficient of determination and errors (BBL, S7P) or decreasing error with less match-ups (GDT, GAL, ZEB). These sites are related to Case 2 waters. In oligotrophic waters there seems not to be much change (CSP, S7P), and only one site shows worse results than the nominal gains (USC).

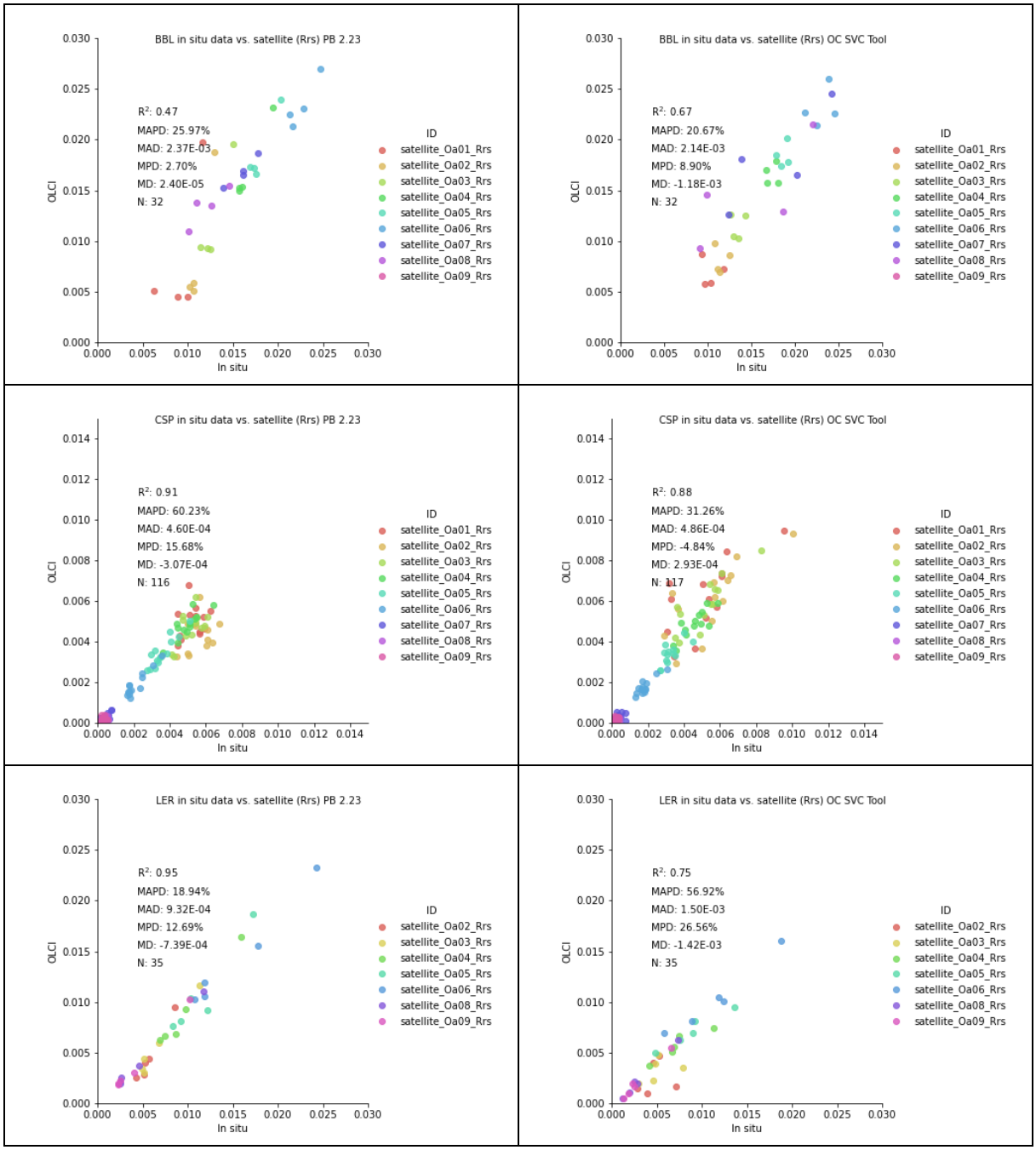

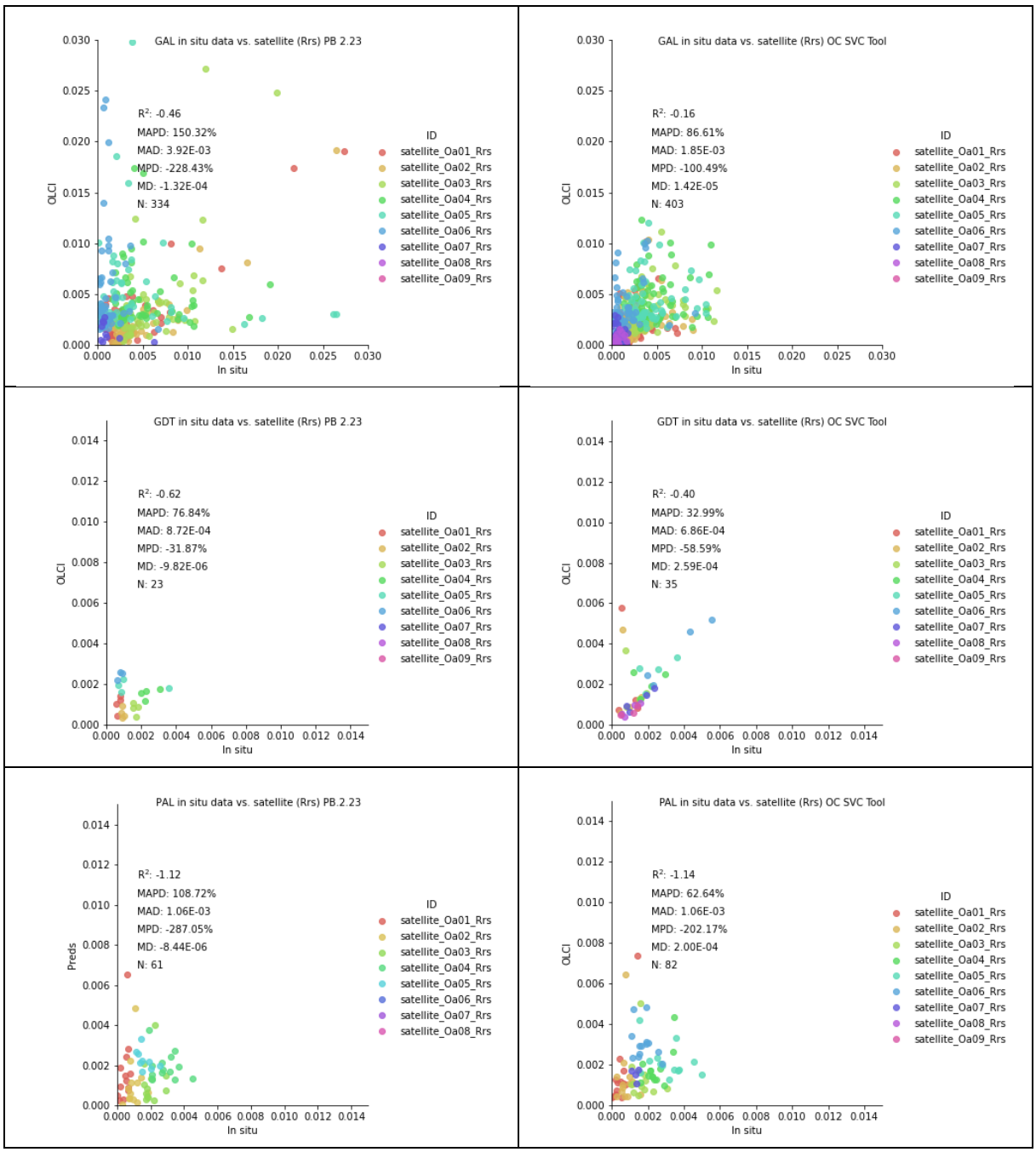
GAL in situ data vs. satellite (Rrs) PB 2.23
R²: -0.46
MAPD: 150.32%
MAD: 3.92E-03
MPD: -228.43%
MD: -1.32E-04
N: 334
OLCI
In situ
ID
satellite_Oa01_Rrs
satellite_Oa02_Rrs
satellite_Oa03_Rrs
satellite_Oa04_Rrs
satellite_Oa05_Rrs
satellite_Oa06_Rrs
satellite_Oa07_Rrs
satellite_Oa08_Rrs
satellite_Oa09_Rrs
GAL in situ data vs. satellite (Rrs) OC SVC Tool
R²: -0.16
MAPD: 86.61%
MAD: 1.85E-03
MPD: -100.49%
MD: 1.42E-05
N: 403
GDT in situ data vs. satellite (Rrs) PB 2.23
R²: -0.62
MAPD: 76.84%
MAD: 8.72E-04
MPD: -31.87%
MD: -9.82E-06
N: 23
GDT in situ data vs. satellite (Rrs) OC SVC Tool
R²: -0.40
MAPD: 32.99%
MAD: 6.86E-04
MPD: -58.59%
MD: 2.59E-04
N: 35
PAL in situ data vs. satellite (Rrs) PB.2.23
R²: -1.12
MAPD: 108.72%
MAD: 1.06E-03
MPD: -287.05%
MD: -8.44E-06
N: 61
Preds
PAL in situ data vs. satellite (Rrs) OC SVC Tool
R²: -1.14
MAPD: 62.64%
MAD: 1.06E-03
MPD: -202.17%
MD: 2.00E-04
N: 82

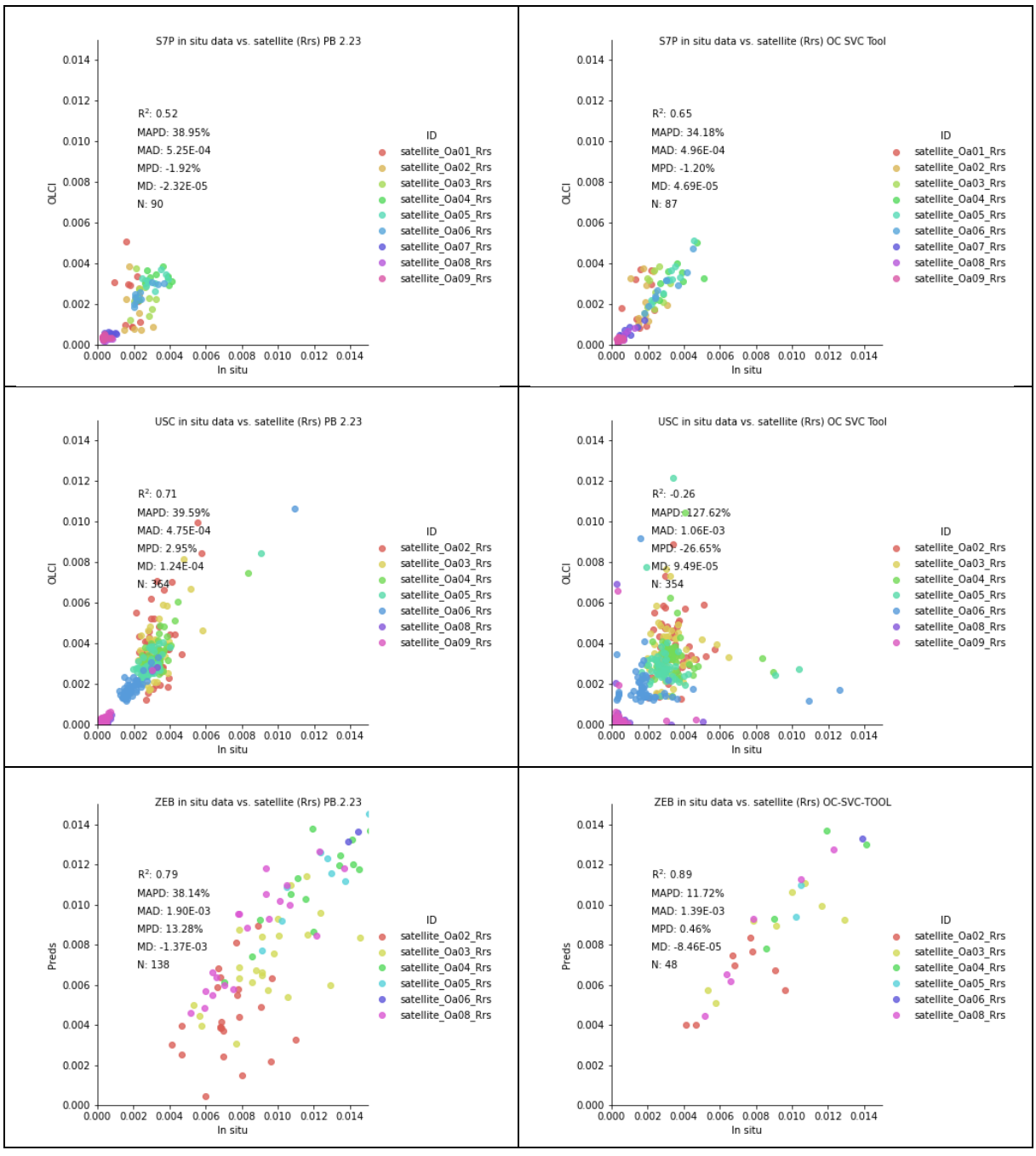

Figure 46 Scatterplots and statitstic calculated for all bands in different sites of the EUMETSAT-AERONET-OC MBD (only PAL and ZEB do not use the common match-ups)

Spectral bias

A better analysis of the statistics can be made using line plots and comparing values of each band per site for the different measurements (Figure 9). We can observe a general decrease of the MAPD (left column) and MPD (right column) in the blue bands with the OC-SVC data practically in all sites except in HLH, LER and USC. For many sites we can also find a reduction in the percentage of error in the red and NIR bands, with the exception again of HLH, LER and USC.

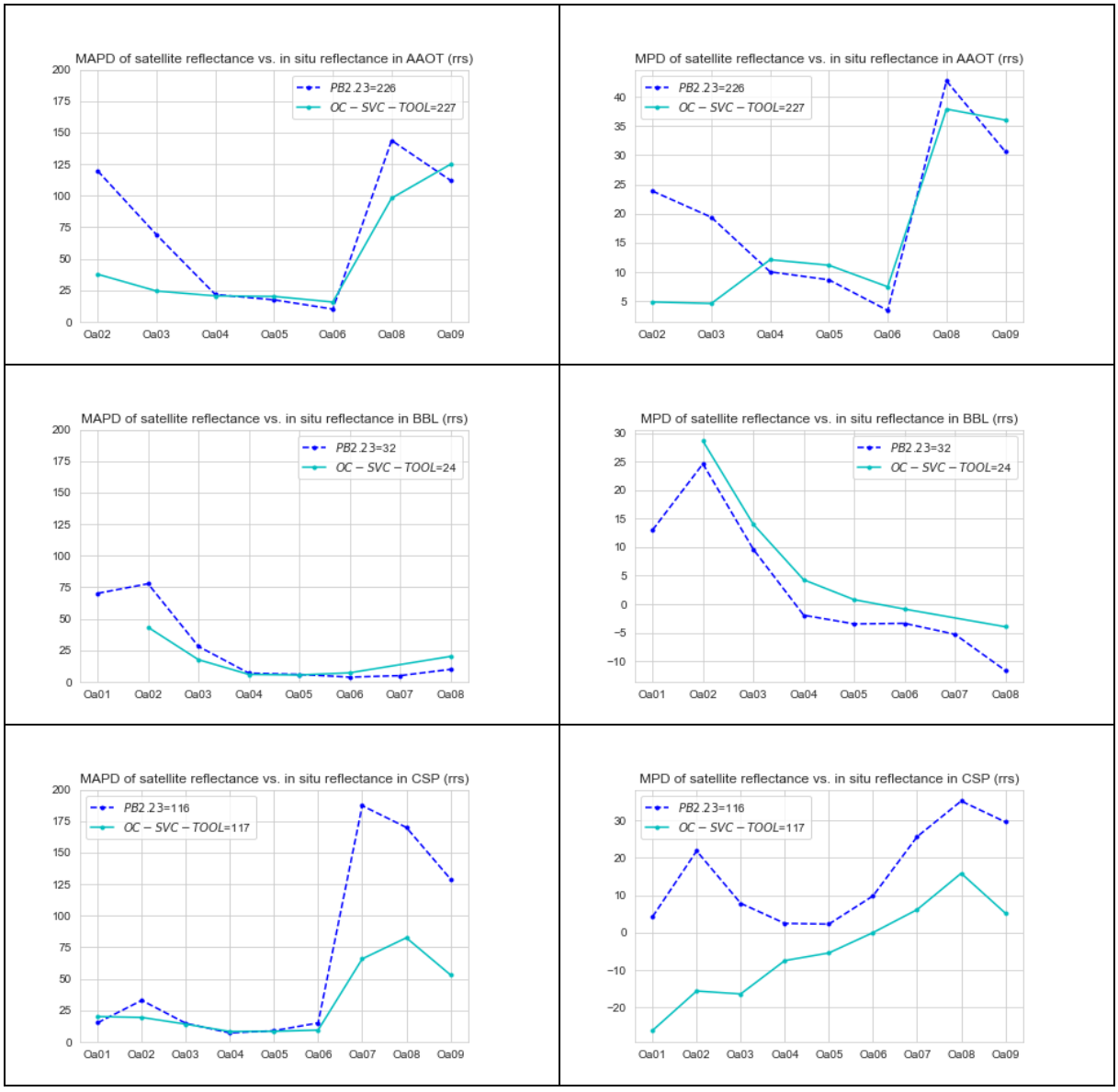

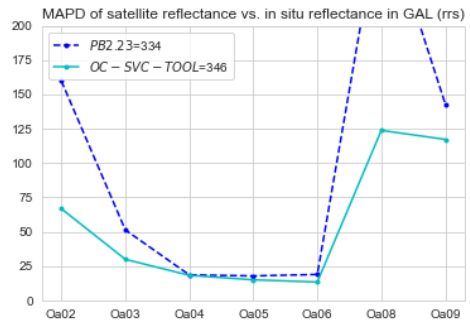
MAPD of satellite reflectance vs. in situ reflectance in GAL (rrs)
PB2.23=334
OC – SVC – TOOL=346
Oa02
Oa03
Oa04
Oa05
Oa06
Oa08
Oa09

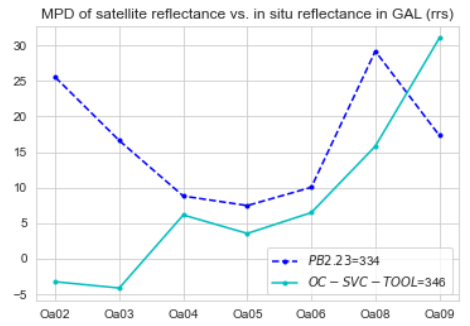
MPD of satellite reflectance vs. in situ reflectance in GAL (rrs)
PB2.23=334
OC – SVC – TOOL=346
Oa02
Oa03
Oa04
Oa05
Oa06
Oa08
Oa09

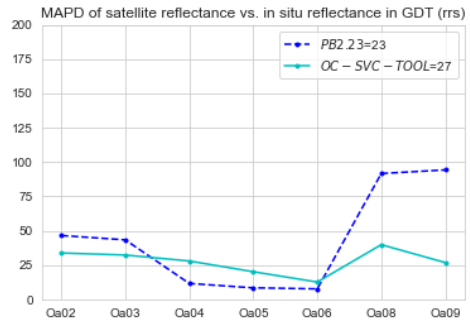
MAPD of satellite reflectance vs. in situ reflectance in GDT (rrs)
PB2.23=23
OC – SVC – TOOL=27
Oa02
Oa03
Oa04
Oa05
Oa06
Oa08
Oa09

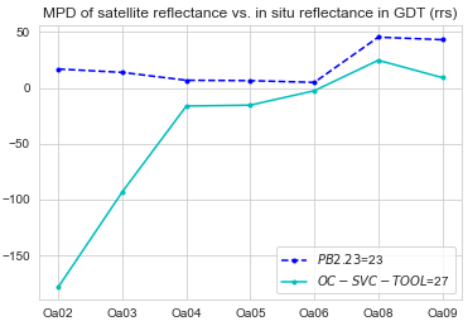
MPD of satellite reflectance vs. in situ reflectance in GDT (rrs)
PB2.23=23
OC – SVC – TOOL=27
Oa02
Oa03
Oa04
Oa05
Oa06
Oa08
Oa09

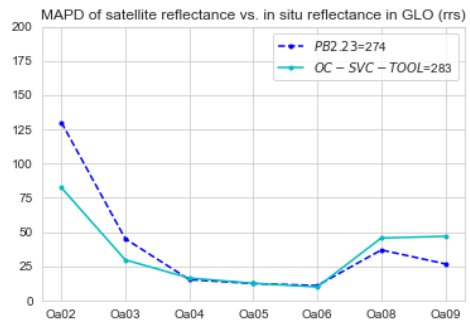
MAPD of satellite reflectance vs. in situ reflectance in GLO (rrs)
PB2.23=274
OC – SVC – TOOL=283
Oa02
Oa03
Oa04
Oa05
Oa06
Oa08
Oa09

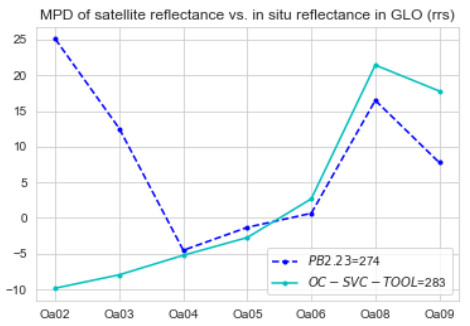
MPD of satellite reflectance vs. in situ reflectance in GLO (rrs)
PB2.23=274
OC – SVC – TOOL=283
Oa02
Oa03
Oa04
Oa05
Oa06
Oa08
Oa09

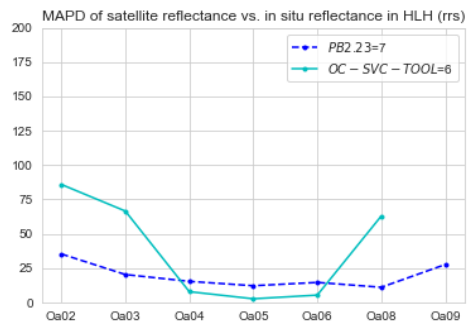
MAPD of satellite reflectance vs. in situ reflectance in HLH (rrs)
PB2.23=7
OC – SVC – TOOL=6
Oa02
Oa03
Oa04
Oa05
Oa06
Oa08
Oa09

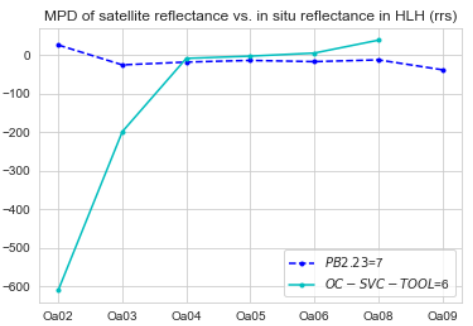
MPD of satellite reflectance vs. in situ reflectance in HLH (rrs)
PB2.23=7
OC – SVC – TOOL=6
Oa02
Oa03
Oa04
Oa05
Oa06
Oa08
Oa09

Figure 9. Line-plots with comparison of Mean Absolute Percentage Difference (MAPD, left) and Mean Percentage Differece (MPD, right) for all EUMETSAT MDB sites

4.5.2 IMPACT ON OLCI-B MATCH-UPS

Venice Tower (AAOT)

AAOT shows a clear improvement of values when using OC-SCV-TOOL gains both in coefficient of determination and error (Figure 47). This is visible even better when plotting all bands together, how the dispersion of the points decreases.

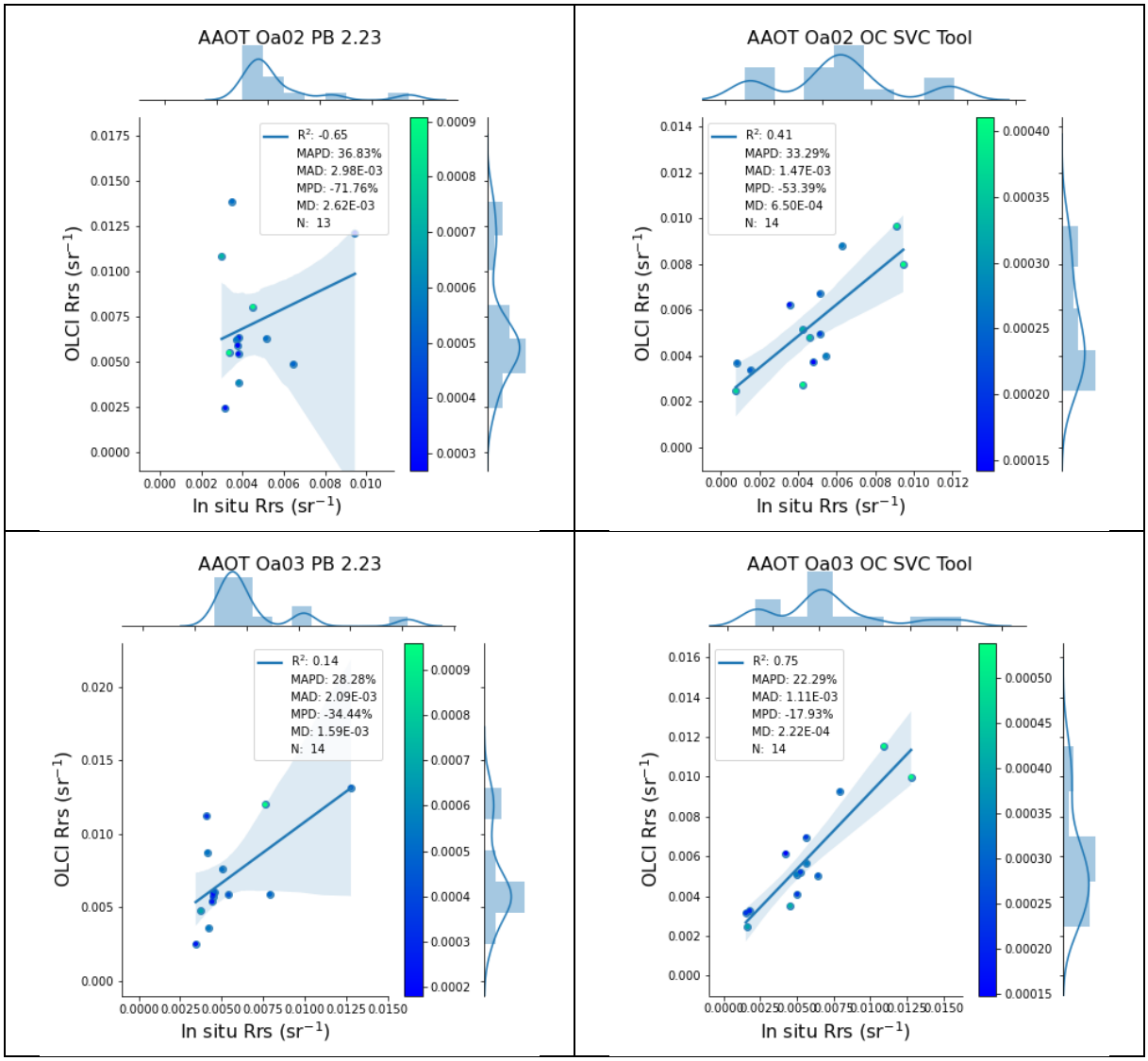

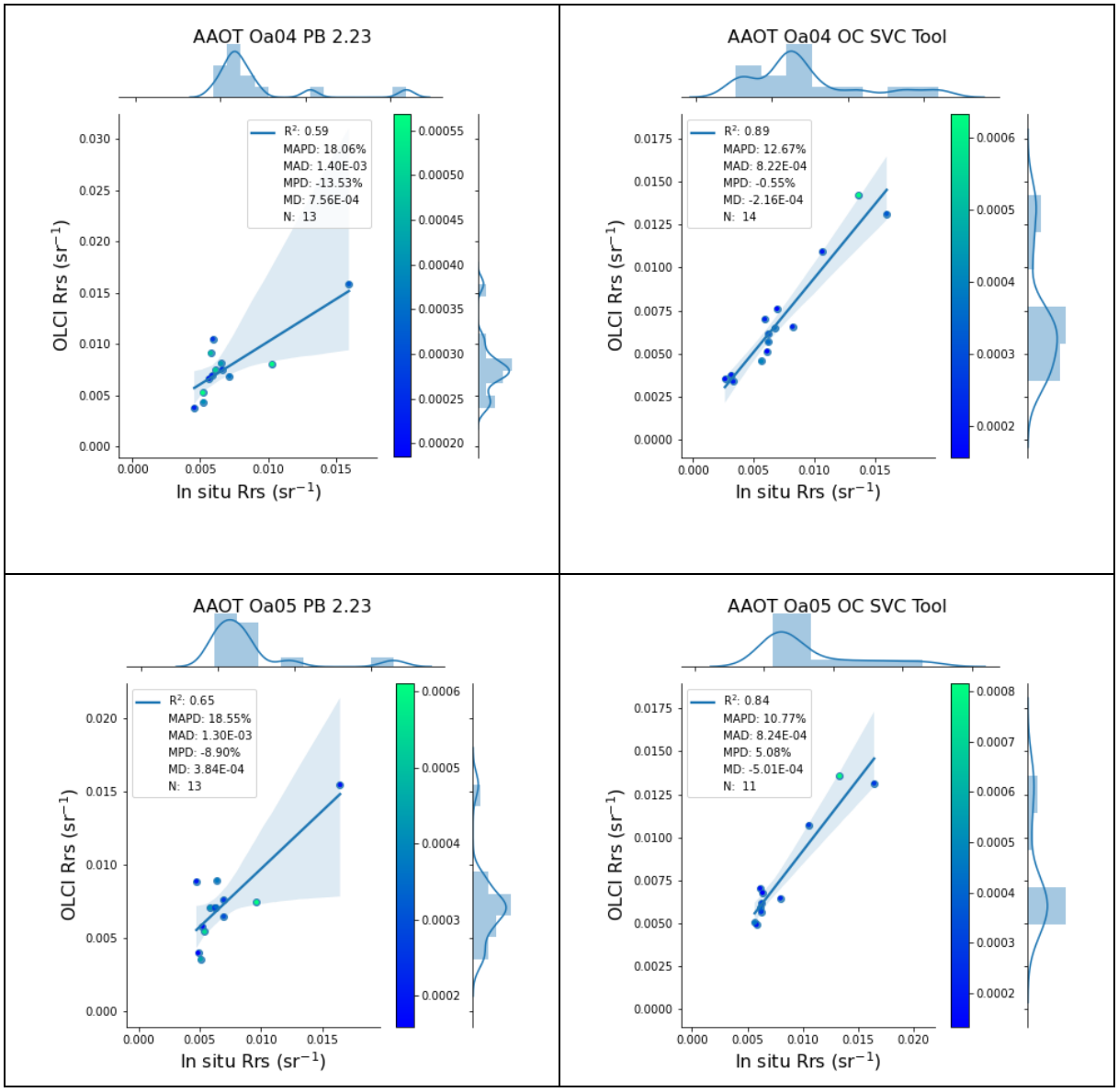
AAOT Oa04 PB 2.23
R²: 0.59
MAPD: 18.06%
MAD: 1.40E-03
MPD: -13.53%
MD: 7.56E-04
N: 13
OLCI Rrs (sr⁻¹)
In situ Rrs (sr⁻¹)
AAOT Oa04 OC SVC Tool
R²: 0.89
MAPD: 12.67%
MAD: 8.22E-04
MPD: -0.55%
MD: -2.16E-04
N: 14
OLCI Rrs (sr⁻¹)
In situ Rrs (sr⁻¹)
AAOT Oa05 PB 2.23
R²: 0.65
MAPD: 18.55%
MAD: 1.30E-03
MPD: -8.90%
MD: 3.84E-04
N: 13
OLCI Rrs (sr⁻¹)
In situ Rrs (sr⁻¹)
AAOT Oa05 OC SVC Tool
R²: 0.84
MAPD: 10.77%
MAD: 8.24E-04
MPD: 5.08%
MD: -5.01E-04
N: 11
OLCI Rrs (sr⁻¹)
In situ Rrs (sr⁻¹)

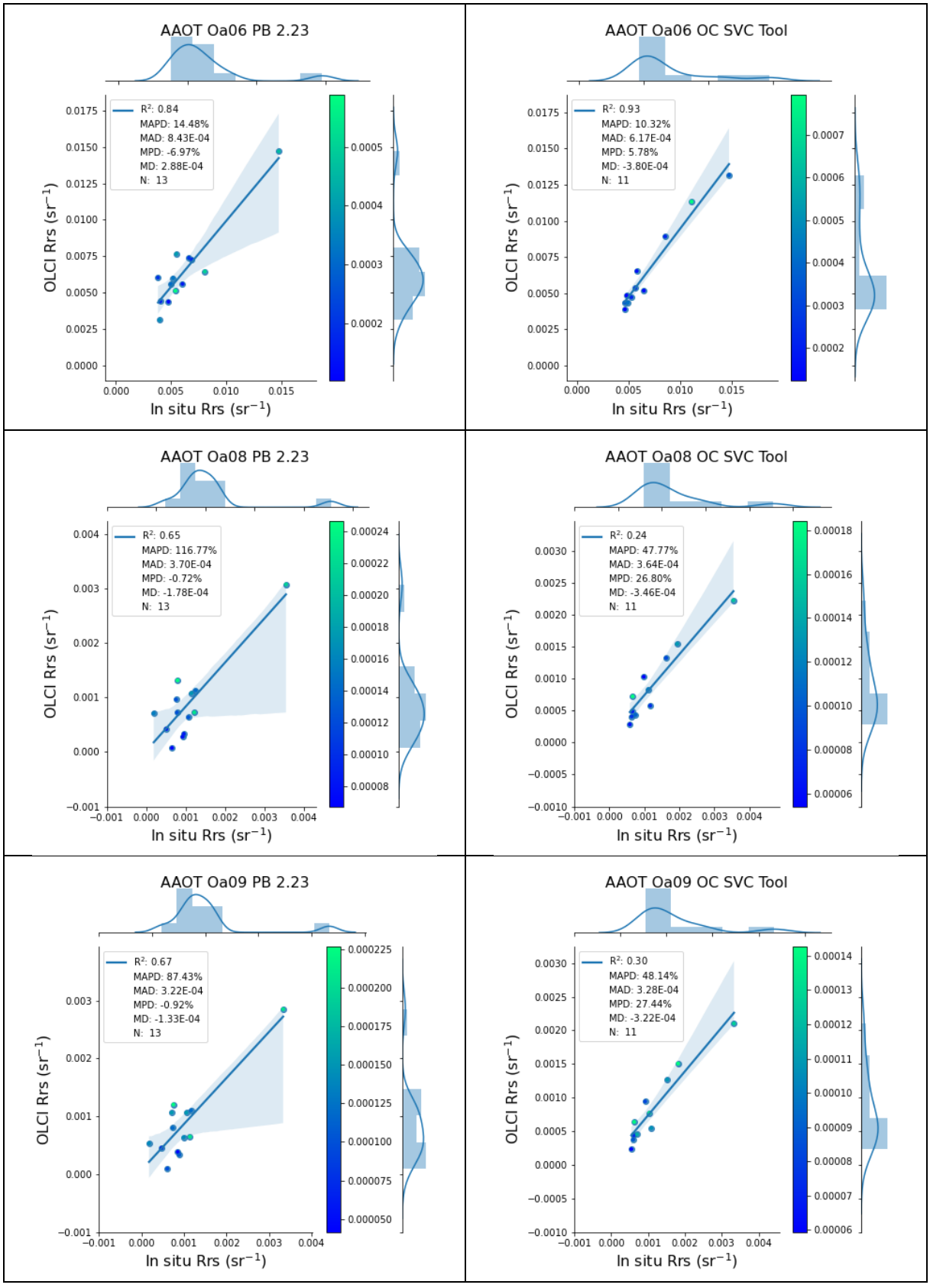
AAOT Oa06 PB 2.23
R²: 0.84
MAPD: 14.48%
MAD: 8.43E-04
MPD: -6.97%
MD: 2.88E-04
N: 13
OLCI Rrs (sr⁻¹)
In situ Rrs (sr⁻¹)
AAOT Oa06 OC SVC Tool
R²: 0.93
MAPD: 10.32%
MAD: 6.17E-04
MPD: 5.78%
MD: -3.80E-04
N: 11
OLCI Rrs (sr⁻¹)
In situ Rrs (sr⁻¹)
AAOT Oa08 PB 2.23
R²: 0.65
MAPD: 116.77%
MAD: 3.70E-04
MPD: -0.72%
MD: -1.78E-04
N: 13
OLCI Rrs (sr⁻¹)
In situ Rrs (sr⁻¹)
AAOT Oa08 OC SVC Tool
R²: 0.24
MAPD: 47.77%
MAD: 3.64E-04
MPD: 26.80%
MD: -3.46E-04
N: 11
OLCI Rrs (sr⁻¹)
In situ Rrs (sr⁻¹)
AAOT Oa09 PB 2.23
R²: 0.67
MAPD: 87.43%
MAD: 3.22E-04
MPD: -0.92%
MD: -1.33E-04
N: 13
OLCI Rrs (sr⁻¹)
In situ Rrs (sr⁻¹)
AAOT Oa09 OC SVC Tool
R²: 0.30
MAPD: 48.14%
MAD: 3.28E-04
MPD: 27.44%
MD: -3.22E-04
N: 11
OLCI Rrs (sr⁻¹)
In situ Rrs (sr⁻¹)

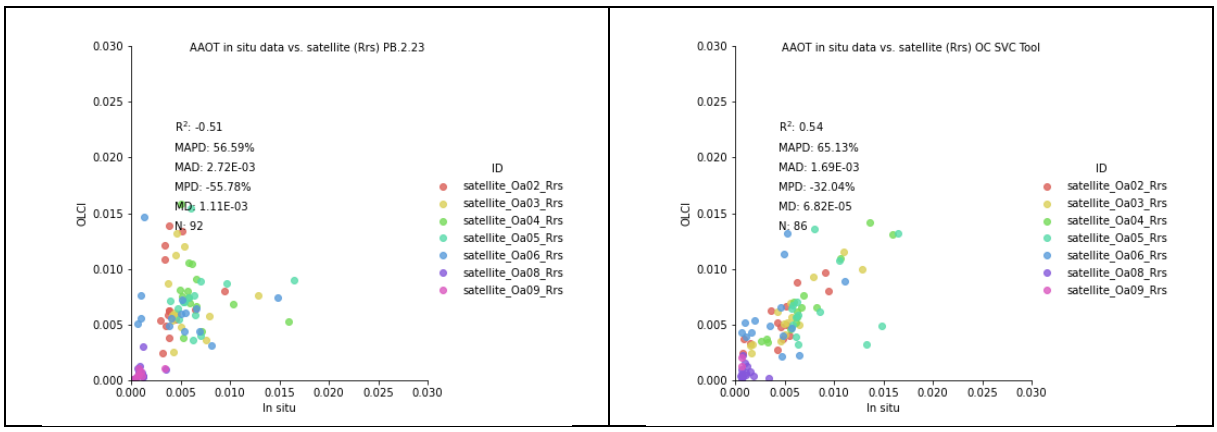

Figure 47. AAOT common matchups analysis for PB 2. 23 and OC-SVC-Tool results

Other sites

For other sites, scatter plots using all band together, and their associated statistics are shown in Figure 48. There is a general improvement for BBL, GAL and USC when using the gains. CSP and S7P lose accuracy and increases dispersion.

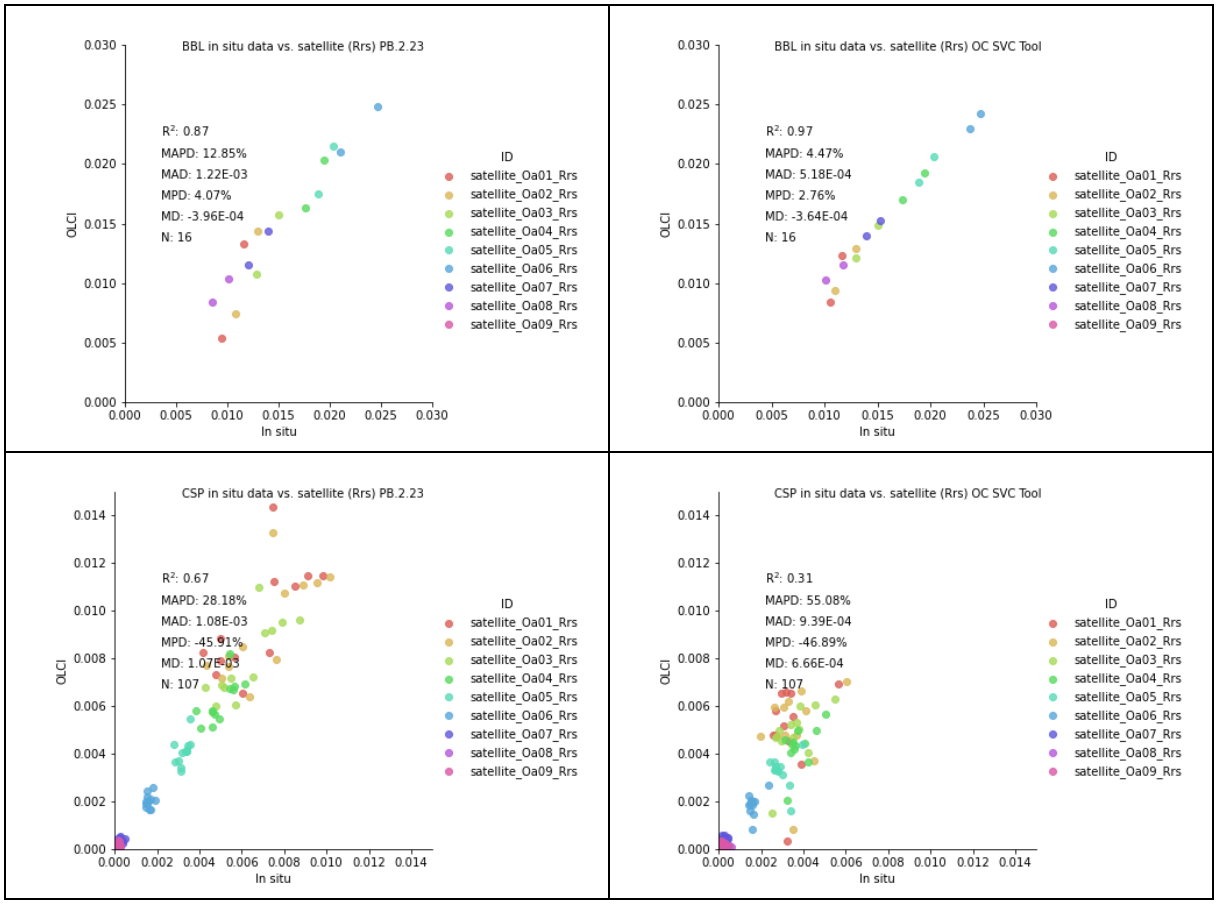

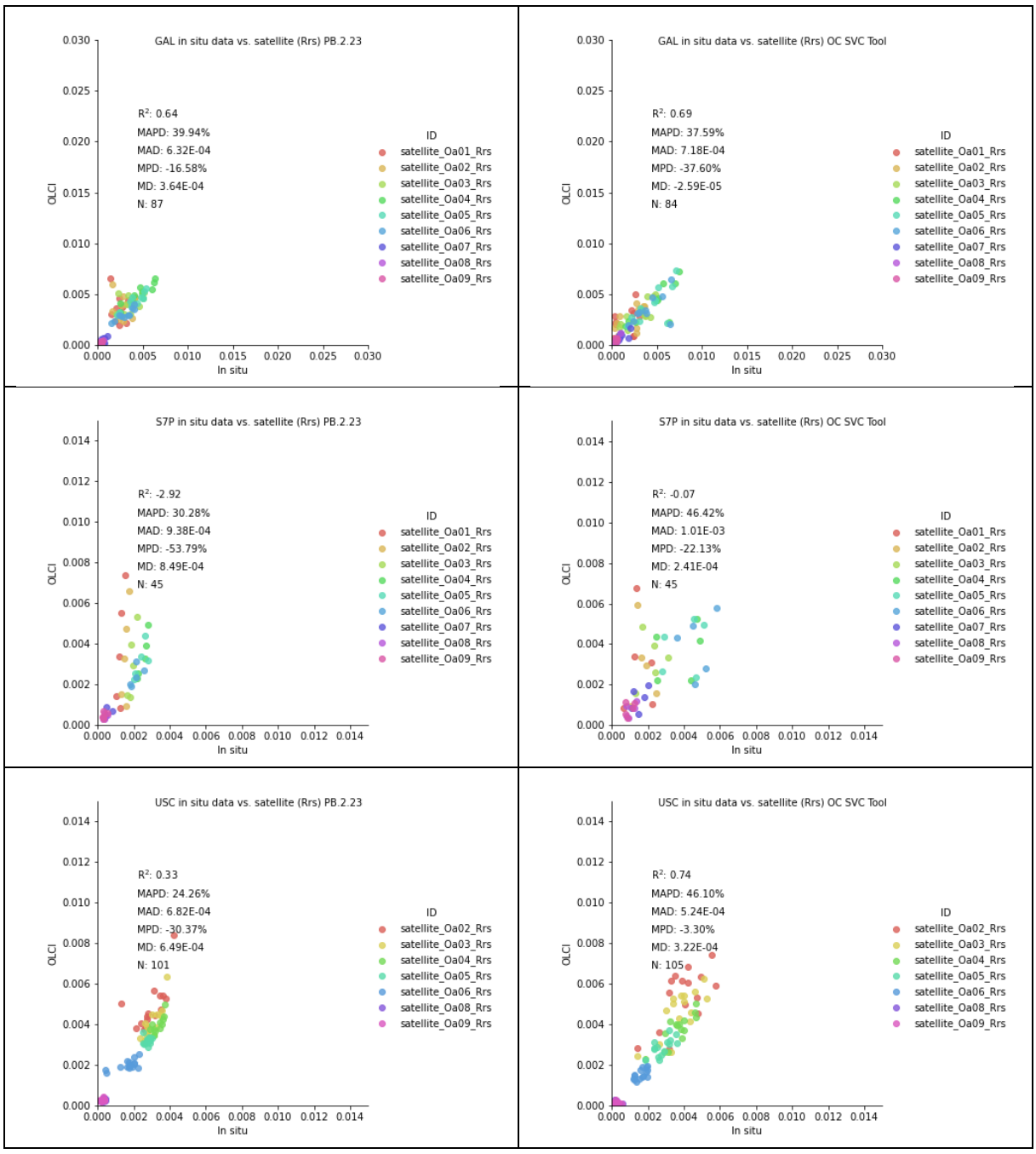

Figure 48. Scatterplots and statitstic calculated for all bands in different sites of the EUMETSAT-Aeronet MBD for the common match-ups

Spectral bias

The OC-SVC gains improve the MAPD and MPD in the blue bands except for CSP and GAL. In the red and NIR the improvement is visible is AAOT, GAL; while CSP, S7P and USC are the exception. Bias can be analysed through the MPD, with a clear decrease in AAOT, S7P and USC.

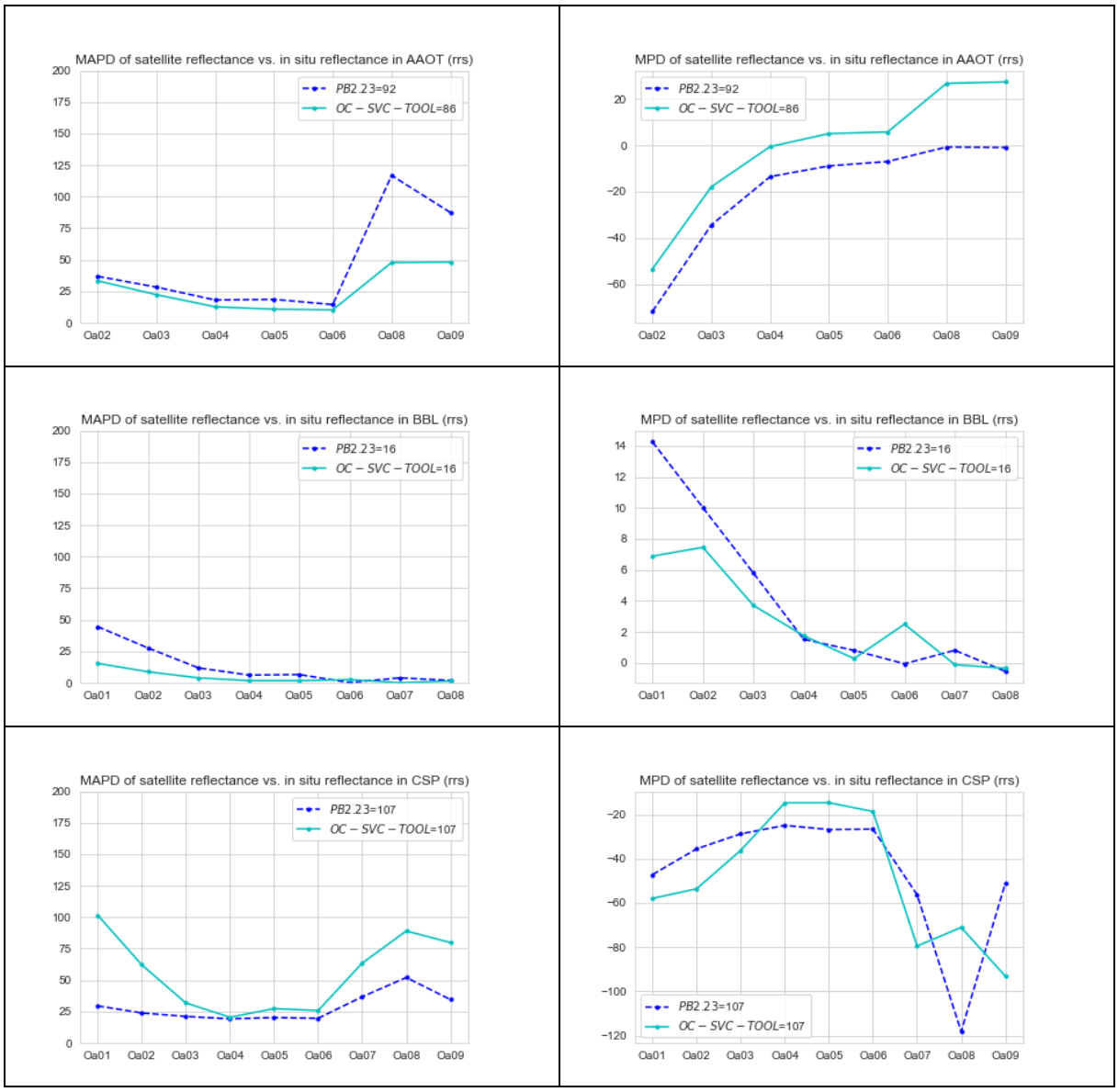

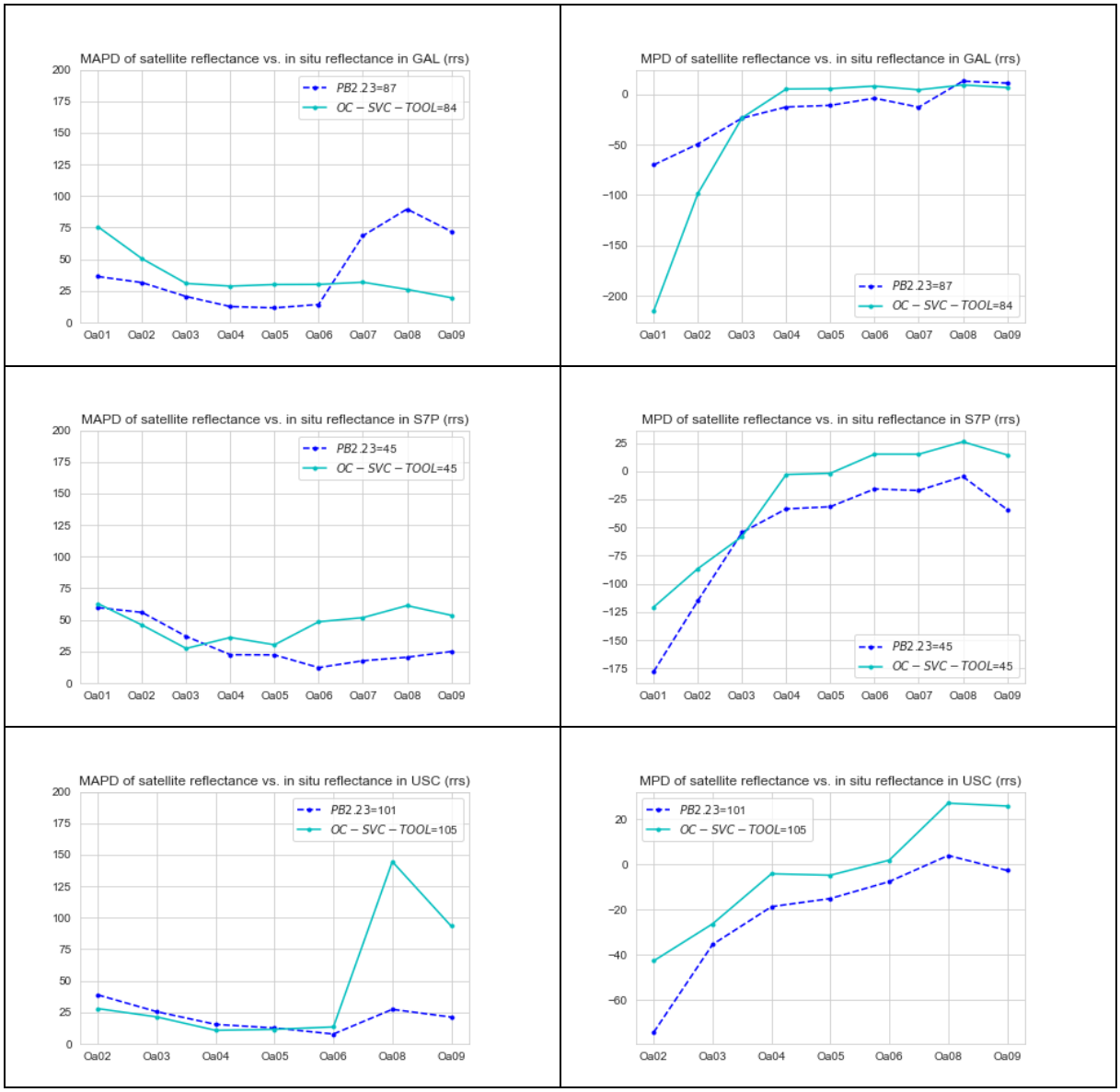

Figure 49. Line-plots with comparison of Mean Absolute Percentage Difference (MAPD), the Mean Percentage Differece (MPD) for all EUMETSAT MDB sites available

4.5.3 ANALYSIS ON LEVEL-3 PRODUCTS

Monthly Level-3 products of OLCI-A and OLCI-B marine reflectance have been generated by EUMETSAT from July 2018 to July 2020, for current PB2.23 and the more recent IPF with OC-SVC-TOOL gains. The analysis is done over different water types: oligotrophic, mesotrophic and eutrophic waters. When bands are relevant, Level-3 of MODIS-Aqua reflectance are also displayed, but it should be emphasized that the wavelengths are not strictly identical to OLCI and may produce differences (no band shift was applied).

Note also that reflectance at some bands in the NIR (753, 779, 865, 885) are not directly comparable between the two OLCI processors: IPF 2.23 provides output of BPC while IPF used for the OC-SVC-TOOL provides output of CWAC.

The excellent agreement between OLCI-A and OLCI-B shown in the next plots for the OC-SVC-TOOL configuration demonstrates the importance to have a consistent SVC process for data harmonization: harmonized database of high-quality in-situ data, with harmonized protocols and process.

4.5.3.1 OLIGOTROPHIC WATERS

The new SVC shows a clear improvement (Figure 50): relative difference between OLCI-A and OLCI-B is below 2.5% at all bands from 400 to 560 nm, through the full time-series, while it is over 10% for PB2.23. A good comparison with MODIS can also be seen at bands 412, 443, but not 490, 560 and 665 where spectral differences are higher.

There is also an improved agreement between OLCI-A and OLCI-B in the red, up to 1020 nm despite over such clear waters the signal is extremely small and relative difference become meaningless.

PB2.23	OC-SVC-TOOL
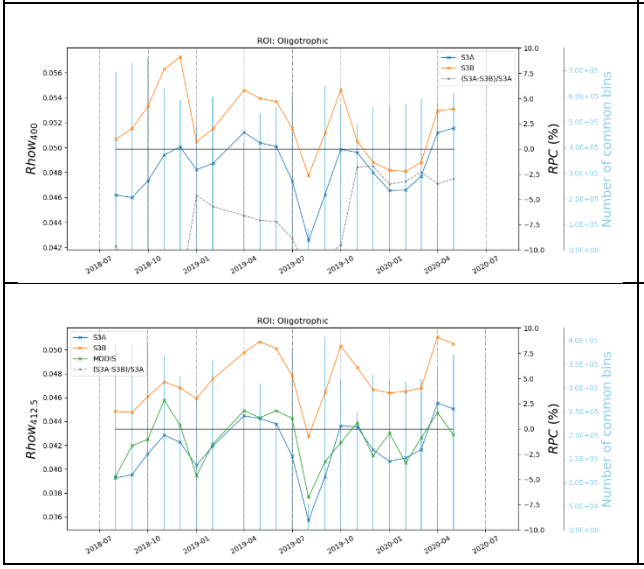	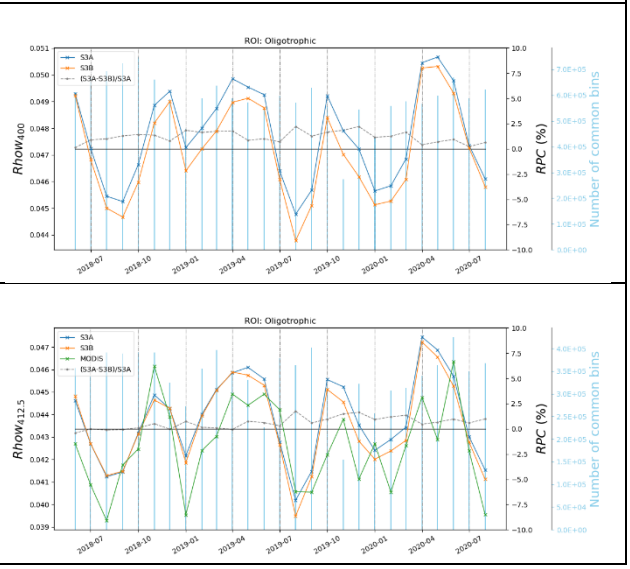

PB2.23	OC-SVC-TOOL
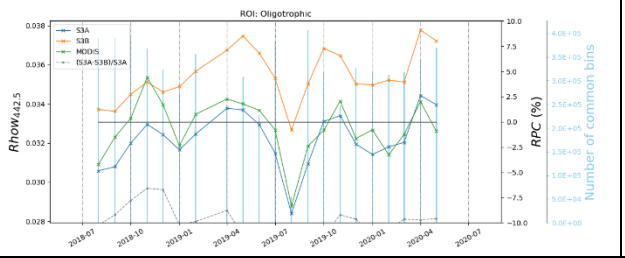	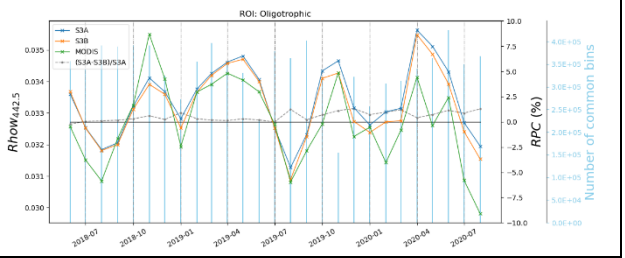
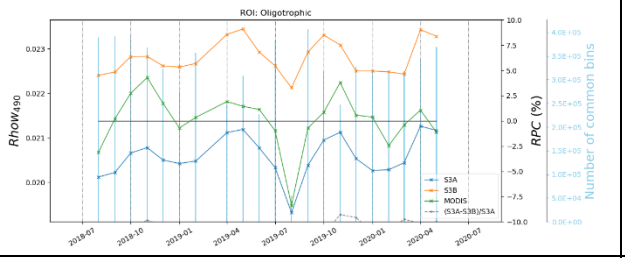	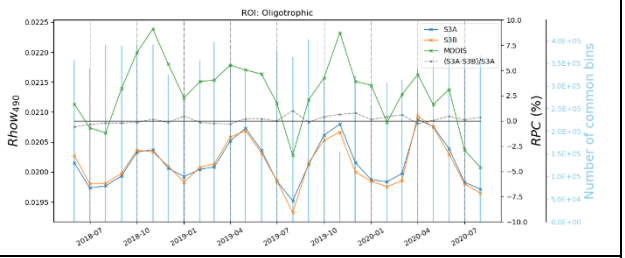
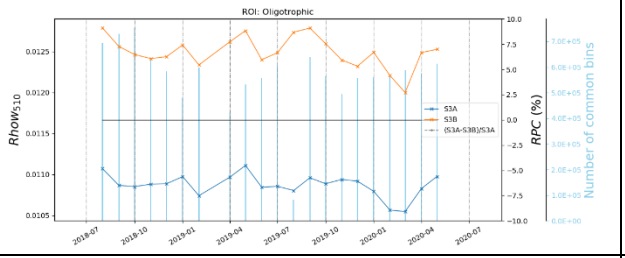	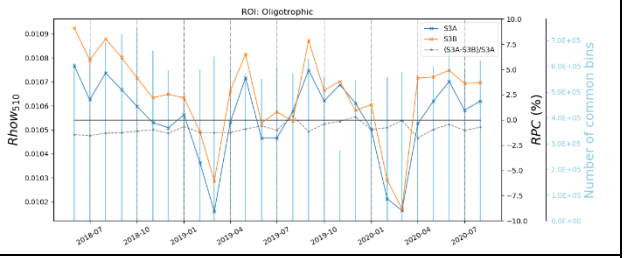
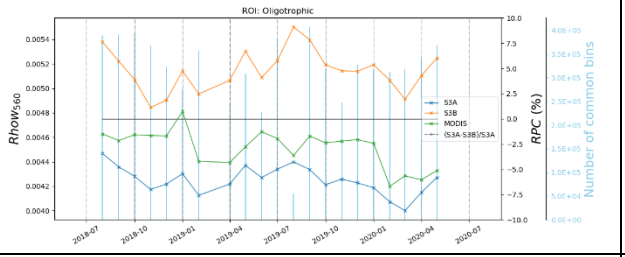	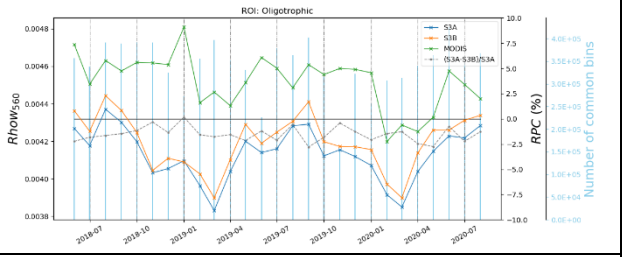
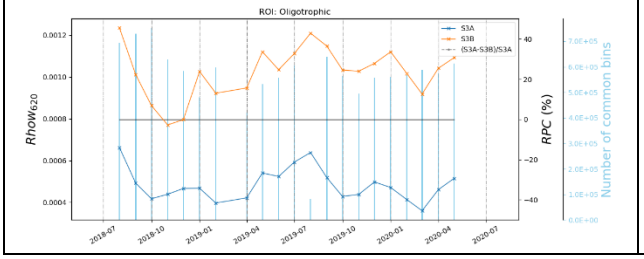	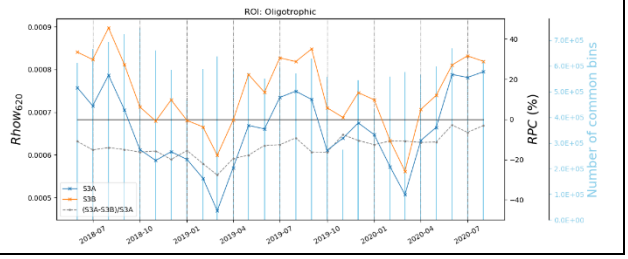

PB2.23	OC-SVC-TOOL
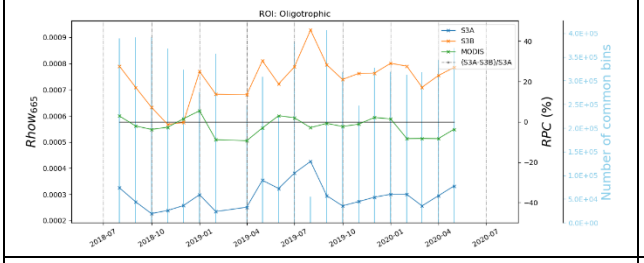	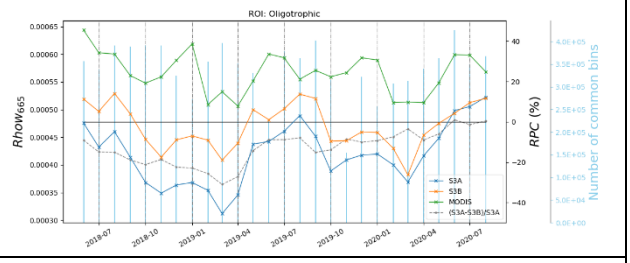
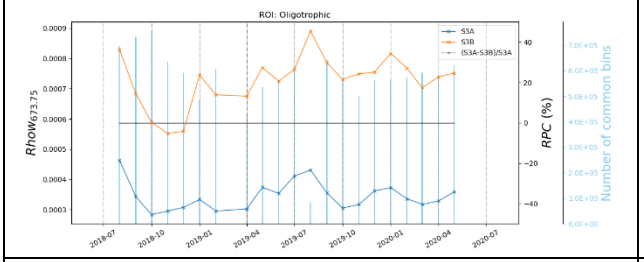	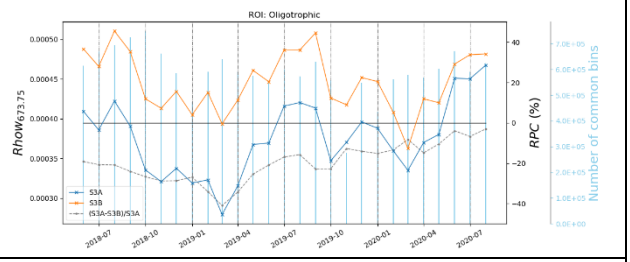
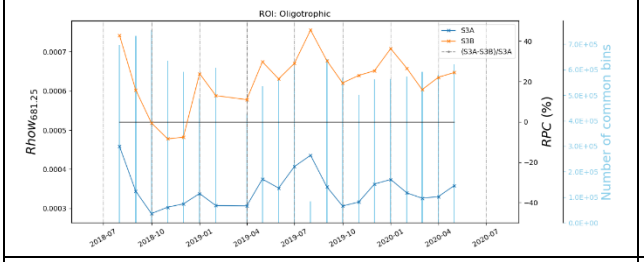	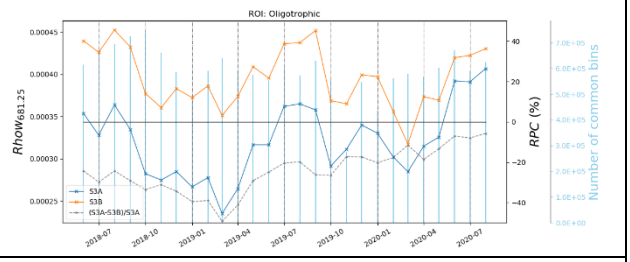
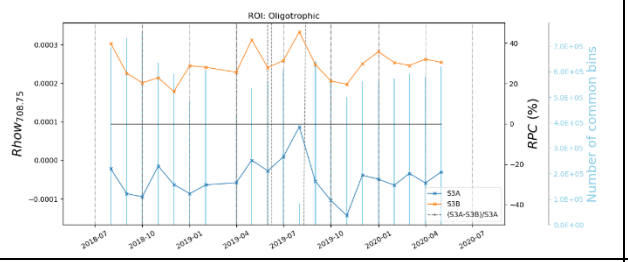	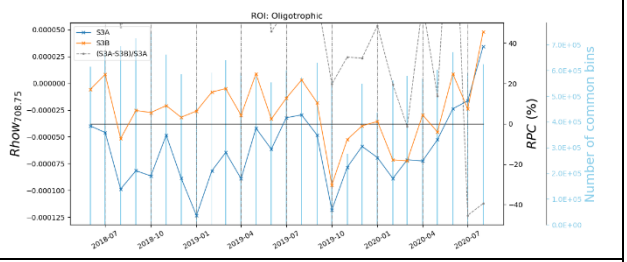
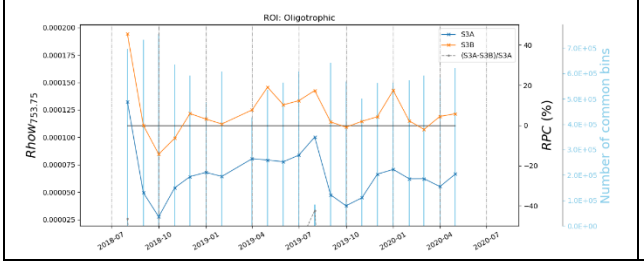	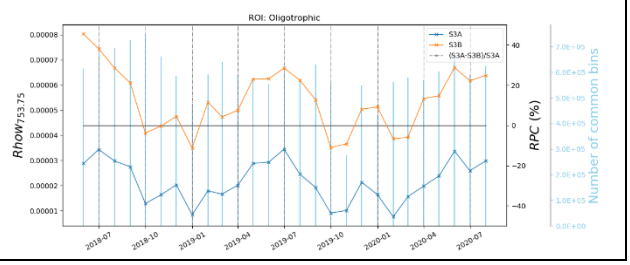

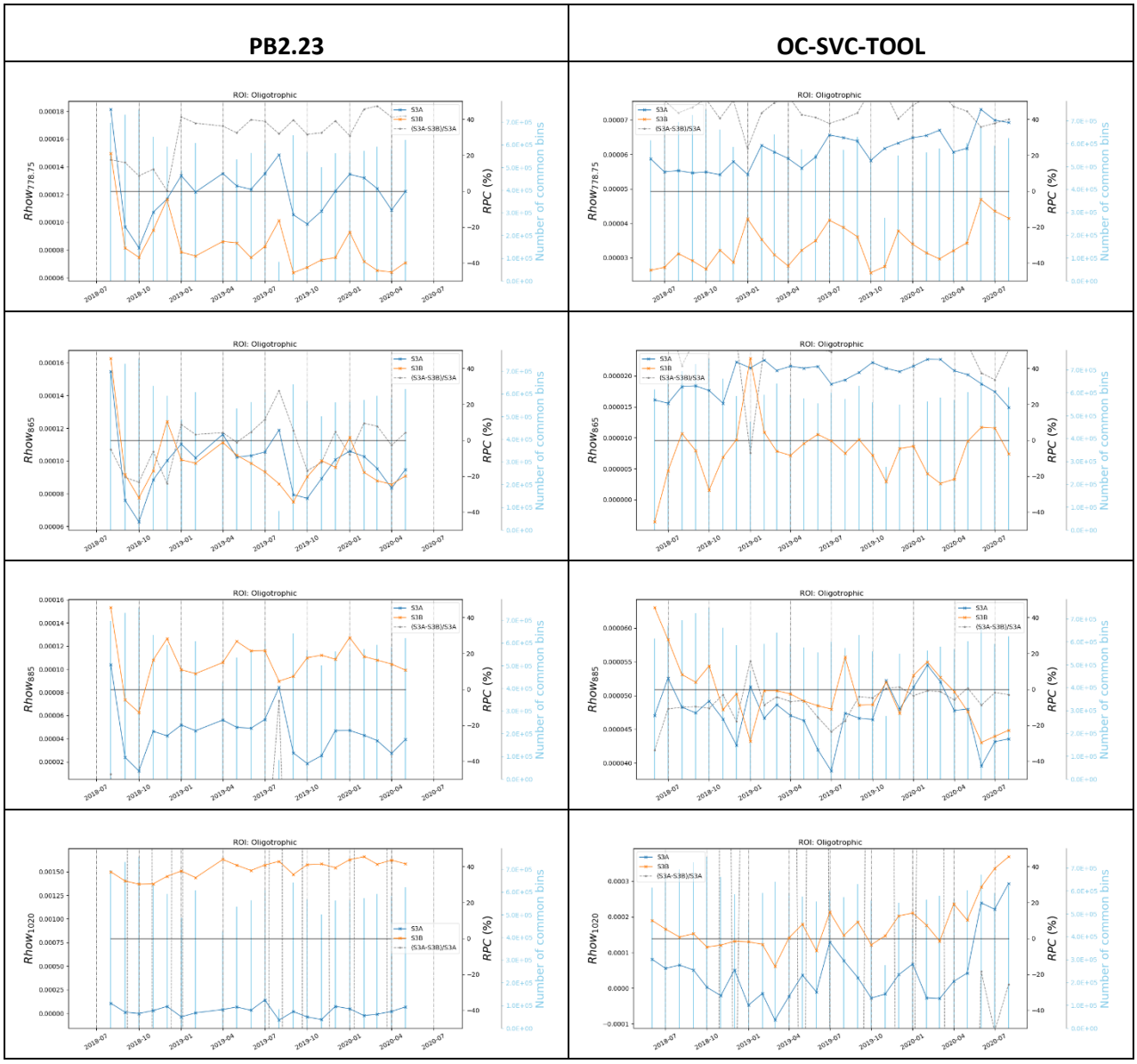

Figure 50 Time-series of Level-3 marine reflectance over oligotrophic waters at all VIS and NIR bands (top to bottom) for OLCI-A (orange), OLCI-B (blue) and, when relevant, MODIS-Aqua (green). Relative difference between S3A and S3B in grey (second y-axis). Left: OLCI data from PB2.23, right with new IPF and OLC-SVC-TOOL gains.

4.5.3.2 MESOTROPHIC WATERS

We observe again a large improvement with the OC-SVC-TOOL gains (Figure 51), with relative difference between OLCI-A and OLCI-B below 2.5 % while they were out of scale for PB2.23. In the red, up to 681 nm, agreement is within 20%, half of that of PB.2.23

PB2.23	OC-SVC-TOOL
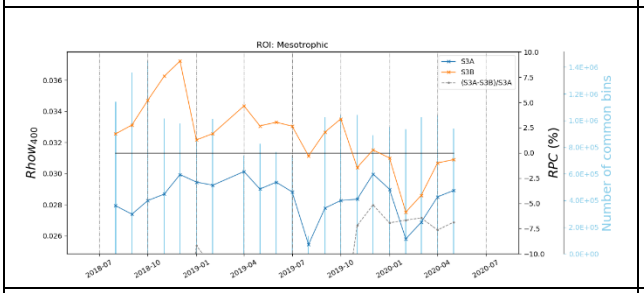	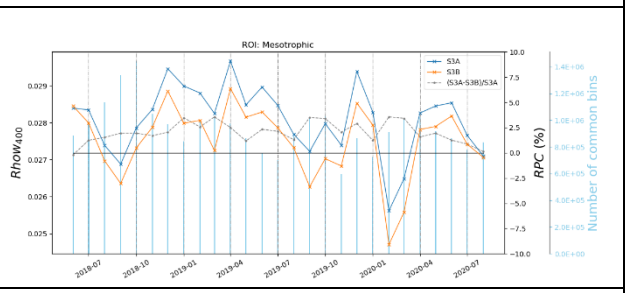
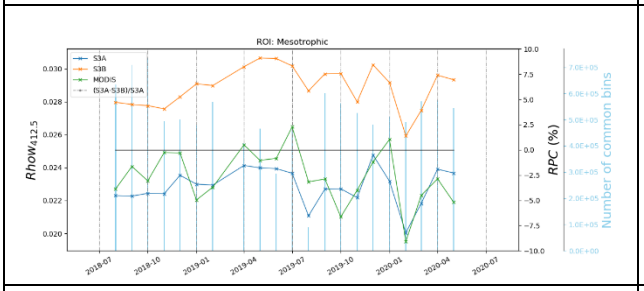	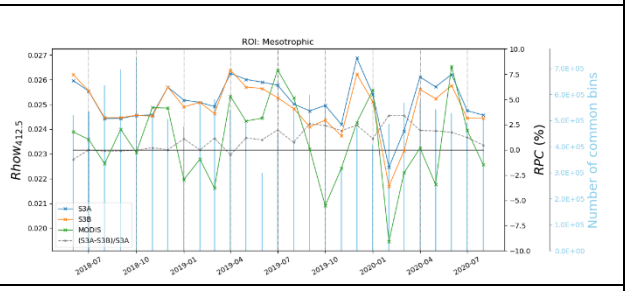
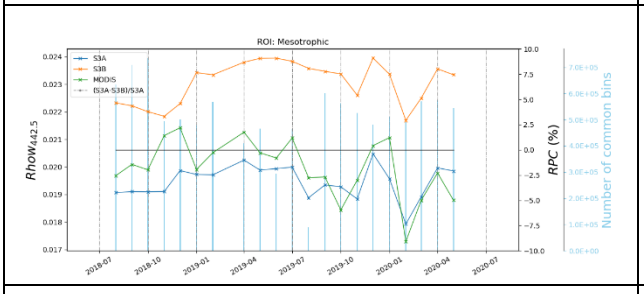	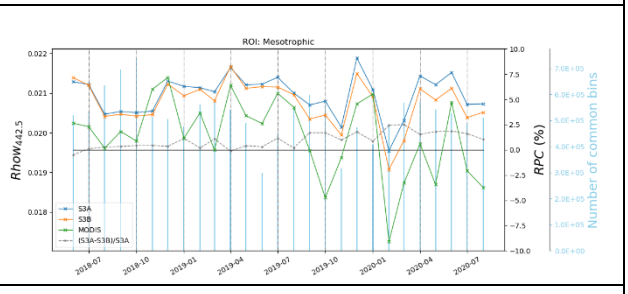
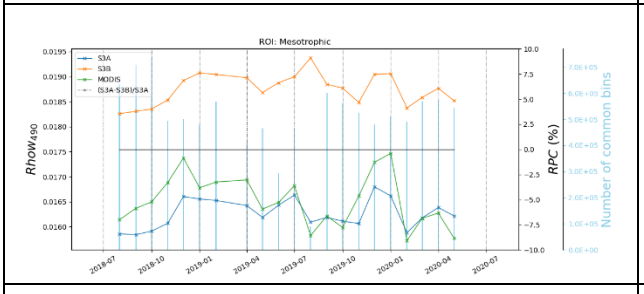	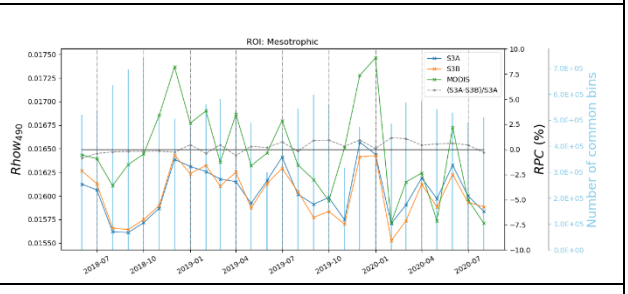
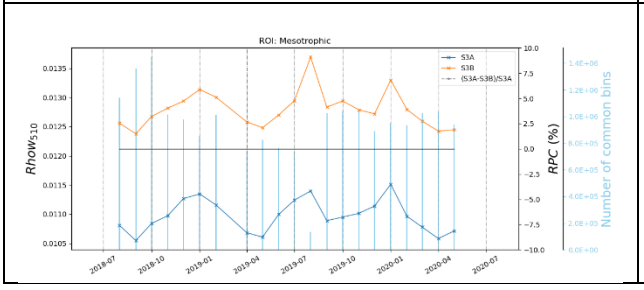	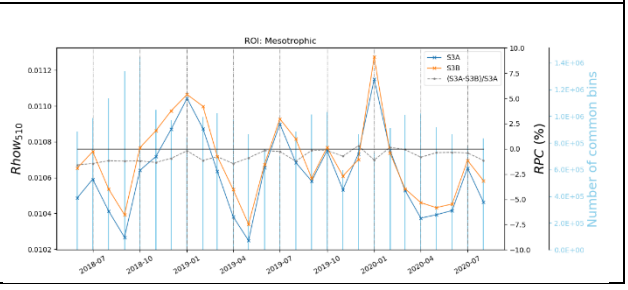

PB2.23	OC-SVC-TOOL
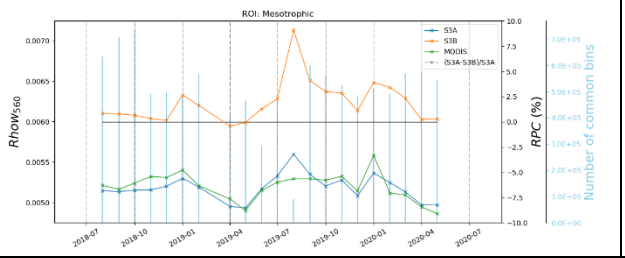	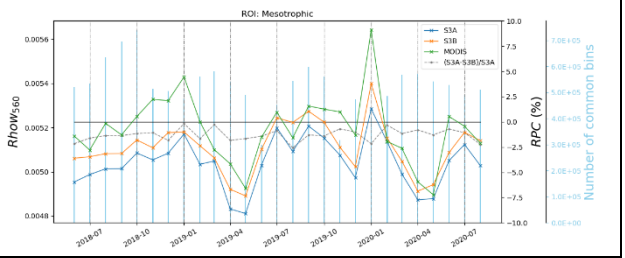
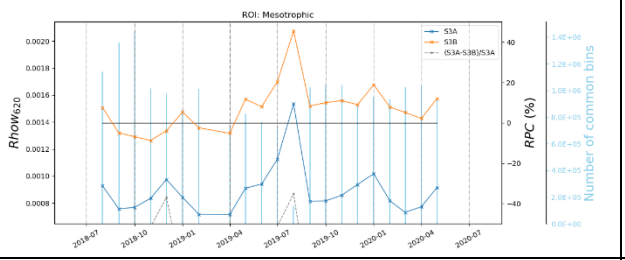	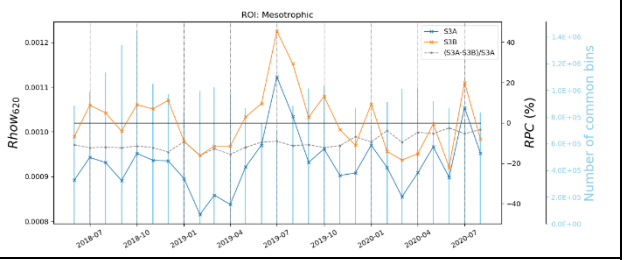
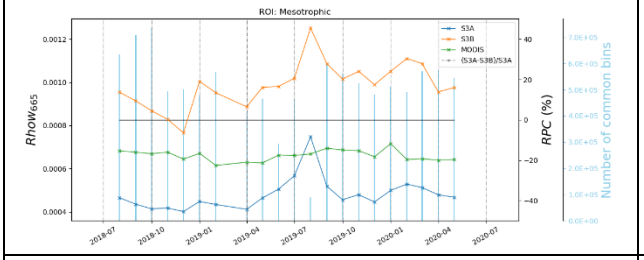	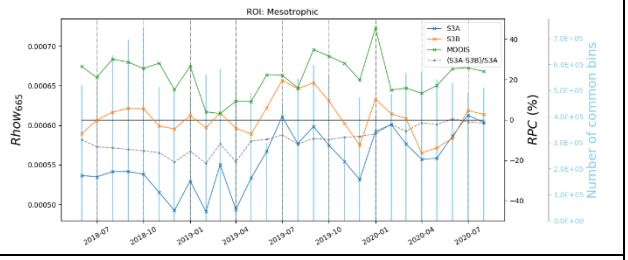
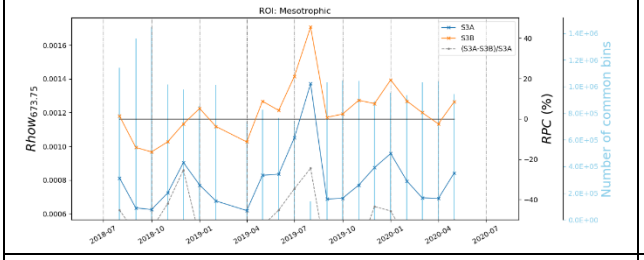	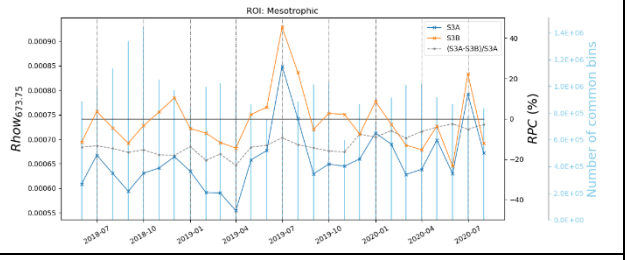
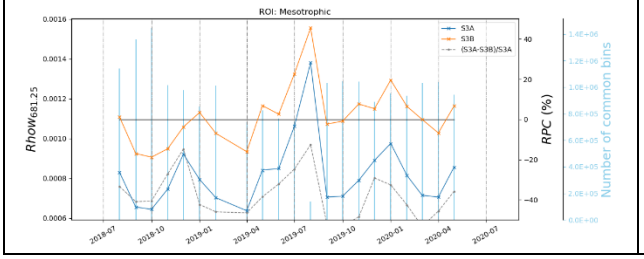	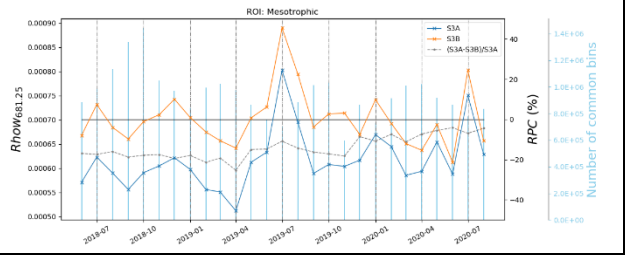

PB2.23	OC-SVC-TOOL
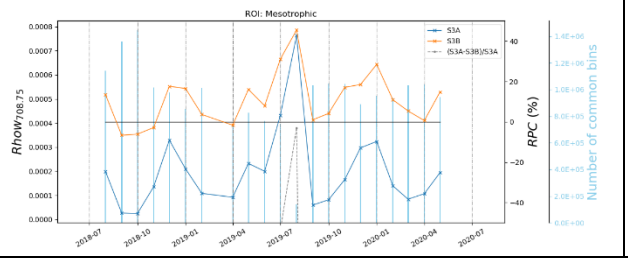	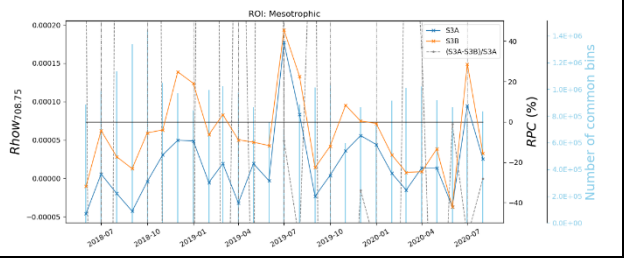
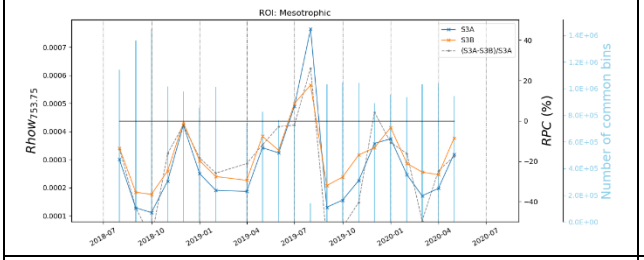	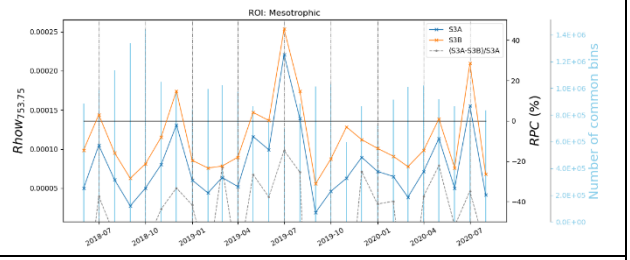
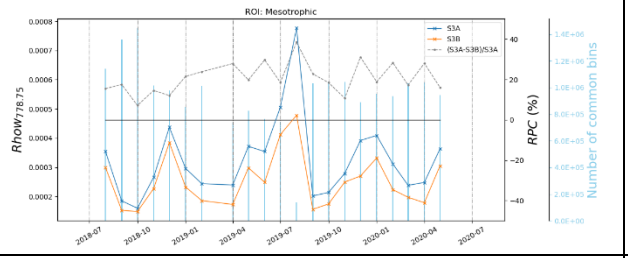	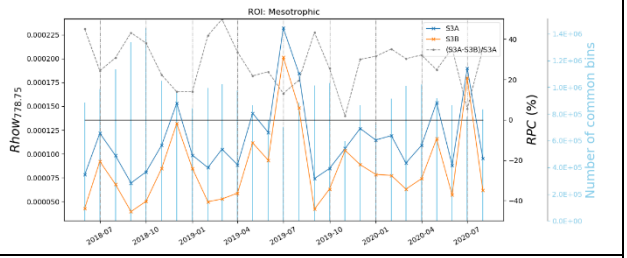
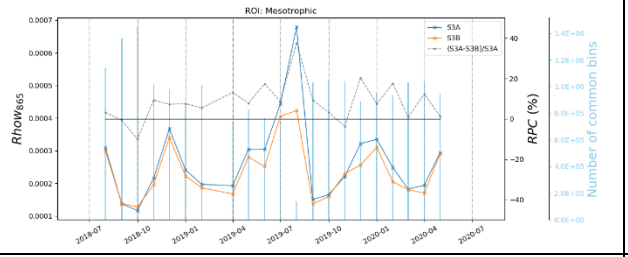	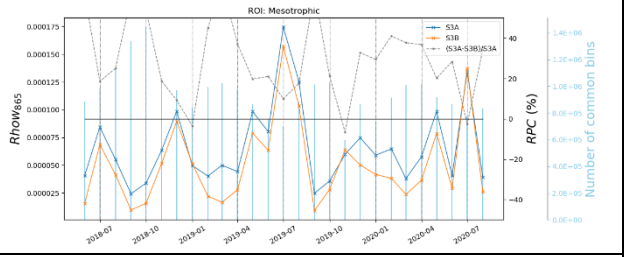
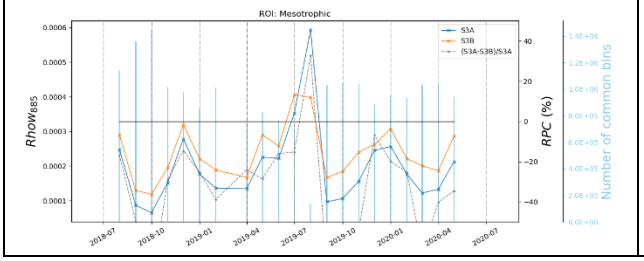	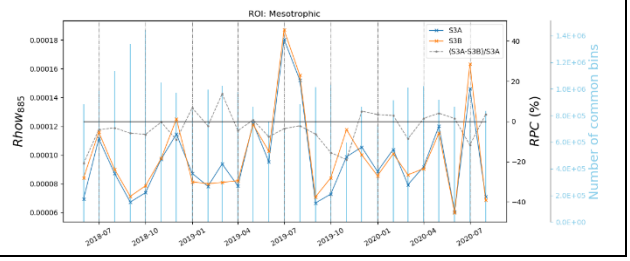

PB2.23	OC-SVC-TOOL
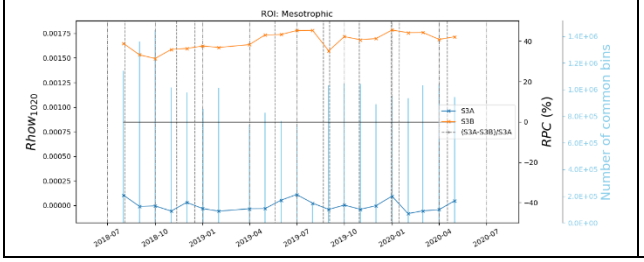	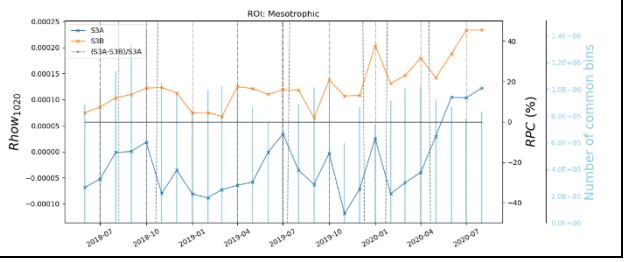

Figure 51 Time-series of Level-3 marine reflectance over mesotrophic waters at all VIS and NIR bands (top to bottom) for OLCI-A (orange), OLCI-B (blue) and, when relevant, MODIS-Aqua (green). Relative difference between S3A and S3B in grey (second y-axis). Left: OLCI data from PB2.23, right with new IPF and OLC-SVC-TOOL gains.

4.5.3.3 EUTROPHIC WATERS

Over such waters, the effect of the atmospheric correction is at least as strong as the TOA calibration and spectral features change (at 400 nm, the signal is about 5 times smaller than over clear waters). There is still a clear improvement for all bands between 443 nm and 681 nm, with relative difference between OLCI-A and OLCI-B within 5%, and even less in the green bands. There is still an excellent agreement between the two sensors in the NIR band, where the signal starts to be non-negligible.

PB2.23	OC-SVC-TOOL
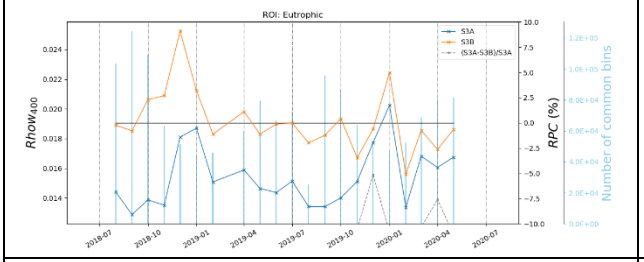	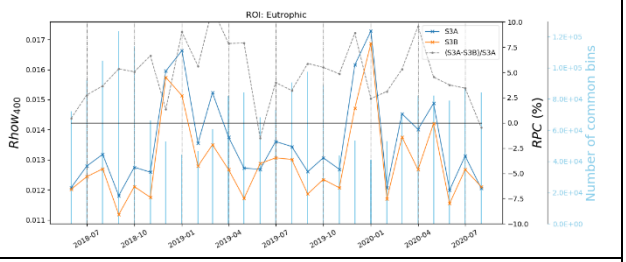
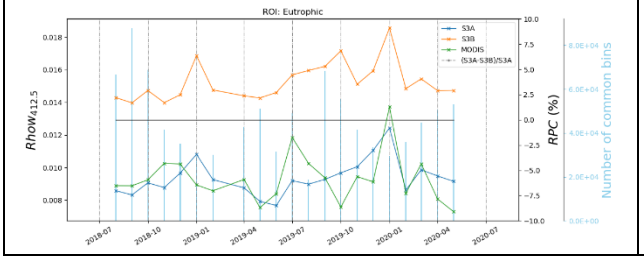	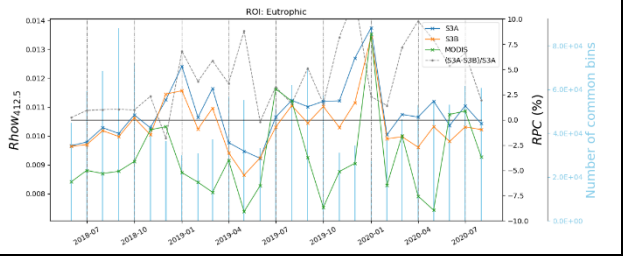

Figure 52 Time-series of Level-3 marine reflectance over eutrophic waters at all VIS and NIR bands (top to bottom) for OLCI-A (orange), OLCI-B (blue) and, when relevant, MODIS-Aqua (green). Relative difference between S3A and S3B in grey (second y-axis). Left: OLCI data from PB2.23, right with new IPF and OLC-SVC-TOOL gains.

PB2.23	OC-SVC-TOOL
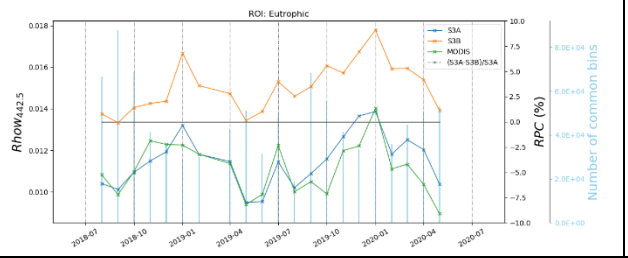	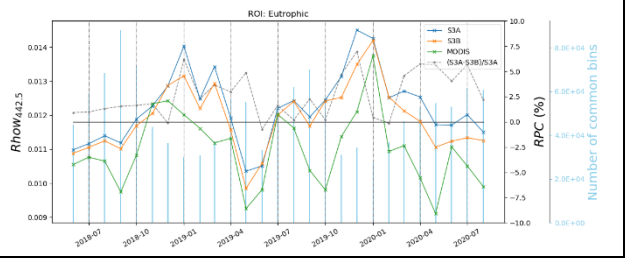
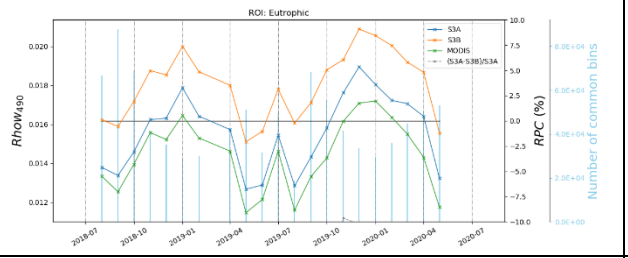	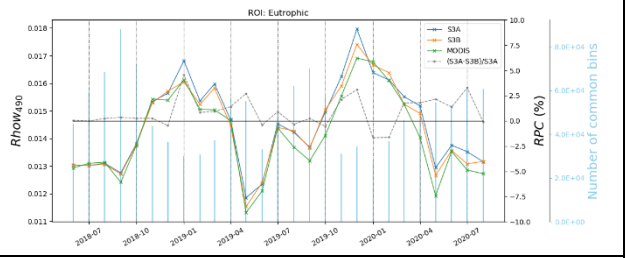
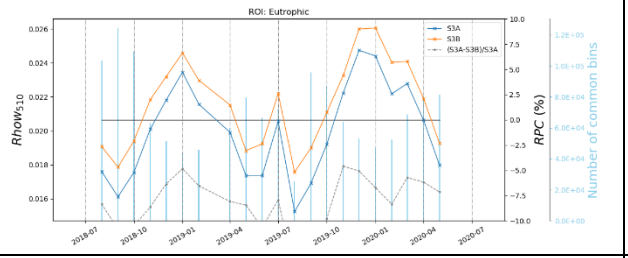	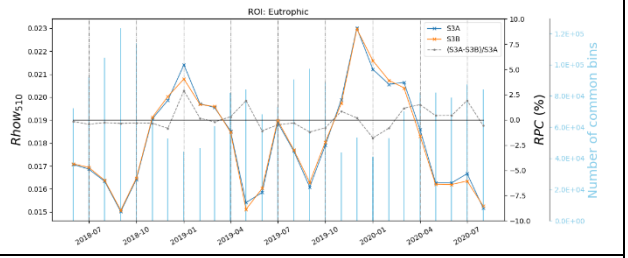
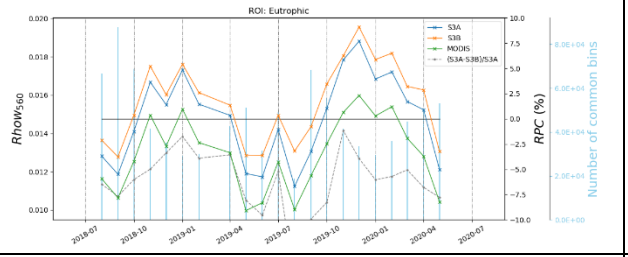	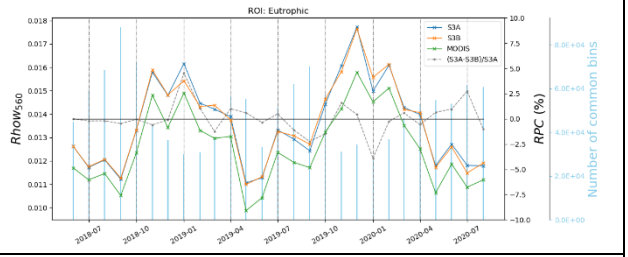
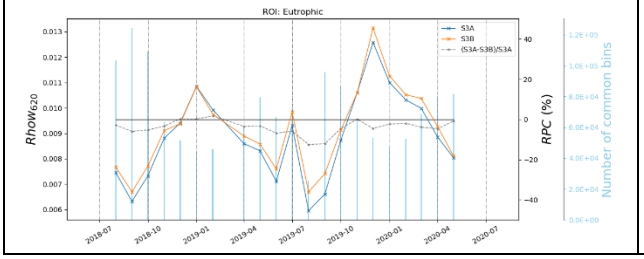	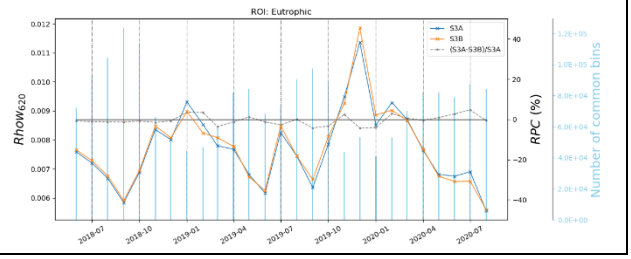

PB2.23	OC-SVC-TOOL
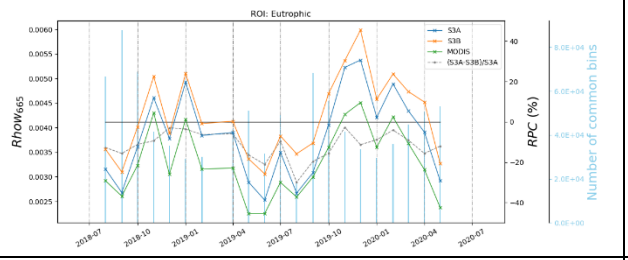	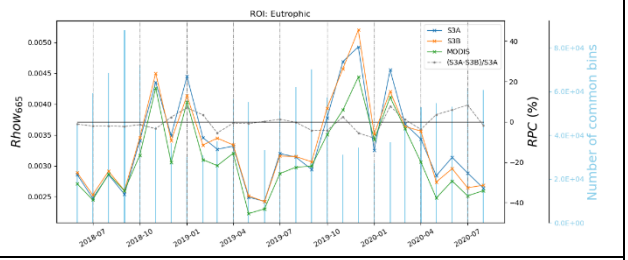
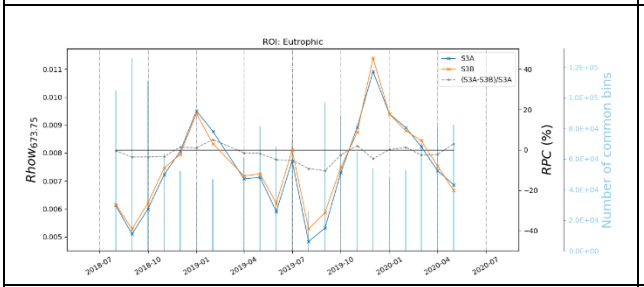	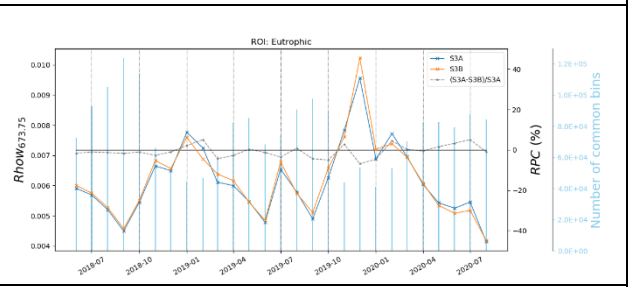
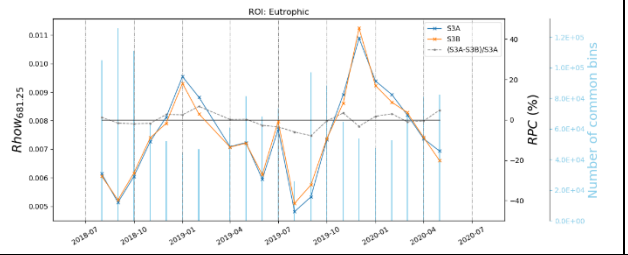	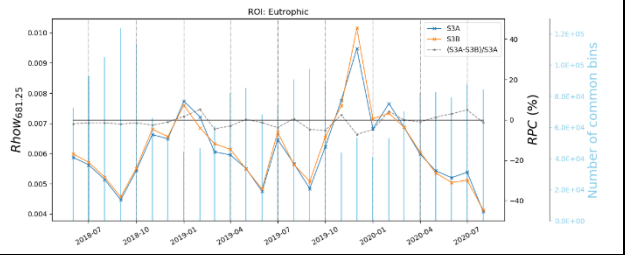
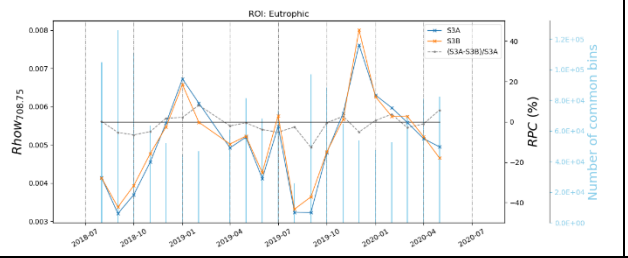	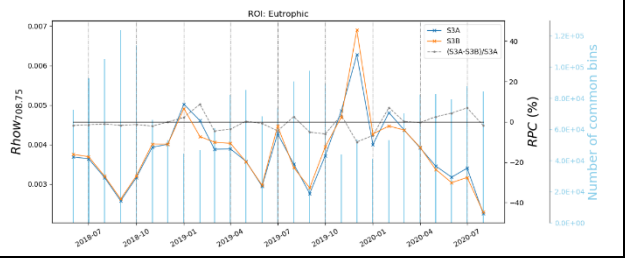
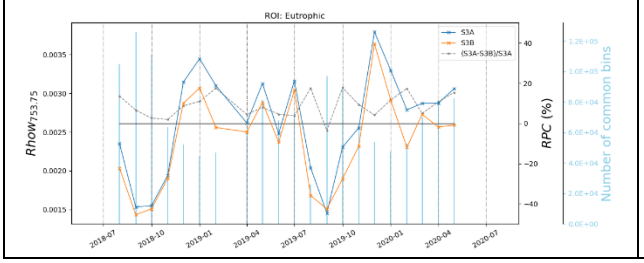	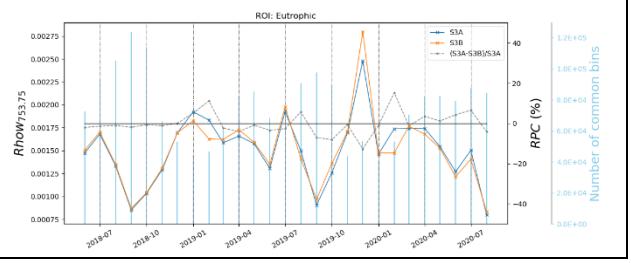

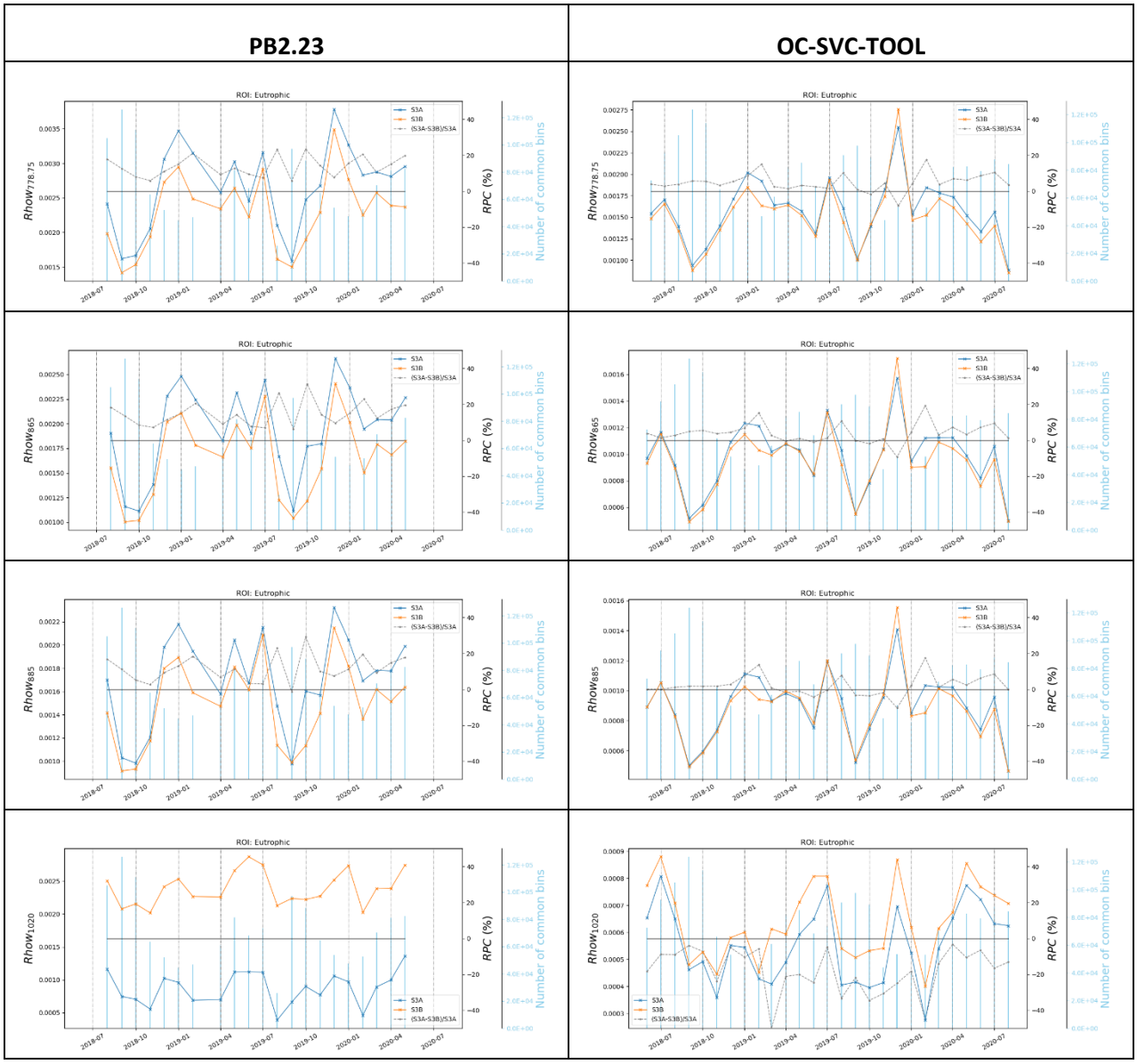

Figure 52 Time-series of Level-3 marine reflectance over eutrophic waters at all VIS and NIR bands (top to bottom) for OLCI-A (orange), OLCI-B (blue) and, when relevant, MODIS-Aqua (green). Relative difference between S3A and S3B in grey (second y-axis). Left: OLCI data from PB2.23, right with new IPF and OLC-SVC-TOOL gains.

5 POTENTIAL LIMITATIONS

We list here a series of potential limitation or assumptions that could be revised for future computations of the gains:

- For the standard AC, the BRDF correction in Eq. (7) induces a small spectral coupling in the marine reflectance because C_{BRDF} comes from a LUT indexed on chlorophyll, itself computed from R_{rs} at various bands (Morel et al., 2002). The numerical inversion seems to handle correctly this small non-linearity, as checked on the impact of individual gains. Still, two alternative approaches could make the problem fully linear:
    - Either deactivate the normalization and conduct SVC with directional reflectance. This requires to de-normalize in the MDB the in situ data to the sensor/illumination geometry through the same BRDF process (i.e. using the in situ R_{rs}^t to compute chlorophyll). Convergence on directional reflectance would imply convergence on fully-normalized reflectance.
    - Or change the Level-2 processor by normalizing the satellite reflectance by the C_{BRDF} factor computed with the in situ R_{rs}^t.
- SVC in the NIR assumes perfectly negligible R_{rs}^t on the SPG site. A small residual signal due to pure water exists at 709 nm. Alternatively, the marine reflectance stored in the MDB at SPG could be recomputed with the pure water model used in the Level-2 processor.
- Digitization of marine reflectance in OLCI Level-2 products create very small errors (maximum being half of the scaling factor, i.e. about 9.2 10^{-6}) that may propagate in the Jacobian matrix computation. In the NIR, at SPG, where the marine signal is extremely small, this may explain the non-perfect retrieval of zero Rrs after individual gains.
- The time-series of MOBY measurements shows various gaps, due to problems of the buoy itself (see Figure 9). Since a seasonal trend can be seen on this plot, some bias could be due to missing data. It is advised to relaunch SVC process regularly when more in situ data become available to see any deviation on the mission average gains.

6 REFERENCES

Antoine, D. and A. Morel (1999). A multiple scattering algorithm for atmospheric correction of remotely-sensed ocean colour (MERIS instrument): principle and implementation for atmospheres carrying various aerosols including absorbing ones, IJRS, 20, 1875-1916.

Bailey, S.W., and P. J. Werdell (2006). A multi-sensor approach for the on- orbit validation of ocean color satellite data products. Remote Sens. Environ. 102(1-2), 12–23

Cazzaniga, I., Kwiatkowska, E., Dzierzon, H., Fomferra, N., Block, T., et al. (2019a). Copernicus Database for Bio-Optical in situ Fiducial Reference Measurements. Presentations from S3VT-2019 meeting, Ocean Colour sessions

Cazzaniga, I., Kwiatkowska, E., Taberner, M., Obligis, E. (2019b). Sentinel3-A/B OLCI Ocean Colour

Product Validation with In Situ Measurements

Clark, D.K., Yarbrough, M. A., Feinholz, M. E., Flora, S., Broenkow, W., Kim, Y. S., Johnson, B. C., Brown, S. W., Yuen, M., and Mueller, J. L. (2003). MOBY, a radiometric buoy for performance monitoring and vicarious calibration of satellite ocean color sensors: Measurement and data analysis protocols, in Ocean Optics Protocols for Satellite Ocean Color Sensor Validation, Revision 4, Volume VI: Special Topics in Ocean Optics Protocols and Appendices. NASA/TM-2003-211621/Rev4-Vol.VI:3-34, Greenbelt, MD.

Deru, A., C. Lerebourg, L. Bourg, S. Dransfeld, E. Kwiatkowska, (2019). S3B System Vicarious Calibration. Presentations from S3VT-2019 meeting, Ocean Colour sessions.

Franz, B.A., S.W. Bailey, P.J. Werdell, and C.R. McClain (2007). Sensor-independent approach to the vicarious calibration of satellite ocean colour radiometry. Applied Optics, 46: 5068–5082

Lamquin, N., Clerc, S., Bourg, L., Donlon, C. (2020). OLCI A/B Tandem Phase Analysis, Part 1: Level 1 Homogenisation and Harmonisation. Remote Sensing, 12, 1804.

Mazeran, C., Ruddick; K., Voss, K., Zagolski, F. and Kwiatkowska, E. (2017). Requirements for Copernicus Ocean Colour Vicarious Calibration Infrastructure. Report of the EUMETSAT study ref EUM/CO/16/4600001772/EJK, issue 1.3

Mazeran (2018). Optimal System Vicarious Calibration without derivative: application to S3-A/OLCI data processed by C2RCC and POLYMER. ESA OC-CCI report to Brockmann Consult, ref. SOLVO/BRC/17/OCC/DR2.

Mazeran, C., C. Brockmann, A. Ruescas, F. Steinmetz (2019). System Vicarious Calibration for non-standard ocean colour algorithm: Application to SeaWiFS, MODIS, MERIS and VIIRS data processed by POLYMER. ESA OC-CCI (Phase 3) ATBD.

Morel, A., Antoine, D. and B. Gentili (2002). Bidirectional reflectance of oceanic waters: Accounting for Raman emission and varying particle phase function. Applied Optics, 41, 6289-6306.

Sentinel-3 OLCI protocol for matchups to derive Ocean Colour System Vicarious Calibration (OC-SVC) gains in visible bands. EUMETSAT report ref. EUM/RSP/DOC/19/1102651, 2019.

Steinmetz, F., Deschamps, P.-Y. and D. Ramon (2011). Atmospheric correction in presence of sun glint: application to MERIS. Optic Express 19, 9783-9800.

Voss, K.J., H.R. Gordon, S.J. Flora, B.C. Johnson, M.A. Yarbrough, M.E. Feinholz, and T. Houlihan (2017). A method to extrapolate the diffuse upwelling radiance attenuation coefficient to the surface as applied to the marine optical buoy (MOBY). Journal of Atmospheric & Oceanic Technology, 34: 423-1432

Werdell, J., Bailey, S., Franz, B., Morel, A. and McClain, C R. (2007). On-orbit vicarious calibration of ocean color sensors using an ocean surface reflectance model. Applied Optics, 46, 5649—5666.

Zibordi, G., Melin, F., Voss, K., Johnson, B., Franz, B., Kwiatkowska, E., Huot J-P., Wang, M., and Antoine D. (2015). System vicarious calibration for ocean color climate change applications: Requirements for in situ data. Remote Sensing of Environment. 159 361-369.

Zibordi, G. and Voss, K. (2019). Vicarious calibration and validation protocols. Proceeding of IOCS meeting, South Korea, 2019. Available at https://iocs.ioccg.org.